



**University of  
Nottingham**  
UK | CHINA | MALAYSIA

**Artificial Neural Network Intelligent Technique and Multiple Nonlinear  
Regression for Prediction and Optimization of the Transmittance of  
Lightpipes and Implementation in BIM**

**by**

**Li ZHANG**

**BArch, MArch**

Student ID: 4248704

Supervisors: Dr. Yuehong Su, Dr. Gadi Mohamed

Thesis Submitted in Partial Fulfilment of the Requirements for the Degree of

**Doctor of Philosophy**

in the Department of Architecture and Built Environment

Faculty of Engineering

University of Nottingham

I hereby certify that this is entirely my own work unless otherwise stated, and I have all necessary rights and consents to publicly distribute this dissertation via the University of Nottingham's eTheses archive.

31 October 2020

## ABSTRACT

Daylighting features prominently in sustainable building design. It has been proven that daylighting not only saves the electric lighting energy consumption, but also improves the visual comfort and occupants' health. A number of daylighting designs and control strategies have been presented and practised. Performance prediction of these designs is essential in daylighting research. The innovation of natural daylighting light pipe took place more than thirty years ago. However, no efficient and accurate prediction method, which includes the efficiency of straight light pipe, especially the bended light pipe has been made available. Therefore, a prediction model for light pipes is desirable to assess and predict its efficiency and potential in energy saving. This thesis attempts to develop an Artificial Neural Networks (ANNs) based prediction model for the performance of lightpipes and implement it in the Building Information Modelling (BIM) platform to help the designers, engineers and asset managers make informed decisions in daylighting lightpipes design. A comprehensive and critical literature review is first introduced covering the advanced artificial neural network intelligent technique in the application of the luminance and illuminance prediction, energy saving, daylighting controls and the optical property of lightpipes. An optical analysis software Photopia is employed to simulate the daylighting performance of light pipes to generate the real database and calculate the efficiency of the light pipes. It is then followed by ANNs simulations in Matlab for forming a forecasting model for light pipe performance. To empower the prediction model and make it easy and friendly to be used, the developed ANNs model for lightpipe performance is innovatively implemented in BIM software Revit, as a plug-in application tool. This tool in Revit enables the prediction of the transmittance of lightpipes directly without running the programme in Matlab. It can help the designers or users choose the lighpipe parameters easily and accurately and therefore add value to the industry and the research community.

## PUBLICATIONS

Zhang, L., Su, Y. and Ullah, I., 2020. A review on daylighting prediction by using Artificial Neural Network techniques. *Journal of Daylighting*, in press.

Tian, M., Zhang, L., Su, Y., Xuan, O., Li, G. and Lv, H., 2019. An evaluation study of miniature dielectric crossed compound parabolic concentrator (dCCPC) panel as skylights in building energy simulation. *Solar Energy* 179: 264-278.

Duan, Z., Zhang, L., Lin, Z., Fan, D., Saafi, M., Castro-Gomes, J. and Yang, S., 2018. Experimental test and analytical modeling of mechanical properties of graphene-oxide cement composites. *Journal of Composite Materials* V52 (22) pp. 3027-3037.

Bottarelli, M., Zhang, L., Bortoloni M. and Su, Y., 2016. Energy performance of a dual air and ground-source heat pump coupled with a flat-panel ground heat exchanger. *Bulgarian Chemical Communications* 48(A): 64-70.

Zhang, L., Tian, M. and Su, Y., 2015. A case study of energy efficiency retrofit and renewable technology utilisation in a UK school group, in *14th International Conference on Sustainable Energy Technologies -SET 2015*. Nottingham, UK.

Yao, G., Han, D., Zhang, L. and Duan, Z., 2021. The thermal performance of Chinese vernacular skywell dwellings. *Advances in Civil Engineering*, V.2021, 6666701.

## **ACKNOWLEDGEMENTS**

The author is extremely indebted to her supervisor, Dr Yuehong Su. He has guided the author through every stage of this research and contributed many ideas to its development. His constant encouragement and unwavering support are greatly appreciated and his guidance has proved invaluable.

Grateful thanks are extended to my co-supervisors, Dr. Gadi Mohamed and Dr. Guohui Gan, who gave me their time and expert advice without hesitation.

Thanks to colleagues and friends within the research unit at the University of Nottingham who provided the laughs and social relief through the years.

Specifically, and finally, I wish to express my greatest appreciation to my parents, for their support, throughout the course of this work. This would not have been possible without them. When writing up this thesis, I gave birth to my son Andrew. Although the past year was extremely difficult for me to balance the work and caring Andrew as affected by Covid19, the birth of Andrew gave me the most happiness in my life. This thesis is dedicated to him.

# Contents

ABSTRACT.....	III
PUBLICATIONS.....	IV
ACKNOWLEDGEMENTS.....	V
List of Tables.....	X
List of Figures.....	XII
Chapter 1 Introduction.....	1
1.1 Background.....	2
1.2 Motivation and objectives.....	5
1.3 Thesis structure.....	8
Chapter 2 A review on daylighting prediction by using Artificial Neural Network techniques .....	11
2.1 Introduction.....	12
2.2 Daylighting prediction methods.....	15
2.2.1 Physical model.....	15
2.2.2 Analytical formulae.....	17
2.2.3 Daylighting calculation software.....	18
2.2.4 Artificial Neural Network.....	21
2.3 Application of Artificial Neural Networks Techniques in Daylighting Prediction ..	27
2.3.1 Luminance and Illuminance Prediction.....	27
2.3.2 Prediction of energy saving due to daylighting.....	38
2.3.3 Daylighting Controls.....	43
2.4 Discussion on research gaps.....	52
2.5 Summary.....	54

Chapter 3 Performance of lightpipes and Artificial Neural Network (ANN) model development for predicting the transmittance of lightpipes .....	56
3.1 Introduction .....	57
3.1.1 Background.....	57
3.1.2 Outline of the principles of Artificial Neural Network .....	58
3.1.3 Research significance .....	60
3.2 Methodology .....	61
3.2.1 Simulation data acquisition in Photopia .....	62
3.2.2 Configuration of Artificial Neural Network.....	69
3.2.3 Evaluation metrics .....	76
3.3 Efficiency of various lightpipes under clear sky.....	77
3.3.1 Efficiency of various aspect ratio of lightpipes under clear sky.....	77
3.3.2 Efficiency of various bended angle of lightpipes under clear sky.....	79
3.3.3 Efficiency of lightpipes with various solar altitude under clear sky .....	81
3.3.4 Efficiency of lightpipes with various solar azimuth under clear sky .....	83
3.4. Efficiency of various lightpipes under intermediate sky.....	84
3.5 Artificial neural network prediction.....	88
3.5.1 Straight lightpipe prediction by Artificial Neural Network.....	88
3.5.2 Straight and bended lightpipe prediction by Artificial Neural Network .....	89
3.5.3 Artificial Neural Network limitations and improvements.....	95
3.6 Summary .....	98
Chapter 4 Predicting the transmittance of lightpipes by multiple nonlinear regression model and comparing with Artificial Neural Network (ANN) model .....	100
4.1 Introduction .....	101
4.2 Summary of previous work on mathematical models .....	102

4.2.1 Straight lightpipe .....	102
4.2.2 Elbow lightpipe.....	103
4.2.3 Su et al. regression formula .....	105
4.3 Methodology .....	109
4.3.1 Models of lightpipes .....	109
4.3.2 Multiple nonlinear regression .....	112
4.3.3 Variables settings.....	113
4.4 Results of regression .....	115
4.5 Comparison between multiple nonlinear regression and ANN model for predicting the transmittance of lightpipes .....	125
4.6 Summary .....	128
Chapter 5 Integrating Artificial Neural Network (ANN) and BIM Revit via Application Programming Interface (API) to predict the daylighting performance of lightpipes.....	130
5.1 Introduction .....	131
5.1.1 BIM.....	131
5.1.2 Autodesk Revit API overview .....	133
5.2 Fundamentals of hybrid ANN and C#.NET.....	135
5.2.1 Artificial Neural Network in the simple retrospect .....	136
5.2.2 An overview of integrating ANN and C#.NET methods .....	137
5.2.3 The process of calling for Artificial Neural Network (ANN) in C#.NET.....	139
5.3 Methodology .....	141
5.3.1 Define valid parameter file .....	142
5.3.2 Hybrid programme with ANN and C#.NET .....	144
5.3.3 Edit the model translator.....	146

5.3.4. Running the prototype programs in Revit .....	150
5.4 Case study and validation.....	151
5.5 Summary .....	155
Chapter 6 Conclusions and Future Work .....	157
6.1 Conclusions .....	158
6.2 Limitations and future work.....	159
REFERENCES .....	161

## List of Tables

Table 2.1 Statistics indexes to evaluate ANNs’ prediction accuracy [58].	22
Table 2.2 Summary of typical methods for daylighting prediction	26
Table 2.3 The performance of ANN and CIE model for predicting the sky luminance between predicted and measured data in Nakhon Pathom and Songkhla [69].	29
Table 2.4 The RMSE (%) of each ANN configurations [70]	31
Table 2.5 Performance of Perez, ANN, Robledo model [71]	32
Table 2.6 Summary of prediction power of Sine, Novel sine and ANN model to illuminance	33
Table 2.7 Compared results of various prediction methods [74]	35
Table 2.8 Summary of ANN applied to predict daylighting in literatures	48
Table 3.1 Brief description of the basic lightpipe parameters for simulation	64
Table 3.2 The parameters with Degree Measure and corresponding Radian Measure	71
Table 3.3 The parameters with Degree Measure and corresponding Radian Measure	72
Table 3.4 The parameters for the sky clear index	74
Table 3.5 The input parameters and output parameters in ANN models	74
Table 3.6 The correlation coefficients of trained ANN models of straight lightpipes	89
Table 3.7 Comparison between results obtained using transfer functions logsig and tansig	89
Table 3.8 Parameters for the best configuration of ANN model for total lightpipe prediction	90
Table 3.9 The correlation coefficients of trained ANN model models of 0°, 30°, 45° and 60° elbowed angle of lightpipes	95
Table 4.1 Regression constants for elbowed lightpipes	108

Table 4.2 Regression constants for straight lightpipes ..... 108

Table 4.3 Four levels for evaluation of ANNs [60]. ..... 113

Table 4.4 values of the constants ..... 116

Table 4.5 Options for regression for lightpipes ..... 117

Table 4.6 Regressing equations attempted for the correlations of altitude, azimuth and sky clearness factor to the transmittance of lightpipes ..... 121

Table 4.7 The regression constant of 30°, 45° and 60° elbowed lightpipes respectively and assessment of each model ..... 121

Table 4.8 Comparison between the MNL model and the ANN model ..... 126

Table 5.1 Values for material parameters used in TEST example of the prototype ..... 153

Table 5.2 Values for ANN parameters used in TEST example of the prototype..... 153

Table 5.3 Mathematics calculated the average reflectance of the material “lightpipe” (set as the transmittance of lightpipes in this modelling)..... 155

## List of Figures

Figure 1.1 Buildings share of UK carbon dioxide emissions [3].....	2
Figure 1.2 An illustration of innovative daylighting devices lightpipes .....	4
Figure 1.3 The workflow of the Thesis .....	10
Figure 2.1 Typical methods for daylighting predictions.....	15
Figure 2.2 Four categories of ANNs models [57].....	22
Figure 2.3 The typical sample of multilayer feedforward neural networks [60] .....	23
Figure 2.4 Transfer function used in the neural network [61] .....	25
Figure 2.5 Diagram to explain various zenith angles and the angular distance.....	28
Figure 2.6 ANN model architecture[70] .....	30
Figure 2.7 A diagram of MLP ANN model, which has been trained by supervised apprenticeship [71].....	32
Figure 2.8 The sketch model of simulation room[74] .....	35
Figure 2.9 A graphic of the best performance ANN architecture [39] .....	37
Figure 2.10 Scheme of geometries of test room [76].....	39
Figure 2.11 A sample diagram of cross-validation method [76] .....	39
Figure 2.12 The multi-layer perceptron (MLP) ANN structure [78].....	41
Figure 2.13 A demonstration of optimization using ANN model to determine proper design parameters in application [78] .....	41
Figure 2.14 The schematic of the IDHVAC system [80] .....	43
Figure 2.15 Flow chart of the IDHVAC system optimization [80] .....	43
Figure 2.16 The diagram of automated split-controlled blinds [85] .....	46

Figure 2.17 The flow chart of ANNs application in daylighting control of blind [85] .....	47
Figure 3.1 Mammalian neuron [87] .....	58
Figure 3.2 The typical sample of a multilayer feed-forward neural networks [60] .....	59
Figure 3.3 Illustration of the process of ANN .....	62
Figure 3.4 A single group of a single type of lightpipes .....	63
Figure 3.5 Parameter demonstration of single lightpipes .....	65
Figure 3.6 Solar altitude and solar azimuth. ....	66
Figure 3.7 Lengths of 1000mm, 1500mm and 2000mm of lightpipes. ....	67
Figure 3.8 Diameters of 230mm, 300mm, 450mm and 530mm of lightpipes.....	67
Figure 3.9 Bended angle of 0, 30, 45 and 60 degree of lightpipes .....	68
Figure 3.10 The typical network architecture and work mechanism of neural network .....	70
Figure 3.11 Horizontal global illuminance under the CIE clear sky versus solar altitude [36].....	73
Figure 3.12 Efficiency of various aspect ratio of lightpipes under clear sky.....	78
Figure 3.13 Efficiency of various bended angle of lightpipes under clear sky.....	80
Figure 3.14 Efficiency of straight lightpipes with various solar altitude under clear sky .....	81
Figure 3.15 Efficiency of 30° bended lightpipes at various solar altitude and solar azimuth 50° .....	82
Figure 3.16 Efficiency of 30° elbowed lightpipes at solar altitude 50° and at various solar azimuth under clear sky .....	84
Figure 3.17 Efficiency of various aspect ratio of lightpipes under intermediate sky .....	85
Figure 3.18 Efficiency of various bended angle of lightpipes under intermediate sky .....	86
Figure 3.19 Efficiency of lightpipes with various solar altitude under intermediate sky .....	87

Figure 3.20 Efficiency of lightpipes with various solar azimuth under intermediate sky .....	87
Figure 3.21 ANNs prediction for the efficiency of straight lightpipes .....	88
Figure 3.22 The prediction MSE value of ANN model .....	91
Figure 3.23 The illustration of regression relationship between prediction values and target values in the ANN Training, Validation and Test procedure .....	92
Figure 3.24 A graphic of the best performance ANN architecture (including the input parameters, the output parameters and the neurons number of hidden layer) .....	93
Figure 3.25 Predicted transmittance in ANN versus simulated transmittance of lightpipes in Photopia .....	94
Figure 4.1 The demonstration of the purposely built shed for testing lightpipes [36].....	106
Figure 4.2 Horizontal global illuminance under the CIE clear sky versus solar altitude [36]	107
Figure 4.3 A single group of a single type of lightpipes .....	110
Figure 4.4 Various geometries of lightpipes .....	111
Figure 4.5 Illustration of the schematic of sun positions and lightpipes.....	114
Figure 4.6 Comparison between simulated transmittance and predicted transmittance of lightpipes based on Su's regression mathematical model.....	117
Figure 4.7 Predicted transmittance versus simulated transmittance for total elbowed lightpipes .....	119
Figure 4.8 Predicted transmittance versus simulated transmittance of elbowed 30 degree lightpipes.....	123
Figure 4.9 Predicted transmittance versus simulated transmittance of elbowed 45 degree lightpipes.....	124

Figure 4.10 Predicted transmittance versus simulated transmittance of elbowed 60 degree lightpipes.....	124
Figure 4.11 The comparison between the multiple nonlinear regression model and the ANN model for predicting the transmittance of lightpipes (top is MNLN model and bottom is ANN model) .....	127
Figure 5.1 Analysis indexes of the 3D to nD modelling project [106] .....	133
Figure 5.2 The summary of Revit elements .....	134
Figure 5.3 Possible mappings linking extension to BIM project (Revit Daylighting) .....	135
Figure 5.4 Combining ANN with Revit workflow .....	142
Figure 5.5 The demonstration of C# .NET call for the Matlab ANN toolbox.....	145
Figure 5.6 The demonstration of C# code in .NET interface when writing ANNREVIT prototype .....	146
Figure 5.7 Demonstration of window model choice in Revit .....	147
Figure 5.8 The location of “Glass” material in “Type Properties” .....	148
Figure 5.9 The location of RGB values edited panel in Revit .....	149
Figure 5.10 Loading the ANNREVIT prototype in Revit .....	151
Figure 5.11 Input and output interface in Revit by adding in ANNREVIT prototype .....	152
Figure 5.12 Revit information for “lightpipe” in “Type Properties” .....	152
Figure 5.13 Revit material information for “lightpipe” with custom parameters “Custom Color” .....	154

# **Chapter 1 Introduction**

## 1.1 Background

Carbon dioxide (CO<sub>2</sub>) emission is one of the greatest global challenges that human beings have to overcome in the 21st century. Although the energy consumption in the World still increases, however, due to implementation of various energy saving techniques, the increase rate of energy consumption has slowed down in the last decade. The UK government has set target to reduce 80% of net carbon account by the year 2050 compared with 1990 baseline [1]. Inspiringly, UK net CO<sub>2</sub> emissions were estimated to be 351.5 million tonnes (Mt) in 2019, which was 3.6% less than 2018 of 365.7 Mt [2]. Among these, buildings are responsible for approximately 38% of the CO<sub>2</sub> emissions in UK (Figure 1.1) [3]. Therefore, buildings are the sector with the greatest potential for carbon reduction.

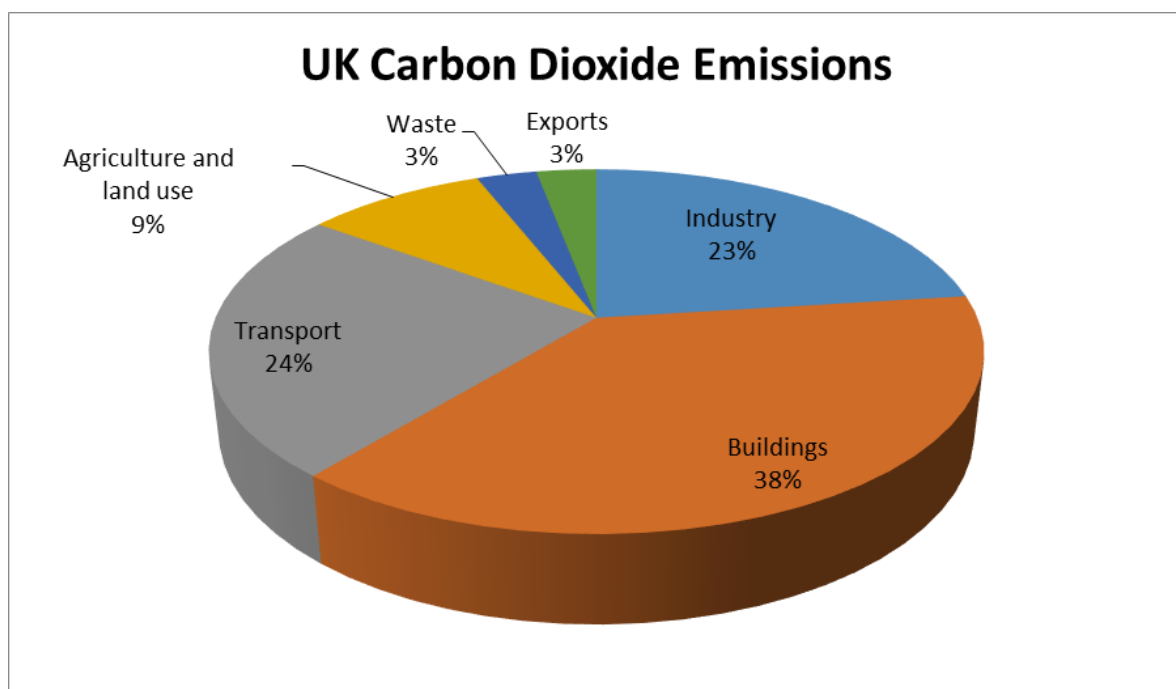


Figure 1.1 Buildings share of UK carbon dioxide emissions [3].

It is found that electric lighting, one of the dominant energy demands, accounts for 17% of total electricity consumption in commercial buildings [4] and 20% in residential properties [5]. Historically, daylight was used as the primary source of luminance during the day. However, as modern cities have been built, artificial lighting has been substantially used in buildings in

the daytime. As a result, massive consumption of artificial lighting and hence energy has brought into attention to numerous scientists and engineers as if it could be reduced or replaced by the natural daylighting. For example, Li and Tsang [6] carried out a survey on some open layout office buildings in Hong Kong and found that 20-25% of electric lighting energy can be saved if half of the occupancy time was served by daylighting with proper artificial lighting control.

Compared with artificial lighting, daylighting does not only save the energy consumption, but also improve the visual comfort and occupants' health, which applies "light vitamin" to people living in the buildings. Begemann et al. [7] have conducted a long-term study and found that the occupants in buildings prefer varying levels of natural lighting cycle to the constant artificial lighting. In addition to the directly save on the energy consumption and personal preference, daylighting can save the cooling cost in air-conditioned buildings. This is due to that the Luminous Efficacy (number of lumens per watt) of daylighting is normally higher than artificial lighting. As such, given the same level of illuminance, less radiant power is required. In other words, natural illumination normally dissipates less heat than artificial illumination and therefore it is considered as an efficient illumination. In an office building with normally extensive use of artificial lighting, significant amount of heat dissipation could be saved by utilizing daylighting instead, which reduce the cooling energy consumption [8].

Light pipe is an innovative design to deliver daylight into deep space where otherwise daylight cannot reach. A schematic of light pipe system is shown in Figure 1.2. An acrylic dome usually is installed at roof level and then transmitted downwards to interior spaces within buildings. The internal surface of the pipe is coated with mirror-finished aluminum with a high reflection

of 98%. This pipe system helps introducing daylight via a light diffuser. The reflecting pipe is adaptable to incorporate any bends around building structural components.



Figure 1.2 An illustration of innovative daylighting devices lightpipes

Because of its main structure as a well-sealed tube, light pipe has added potential advantage in reducing excessive solar gain. In addition, the daylight only emits off from diffuser and as such the output daylight is easier to control. Moreover, the light pipe is flexible in its structure, allowing to put diffusers directly where needed, so as to achieve a good internal daylight distribution. The combined use of windows and light pipes can reduce glare and further improve the balance of daylighting in a room. Exploiting daylighting sometimes is objected due to the excessive glare and shadow it may cause. However, light pipe could solve these issues. By redirecting and diffusing daylighting into deep space, glare from windows is reduced and daylighting is of a better uniformity. Another advantage is light pipe could be applied in

multi-story buildings, while the use of daylight is usually limited to the perimeter zone of a building.

Due to various potential advantages as mentioned, light pipes have been widely used in the USA and Australia and developed in the UK and Europe. Researches evaluating the performance of light pipe is thus justified to reveal its full potentials and to push forward its development.

## **1.2 Motivation and Objectives**

The prediction of daylighting in building design is a key part of the whole design process. As is widely accepted, daylight condition is highly dynamic throughout a day and a year, which brings difficulty to the prediction of daylight. Early work about daylighting prediction always employed sensitivity and regression analysis to deal with annual energy using situation. However, such analysis methods considerably relied on well-understood energy consumption data. Due to the non-linear nature of daylight, artificial neural networks (ANNs) had been introduced to daylighting prediction, which has advantages in solving nonlinear problems [9].

In the last twenty years, ANNs has been applied in various fields of research, including refrigeration, air conditioning and heat pump system [10], heat transfer problem in nuclear engineering [11], sizing of solar photovoltaic systems [12], modelling and control of combustion processes [13], modelling of renewable energy system [14], chemical process control [15], thermal analysis of heat exchangers [16], forecasting [17], and application in the atmospheric sciences [18]. In light of architecture, ANNs has been used to analysing cooling and heating in buildings, electricity usage, sub-level components operation and optimization, and parameters estimation. ANNs can model multi-variable problem. As a computational

learning paradigm, ANNs can extract the non-linear complex relationships between the variables by means of training data. In the meantime, compared to other systems, ANNs is speedier and simple in terms of calculation efficiency and processing algorithm.

Regarding the light pipe, the difficulties in identifying all decisive factors that affect the performance and in quantitatively weighing the contributions of these decisive factors are the main barriers to appraising the efficiency of light pipe. The complexity in the mechanism of light pipe transmitting light makes it difficult to appraise the performance by means of physical modelling. Besides, prior to this research, the lack of light pipe performance data, which include both environmental, and geometrical data make it impossible to predict the performance by using mathematical methods as well.

The overall aim of this work is to develop an artificial neural network model for the prediction and optimization of the daylighting performance of light pipe and implemented into BIM platform to enhance the light pipe design capacity. Although the performance of light pipe has been investigated in a number of studies, no methods could predict the bended light pipe because the non-linear relationship between the system parameters and the daylighting performance of light pipe. The final goals are to be achieved following a logical process from raw data simulated by an optical software Photopia collection to evaluate of ANN models. Moreover, developing the ANN as plug-in in fashionable software BIM, which is also filling the gap in forecasting lightpipes' performance in BIM project. The specific objectives of this research are presented as follows.

- To conduct a comprehensive literature review of studies in the relevant field in order to gain sensible understanding of the knowledge and justify the research. It is intended to

summarise the to-date development in light pipes daylighting performance measurement and simulation. The literature search focuses particularly on the prediction of performance of light pipe systems of various designs and under different weather conditions.

- To develop an artificial neural networks model for predicting the daylighting performance of light pipes. Although the complexity in the working mechanism of light pipe makes it difficult to appraise its performance, to the aid of software Photopia, Matlab and high performance computing facility, it is possible to develop a computational model to predict the performance of light pipe especially the bended light pipe due to the non-linear relationship between transmission characteristics and performance. Importantly, the study aims to produce a valid research method, and a framework under which further development in daylighting performance modelling can be conducted in a consistent direction leading to the final solution.
- To derive the mathematical expression for the daylighting performance of lightpipes with various configurations and sky conditions. By analysing the simulated results, this research will build the analytical model relating the input and output parameters and establish the direct/explicit relationship amongst these parameters for light pipe daylighting performance. The analytical expression will be evaluated and compared against the ANN prediction model in terms of prediction accuracy.
- To implement the validated ANN prediction model in the BIM platform as a plug-in for practical applications. Designers and/or practising engineers usually have very limited knowledge in advanced modelling techniques; hence, a handy and reliable tool embedded

in an essential BIM design software such as Revit would significantly help them in their design process of utilizing light pipes.

### **1.3 Thesis structure**

This thesis is organised in six chapters. Figure 1.3 shows the workflow of this research.

Chapter 1 outlines the research in overall. Introduction of research background and research objective are proposed in this chapter. Novel methodology to solve the problem is also introduced. Moreover, the thesis structure is listed at the end of Chapter 1.

Chapter 2 presents the state-of-the-art of the application of ANNs in predicting daylighting performance, which covers solar luminance and illuminance, daylighting control scheme and energy saving strategies. Strengths by using ANNs are highlighted and evaluated. Moreover, the research gaps have been identified and discussed. Further improvement for accuracy of ANNs and its application in daylighting study are suggested.

In Chapter 3, an optical analysis software Photopia has been employed in simulating the daylighting performance of light pipes and the efficiency of each light pipe is calculated by Microsoft Excel. It is followed by using Matlab Artificial Neural Networks (ANNs) simulation for forming a forecasting model for light pipe efficiency. Additionally, data requirement and future improvements of ANNs for more accurate daylighting prediction are discussed.

Chapter 4 presents the mathematic form of prediction model for daylight performance of lightpipes. These formulas are derived by various nonlinear multiline regression by a large amount of data from Photopia simulations. The formulae can be used to determine the transmittance of lightpipes straightway by knowing the local sun position, parameters of

lightpipes and clearness factor of the sky. Meanwhile, the ANN models, which has been established in Chapter 3, is compared to the mathematic model in this chapter. The strengths and weaknesses of two type of models are compared in terms of the prediction accuracy.

Chapter 5 is to link the ANN model with BIM platform Revit by translating the results from ANN into Revit input files and automatically performing the simulation. A plug-in is developed to accurately translate the results that were predicted by ANN for lightpipe transmittance into Revit models. The subsequent simulation in Revit is automatic without any manual intervention. One main driver of this research project is to make the prediction process fast, accurate and friendly to architects and practising engineers.

Chapter 6 is the conclusions and future work. The main contributions of this research are summarized first. It is then followed by the recommended further work which includes some ideas to improve the ANN model configuration in the future and the API development in BIM system.

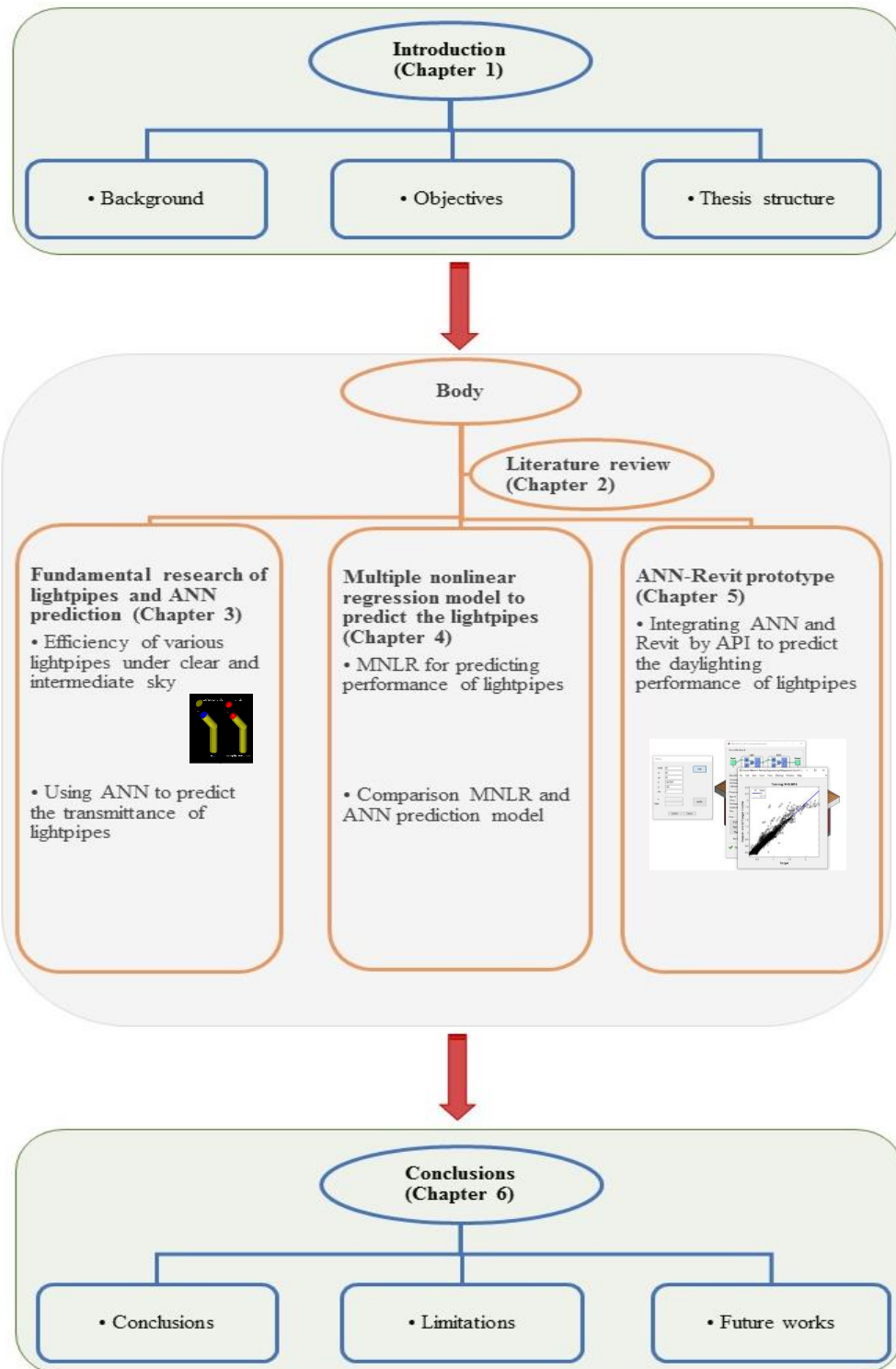


Figure 1.3 The workflow of the Thesis

**Chapter 2 A review on daylighting  
prediction by using Artificial Neural  
Network techniques**

## 2.1 Introduction

Artificial lighting consumes around 20% of global generated electricity[19]. Therefore, exploring novel techniques that could replace artificial lighting has been attracting massive interest in sustainable building designs. Daylighting has been considered as an effective sustainable technique, which has significant potentials to replace artificial lighting, leading to vast benefits to view comfort and health of occupants and hence benefits to economy and society as well. Compared to artificial lighting, daylighting can reduce the consumption of electrical energy and hence the greenhouse gas emission produced by the conventional electricity generation. Moreover, according to psychology, occupants prefer daylighting more than artificial lighting due to its vivid colour rendering to offer visual comfort and delightful environment, which promote the productivity and health of occupants [13].

The conspicuous contribution of daylighting has been confirmed in a number of literatures [6], [7], [8], [20], [21], [22], [23], [24], [25]. In terms of energy saving, Li and Tsang [6] surveyed 35 open layout office buildings in Hong Kong and found that 20-25% of electric lighting energy can be saved with appropriate fenestration and daylighting control. Moreover, McHugh et al. [26] estimated that around annual 24,000 GWh electric power could be reduced by appropriate photo controls under skylights for 5.388 billion m<sup>2</sup> of commercial floor area in the US. Other researchers revealed that the European Community annual CO<sub>2</sub> emission could be reduced by 223 million tonnes using passive solar design [20, 21]. In a cooling-dominant building, using natural lighting could significantly reduce heat dissipation caused by artificial lighting hence reduce the cooling demand [8]. Furthermore, it has been identified that occupants normally prefer varying levels of natural lighting cycle rather than constant artificial

light [7]. The benefits of psychological aspect of natural light have also been demonstrated [22], [23], [24], [25].

Sufficient and comfortable interior illuminance is the basic criteria in daylighting assessment. Successful daylighting design based on the availability of natural light and the distribution of daylight levels at work plane. Therefore, it is clear that prediction is a key stage of daylighting strategy for buildings. It is necessary to predict the amount of daylight and its distribution in the buildings in order to evaluate visual comfort without glare and energy saving. It would be ideal to forecast the daylighting performance accurately before a real daylighting design is adopted. Successful prediction could bring sufficient daylight into the interior space without any undesirable effects. In light of cost effectiveness, accurate prediction of daylighting performance can bring dramatic benefits in the cases where expensive and/or innovative technologies or systems are employed [27]. However, accurate daylighting prediction is not an easy task because there are usually a large number of underlying parameters affecting the performance of daylighting. The variables can vary from geographical location, time in a day or a year, local sky conditions and architecture geometries and features. Early work about daylighting prediction employ scale model and mathematic formulae to evaluate the daylight level. In the past decades, computer software has been widely used to simulate the daylighting performance as well. However, due to the varying and non-linear nature of daylighting parameters, the above-mentioned analysis methods considerably rely on long-time measurement or exhaustive data to evaluate the daylighting performance, which are time and labour consuming. Recently, a new and attractive method based on ANNs in predicting daylighting performance has been introduced, which has convincing advantages in solving multi-variables problems [9].

In the last two decades, ANNs have been applied in various fields of research, for example, heat transfer in nuclear engineering [11], sizing of solar photovoltaic systems [12], refrigeration, air conditioning and heat pump systems [10], modelling and control of combustion processes [13], modelling of renewable energy systems [14], chemical process control [15], thermal analysis of heat exchangers [16], forecasting [17], and application in the atmospheric sciences [18]. In the field of architecture and built environment, ANNs have been used to analysing cooling and heating in buildings, electricity usage, sub-level components operation and optimization, and parameters estimation. Compared to other methods, ANNs can provide speedy, simply and more accurate prediction. Therefore, it would be very useful to present a state-of-the-art of ANNs application in daylighting prediction. It is in this regard this paper is presented.

This paper attempts to review all the possible methods available for daylighting prediction with a special focus on the potential application of ANNs, as shown in Figure 2.1 (the dashed area is the methods presented in this article). In particular, a discussion will be made to identify potential research gaps. This paper is structurally arranged as follows: firstly, various available daylighting prediction methods are summarised and their strengths and weaknesses are discussed; secondly, ANNs predication models in luminance and illuminance, control systems and energy savings are evaluated; thirdly, research gaps are discussed; finally, the conclusions are presented.

## 2.2 Daylighting prediction methods

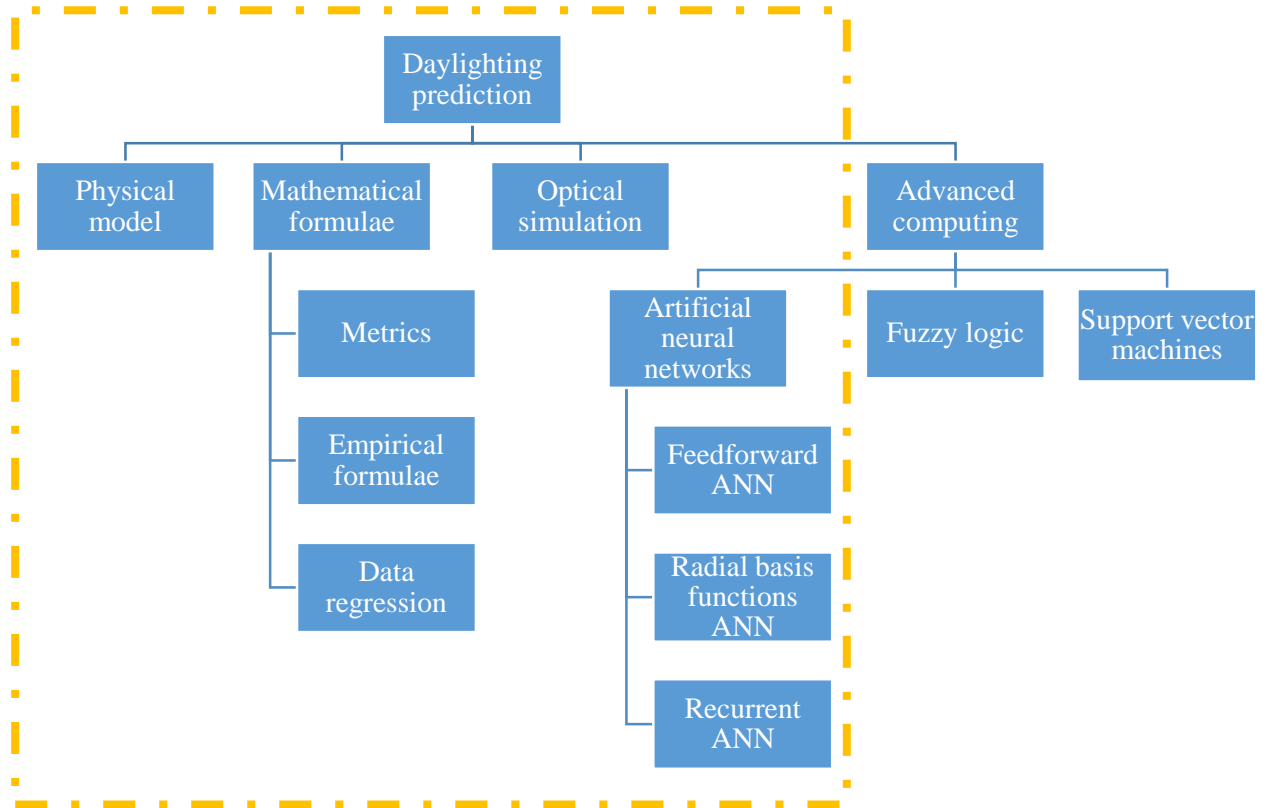


Figure 2.1 Typical methods for daylighting predictions

This section presents an overview of existing daylighting prediction methods including physical model, analytical formulae, computer simulation and ANNs, followed by discussions on the strength and weakness of each method.

### 2.2.1 Physical model

Physical model has been implemented for centuries to evaluate the illuminance quality in the interior of buildings [28]. The models are usually made of card, wood or plastics. The accuracy of evaluation highly depends on measurement position, model geometry and manufacturing details, especially the surfaces reflectance, fenestration and glazing transmittance. The

experiment is usually undertaken under the real sky conditions or Commission Internationale de L'Eclairage (CIE) artificial sky.

Littlefair [29] proposed a scale model to predict daylight level within an atrium building. It evaluated the performance of an atrium and the illuminance level of neighbouring space. Kim et al. [30] built a 1:20 scale model for measuring indoor illuminance of Seoul Art Museum installed with toplights. With the scale model, the building details, including façade, textures, furniture and inner layout or figures, can be considered. A case study has been done by Aghemo et al [31] to simulate daylight environment of a high school classroom with various shading system in Italy. By simulating different sky conditions and sun paths, the best shading scheme can be determined. Some rules should be followed in order to get accurate results [28, 29]. General regulations include using original building structure and geometry, preventing light leaking, and choosing the same material property. Further, specialized rules include using appropriate model size and scale varying from 1:500 to 1:1 based on different modelling purpose, the test sensor size and position in the model, etc. The advantage of this method is able to analyse the daylighting performance quantitatively and qualitatively at the same time. Normally, the daylight factor can be measured by photocells and visual impact could be directly presented. However, several studies have revealed that it is difficult to completely match the results from the physical models to those from the actual buildings. Further, it has been found that the daylighting performance in physical models tends to be overvalued. Therefore, using the scaled physical model alone would not be a reliable option.

### 2.2.2 Analytical formulae

The use of mathematical formulae is another useful method in predicting daylighting performance. This approach may be applied at three different levels, basic metrics, empirical formulae, data regression model.

Daylight factor (DF) is one of the most accepted and basic daylighting performance indicator, as defines below,

$$DF = \left( \frac{E_{in}}{E_{ext}} \right) \times 100\% \quad (2.1)$$

where  $E_{in}$  is the daylight illuminance at a fixed point on the work plane inside the room,  $E_{ext}$  is the outside illuminance on the horizontal plane under a CIE overcast sky or uniform sky [32]. DF is the most widely used metrics of daylighting and adopted as a design criteria in relevant industry standards and guides [33]. As the DF is defined for the overcast sky condition, it does not need to consider the building orientation and location, so it is easy to be determined analytically. However, the solar angles and redirection of sunlight are not considered in the formulation of the DF. This often causes problems if the DF metrics is used for prediction under other sky conditions rather than the overcast sky.

The DF value is generally for certain point, to estimate the average illuminance on a working plane. Littlefair [29] introduced the concept of average daylight factor ( $DF_{av}$ ) and gave an empirical formula,

$$DF_{av} = \frac{WT\theta}{A(1-R^2)} \quad (2.2)$$

where  $W$  is the glazing area ( $m^2$ ),  $T$  is the transmittance of the glazing and  $\theta$  is the angle of visible sky at the centre of the window.  $A$  is the total area of room surfaces, including roof, floor, walls and windows ( $m^2$ ).  $R$  is the average reflectance of these surfaces. Similar to Eq. (1), this formula for daylight is easy to use but it summarises the overall daylighting performance. Love and Navvab [34] proposed a new metrics as an indicator of daylighting performance, which is the vertical-to-horizontal illuminance ratio (VH ratio), that is, the ratio between the illuminance value on a vertical window and outdoors horizontal illuminance value as given by Equation 3. They found that the VH ratio is more stable than the DF under real sky conditions, so more suitable to be used to estimate the illuminance and determine the glare.

$$VH = \frac{E_V}{E_H} \quad (2.3)$$

Besides these basic formulae, advanced mathematical equations can also be extrapolated based on measurement or theoretical derivation. Kim et al. [35] used multiple linear regression method to build a mathematical model to forecast the fluctuation of external daylight illuminance. Kazanasmaz [36] used the fuzzy logic model to examine the uniformity of daylight illuminance in an office. In recent years, for advanced daylight guide and transmission systems, some mathematical models were put forward to predict the daylighting performance of a system. Su et al. [37] proposed a regression model to forecast the output lumen value of a light pipe. Moreover, both [38] and [39] explore the mathematical model to predict the transmission of light pipes.

### **2.2.3 Daylighting calculation software**

Compared to physical model and mathematical formulae, computer optical simulation combines the benefits of both illuminance calculation and interior visualization [29].

Moreover, it does not require any physical materials, which is economic, and environment friendly while significantly saves time. Computer simulation can also be much more accurate in certain cases. Radiosity and raytracing are the fundamental methods to calculate illuminance in computer simulation. Radiosity analyses simple surfaces with diffuse element method while raytracing technique deals with complex surfaces with specular reflection [40]. The common computer modelling tools could be classified into built exclusively for daylighting calculation, such as RADIANCE, LightTools, Photopia, others for lighting such as TracePro, EnergyPlus, IES, DATSIM, Ecotect, Relux and for the other purposes and daylighting is a “feature” such as Dialux, Lightsolve, ADELIN, CODYRUN, SkyCalc, Autodesk, SPOT Pro, Lightscape, RadioRay, Microstation, etc.

Those computer software packages have been used extensively in the recent years to predict daylighting performance and evaluate daylighting designs. For instance, Jovanović et al. used DAYSIM to calculate DF, daylight autonomy (DA) and useful daylight illuminance (UDI) [41]. Li et al. used RADIANCE to simulate the illuminance value in different categories of buildings [6]. Similar studies could be found in literatures [30], [42-44]. Meanwhile, numerical software is also used to guide daylighting design. Andersen et al. employed Lightsolve to simulate the annual daylighting performance, which provided an ideal and reliable design guide for daylighting design in buildings [45]. Similarly, Gagne et al. used Lightsolve Viewer (LSV) for daylighting design and set up an interactive expert system to explore geometries of daylighting and performance goal in initial design stage [46]. Kota et al. [47] integrated BIM tool in Revit with Radiance and DAYSIM to simulate the daylighting situation. Radiance was used to quantify the daylight effect throughout the various simulation stages. When the anidolic system and EC glazing configurations was confirmed, the Radiance was used to

assess the daylight factor at the workplane and room surfaces around the test room. At the same time, visual comfort especial the glare risks were evaluated.

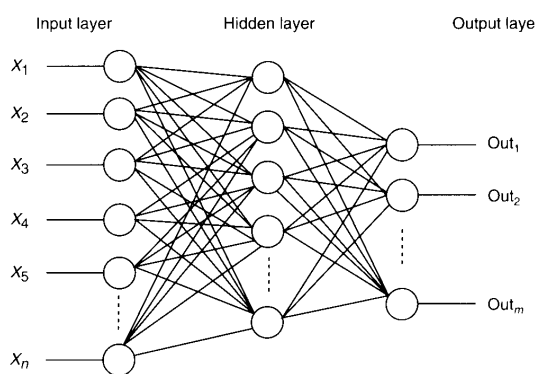
In addition, some studies integrated two or more different types of numerical tools to simulate the daylighting level and predict energy saving. It has been reported in [8], which coupled ADELINe to simulate daylighting and TRNSYS to simulate thermal condition and found that 50% to 80% artificial lighting could be reduced by daylighting which can save 40% energy cost. Chen et al. used Ecotect and RADIANCE to simulate the daylighting value and distribution [48]. Meanwhile, EnergyPlus was used to determine the potential energy saving and some studies can be found in [26], [49-53].

Moreover, simulation techniques have been intensively used in recent years in evaluation of new daylighting systems and technologies. Acosta et al. [54] employed Lightscape to simulate three different shapes of lightscoop skylights in order to choose a proper shape. Dutton et al. [39] used Photopia raytracing to predict the lightpipe transmittance. Ullah et al. [55] used LightTools and Dialux to simulate inner illuminance quality in multi-floor office buildings with installation of an innovative daylighting system which combines LED light with a highly concentrated optical fibre-based daylighting guide system. Page et al. [56] used the raytracing method in RADIANCE to simulate the visual comfort and daylight performance of an office building installed with electrochromic glazing coupled with an anidolic daylighting system. Randance was used to quantify the daylight effect throughout the various simulation stages. When the anidolic system and EC glazing configurations was confirmed, the Randance was used to assess the daylight factor at the workplane and room surfaces around the test room. At the same time, visual comfort especial the glare risks were evaluated.

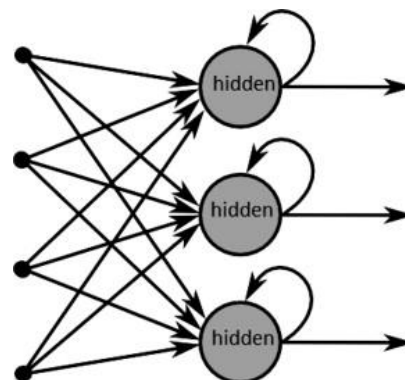
## 2.2.4 Artificial Neural Network

Different from conventional computational methods, ANNs simulation does not require building up any physical model. During the past three decades, ANNs has been used as an alternative approach to conventional prediction methods in many research areas. ANNs is a powerful tool in solving complex and non-linear problems in a number of fields by the means of simulation, identification, prediction, optimization, classification and control.

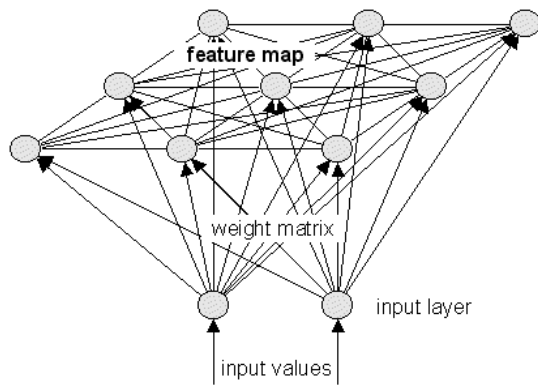
The ANNs simulation is a self-learning and self-training platform or programme. According to different network structures, ANNs models can be classified into 4 categories: Feedforward Neural Network, Feedback Neural Network, Self-organizing Map and Random Neural Network (as shown in **Figure 2.2**). Most of categories are straightforward applications of optimization theory and statistical estimation [57]. ANNs can model multi-variable problems while extracting the non-linear complex relationships between the variables by means of training data. In the meantime, the performance of ANNs could be evaluated by some routine statistics indexes as shown in **Table 2.1**, which represent the accuracy of forecasting. These indexes would be used in section 3 to evaluate the ANN prediction ability.



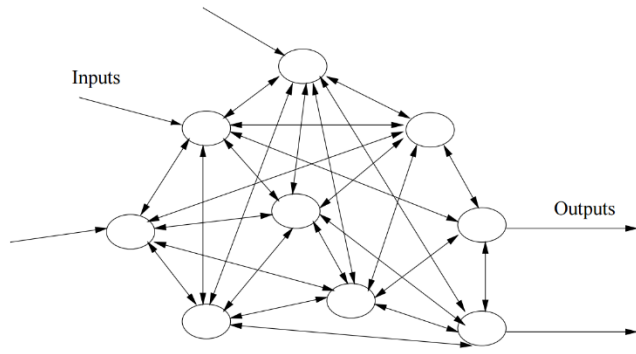
Feedforward Neural Network



Feedback Neural Network



Self-organizing Map



Random neural network

Figure 2.2 Four categories of ANNs models [58].

Table 2.1 Statistics indexes to evaluate ANNs' prediction accuracy [59].

Criteria	Abbreviation	Accuracy preference
Mean Absolute Error	MAE	value $\leq 10\%$ , High
Mean Absolute Percentage Error	MAPE	$10\% \leq \text{value} \leq 20\%$ , Good
Mean Squared Error	MSE	$20\% \leq \text{value} \leq 50\%$ , Reasonable
Root Mean Square Error	RMSE	value $\geq 50\%$ , Inaccurate
Mean Bias Difference	MBD	
Normalised Mean Bias Error	NMBE	
Coefficient of Variation of the RMSE	CVRMSE	
Correlation Coefficient	R	The closer to 1, the more accurate
Squared Correlation Coefficient	R <sup>2</sup>	
Nash-Sutcliffe Efficiency Coefficient	NSEC	

Due to different strengths and requirements, different networks could be used in various fields. Almost all relevant researches in literature used the backpropagation (BP) neural network and its variants, which belongs to feedforward neural network category. BP neural network model is illustrated in Figure 2.3. It is one of the widest applications of ANNs and it is quite convenient and accurate. In fact, it is hard to determine the fastest training algorithm for a given problem. Instead, the most suitable one is always determined by the method of trials and errors. The BP neural network is normally composed of three components [60]. These parts usually consist of one input layer, some hidden layers and one output layer, as shown in Figure 3. Within each layer, there are a certain number of neurons. The procedure for developing an ANNs model includes 3 phases including modelling, training and validating. First, modelling involves analysing data, identifying input parameters and selecting network architecture and internal rules. The prepared data can then be trained, for example, by using BP learning algorithm to establish a model. After the training of data and the establishment of the model, it should be validated before application.

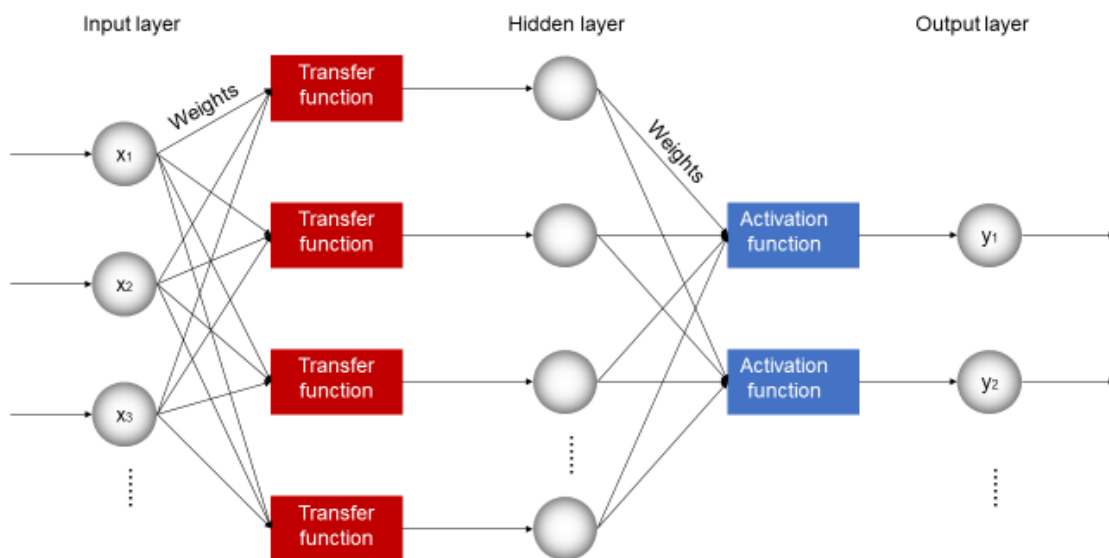


Figure 2.3 The typical sample of multilayer feedforward neural networks [61]

BP algorithm is a gradient descent method. The principle is that they are processing elements (PEs) and each connection of them has an associate weight. Each time it reduces the total error by changing the weights along its gradient to improve the performance of the network [61]. The process of an ANNs simulation starts with weighted summation activation of the neuron through its incoming connections; it is then followed by passing through an activation function and this activated value is the output of the neuron [14]. Specifically, training BP model should assign random values to the weight terms ( $w_{ij}$ ) in all nodes initially. For the output layer for the case of the logistic-sigmoid activation (as shown in Figure 2.4), the error can be computed as follows:

$$\delta_{pi} = (t_{pi} - \alpha_{pi})\alpha_{pi} (1 - \alpha_{pi}) \quad (2.4)$$

For a node in a hidden layer:

$$\delta_{pi} = \alpha_{pi} (1 - \alpha_{pi}) \sum_k \delta_{pk} w_{kj} \quad (2.5)$$

where the subscript  $k$  is a summation over all nodes in the direction of the output layer. The subscript  $j$  is the weight position in each node. Moreover,  $\delta$  and  $\alpha$  for each node are used to calculate an incremental change to each weight via:

$$\Delta w_{ij} = \varepsilon(\delta_{pi}\alpha_{pj}) + mw_{ij}(\text{old}) \quad (2.6)$$

where  $\varepsilon$  is the learning rate which determines the size of the weight adjustments during each training iteration and  $m$  is the momentum factor which is applied to the weight change used in the previous training iteration. The values of  $\varepsilon$  and  $m$  are determined prior to the training cycle and controls the speed and stability of the simulation [13].

In light of non-linear problems, the sigmoid function is the most common logical transfer function in BP algorithm. It includes tansig and logsig algorithms (sometimes purelin algorithm is also used as the transfer function, but it is linear function which is less commonly used) [62]. They are both an “S” shaped transfer function, logsig ranging from 0 to 1 and tansig ranging from -1 to 1, which can be expressed in Figure 2.4.

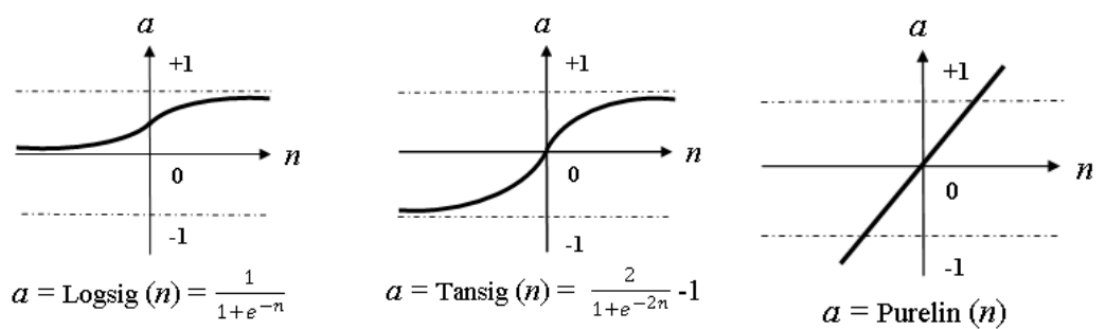


Figure 2.4 Transfer function used in the neural network [62]

Normally, 70% to 90% of dataset is used in training the model and the remaining dataset is used to test and validate the model. Relevant application of ANNs predictions in daylighting would be elaborated in the following section. The summary of daylighting prediction methods is presented in Table 2.2.

Table 2.2 Summary of typical methods for daylighting prediction

Methods	Tools	Strengths	Shortcomings
Physical model [28-31, 63-66]	Card, wood, plastic etc.	<ul style="list-style-type: none"> <li>- The daylighting performance is physically visible;</li> <li>- Building geometrical and façade details could easily be formed;</li> <li>- Cheaper and easier for many people to use;</li> <li>- Easier to make and handle.</li> </ul>	<ul style="list-style-type: none"> <li>- Too many rules needed;</li> <li>- Overestimate daylighting performance;</li> <li>- Material and labour cost;</li> <li>-Time consuming</li> </ul>
Analytical formula [29, 32, 34-39, 67, 68]	<p>E. g. <math>DF = \left(\frac{E_{in}}{E_{ext}}\right) \times 100\%</math>;</p> $DF_{av} = \frac{WT\theta}{A(1-R^2)}; \quad VH = \frac{E_V}{E_H}$	<ul style="list-style-type: none"> <li>- Quickly estimate the daylighting performance;</li> <li>- No cost in materials;</li> <li>- Easier and quick to operate for designers.</li> </ul>	The accuracy is low, so the results always need to be corrected.
Computer simulation [6, 8, 26, 29, 30, 36, 39-56, 69]	RADIANCE, LightTools, Photopia, TracePro, EnergyPlus, IES, DAYSIM, Ecotect, Relux, Dialux, Lightsolve, ADELIN, CODYRUN, SkyCalc, Autodesk, SPOT Pro, Lightscape, RadioRay, Microstation, etc.	<ul style="list-style-type: none"> <li>- Cost effective;</li> <li>- Complex analysis;</li> <li>- Deal with a huge number of variables</li> </ul>	<ul style="list-style-type: none"> <li>- Designers need to have strong background;</li> <li>- Time consuming to build models and simulations with variable parameters;</li> <li>- Computationally expensive</li> </ul>
ANNs	Refer to following Section 3		

## **2.3 Application of Artificial Neural Networks Techniques in Daylighting**

### **Prediction**

In this section, the techniques and applications of ANNs as a prediction tool in daylighting are critically discussed. It mainly covers luminance and illuminance forecasting, daylighting performance combined with energy saving scheme and control system.

#### **2.3.1 Luminance and Illuminance Prediction**

##### **2.3.1.1. External luminance prediction**

Before designing a daylight dominating building, surveying the daylighting environment to estimate whether enough daylight could be utilized is prime. Janjai et al. have demonstrated that ANNs presented outstanding prediction performance compared with CIE models; meanwhile this study filled the gap with no research employing ANN to predict sky luminance in tropics [70]. They chose two cities Nakhon Pathom and Songkhla in Thailand as the measurement locations to obtain the 3-year period (2007-2009) of sky luminance data by utilising EKO sky scanners in monitoring stations. These data according to CIE classification was intentionally selected and grouped into clear, partly cloudy and overcast skies weathers. The study was divided into three stages: first stage, 2007-2008 data from Nakhon Pathom was used to train a new ANN model; second stage, 2009 data of Nakhon Pathom was used to test ANN model and CIE model; finally, data from Songkhla was used to validate the performance of ANN and CIE model.

In their ANN modelling, the input parameters include the zenith angle of the sun ( $Z_s$ ), the zenith angle of the sky element ( $Z$ ) and the angular distance between sun and sky element ( $\chi$ ), as shown in Figure 2.5, and the sky luminance ( $L$ ) is the only output. A multi-layer with BP

algorithm was used to train the model. RMSE and MBD were chosen to evaluate the deviation between ANNs model and CIE model. The performance values of the ANNs and CIE model are listed in Table 2.3. It has been proved that the ANNs model performed more accurate analysis than conventional CIE model. In Songkhla, for the case of overcast (CIE 4), the ANN model presented stronger prediction power with RMSE 17.4% and MBD 1.7% compared with CIE 31.8% and -7.3% respectively. Moreover, for clear sky (CIE 13), the RMSE and MBD of ANN model were 31.0% and 3.3% respectively while these for CIE were 37.9% and 3.3%. In terms of partly cloudy (CIE 7, 8, 10) sky, ANN model presented slightly better than CIE model in forecasting sky luminance.

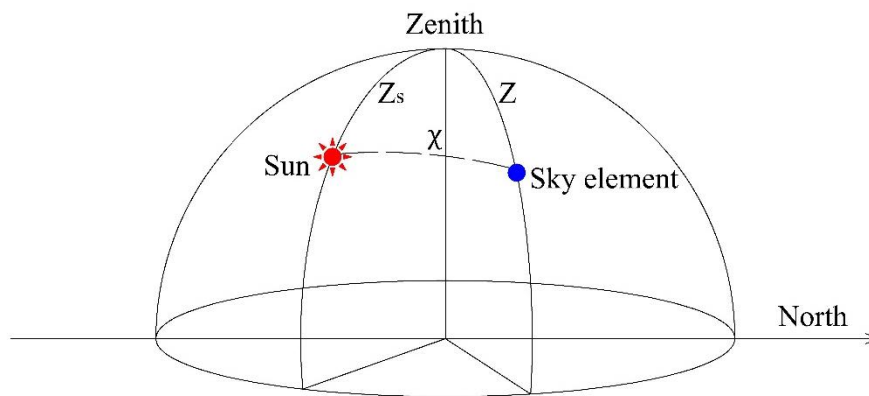


Figure 2.5 Diagram to explain various zenith angles and the angular distance

The prediction model of sky luminance, which only considers the solar position but neglects other effects, could cause the deviation of results. Hence, it would be important and versatile to measure the global radiation and develop a “non-local” model to survey the external illuminance. However, because of atmospheric variables, especially turbidity and water vapour, it is difficult to derive a common model, which could possibly consider all affecting components by conventional methods to determine the solar luminous efficacy. López and Gueymard developed a creative ANNs model to predict solar luminous efficacy components

under clear sky conditions [71]. In order to determinate the simplest input variables and optimized network architecture, but still keep high prediction accuracy of the model, they tried different combinations of 4 parameters, i.e., solar zenith angle ( $\theta_z$ ), perceptible water ( $w_p$ ), diffuse fraction ( $\kappa$ ) and direct transmittance ( $\kappa_b$ ) to obtain direct ( $K_b$ ), diffuse ( $K_d$ ) and global ( $K_g$ ) component of luminous efficacy as the output objectives at the same time. They also tried different network architecture by means of changing the number of neurons in hidden layers (Figure 2.6).

Table 2.3 The performance of ANN and CIE model for predicting the sky luminance between predicted and measured data in Nakhon Pathom and Songkhla [70].

CIE	Nakhon Pathom				Songkhla			
	RMSE (%)		MBD (%)		RMSE (%)		MBD (%)	
	ANN	CIE	ANN	CIE	ANN	CIE	ANN	CIE
Overcast								
CIE 4	17.4	31.8	1.7	-7.3	17.1	39.6	6.7	0.7
Partly cloudy								
CIE 7	41.9	39.7	-4.3	-5.2	36.3	29.5	4.2	1.7
CIE 8	46.3	49.8	-12.4	-12.3	42.2	40.2	-7.1	-6.8
CIE 10	41.2	47.9	2.5	-0.3	35.9	46.7	6.6	2.6
Clear sky								
CIE 13	31.0	37.9	3.3	-7.2	47.7	56.4	-1.3	-9.2

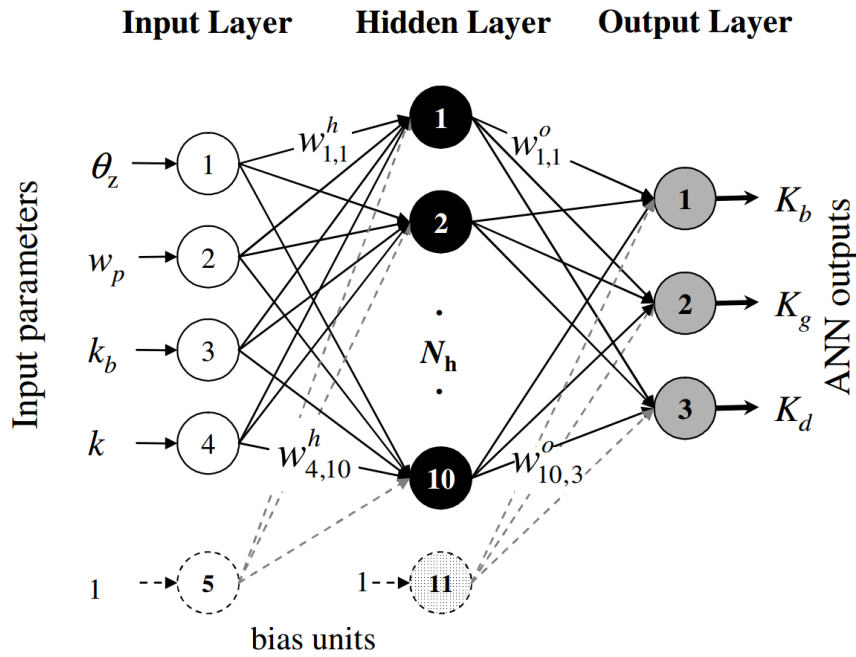


Figure 2.6 ANN model architecture[71]

As shown in Table 2.4, RMSE was used to evaluate the accuracy of the developed ANNs model. All the results showed that RMSE were around 9%, which demonstrated high prediction power. The research found that ANN models could also be used to test the sensibility of each input variable and perceptible water was the important influencing variable. Another interesting finding was whatever the removal of the solar zenith angle did not change the accuracy of prediction. However, removing this parameter means more account number hidden neurons are needed, which can make the model more complex. The study also investigated the impacts of different hidden neurons on the accuracy of the ANNs model. Although 13 hidden neurons slightly improved the prediction power of the ANNs model, it was far too complex and time consuming. Ten neurons were recommended as the proper model architecture for that problem, which has made the error lower than the experimental errors.

Table 2.4 The RMSE (%) of each ANN configurations [71]

$N_h$	Inputs								
	$\{\theta_z, w_p, \kappa_b, \kappa\}$			$\{\theta_z, \kappa_b, \kappa\}$			$\{w_p, \kappa_b, \kappa\}$		
	Outputs								
	$K_b$	$K_d$	$K_g$	$K_b$	$K_d$	$K_g$	$K_b$	$K_d$	$K_g$
22	1.4	1.8	1.6	6.4	3.9	4.8	2.0	2.9	2.9
17	1.7	1.9	1.7	6.8	4.0	4.9	2.1	3.0	2.9
13	2.0	2.1	1.8	6.9	4.4	5.2	2.4	3.1	3.0
10	2.1	2.5	2.4	7.4	5.0	6.0	2.7	3.4	3.4
7	3.4	3.1	2.6	7.8	5.0	5.9	3.7	3.7	3.5
5	4.6	4.5	4.1	7.9	5.9	6.3	4.7	4.5	4.1
3	7.4	5.0	5.3	9.2	6.5	6.8	7.6	5.0	5.3

\*  $N_h$  is the number of hidden neurons in hidden layer.

Similarly, in order to determine natural illumination, Tíba et al. [72] tried to calculate the hourly external luminous efficiency through the solar irradiation available. Illuminance measurement is not included in routine meteorological test in Brazil. Because of the lack of these information, an empirical formula was derived by Perez et al. [73] to determine the luminous efficiency. This formula created a relationship between illumination and solar irradiation combined with some other meteorological data. Subsequently, in order to develop a model, which could use the global irradiation and routine measured data from meteorological station as input variables, ANN was chosen as the tool to predict the solar luminous efficiency. They chose dew point temperature, rain precipitation, darkness of sky, clearness index of Perez

and index of transmittance as the input parameters and only export the hourly luminous efficiency as the output result. A multilayer perceptron (MLP) ANN was chosen to run the simulation (Figure 2.7). The results were used to compare with Perez model and Robledo model (Perez local calibrated model). Two cities of Recife and Pesqueira were chosen to test the accuracy of ANNs model and the Perez and Robledo model. The compared results were evaluated by the MBD and RMSE which were both lower than 5% as shown in Table 2.5.

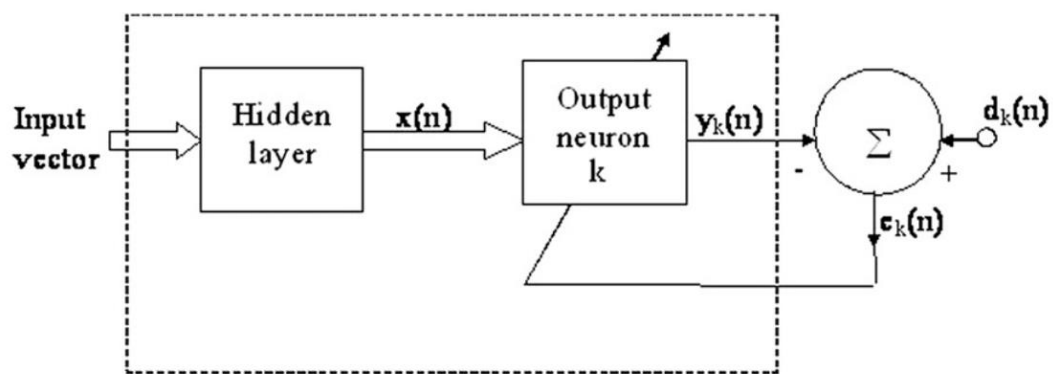


Figure 2.7 A diagram of MLP ANN model, which has been trained by supervised apprenticeship [72].

Table 2.5 Performance of Perez, ANN, Robledo model [72]

Location	RMSE (%)			MBD (%)		
	Perez	ANN	Robledo	Perez	ANN	Robledo
Pesqueira	3.7	3.6	7.2	-0.2	4.1	0.7
Recife	8.5	5.8	5.3	1.3	5.7	0.2

Pattanasethanon et al. [74] compared the performance of an empirical sine model, a novel sine model and an ANN model to forecast the horizontal plane solar illuminance of all sky types at Mahasarakham in Thailand. Frequently used BP algorithm was used to training the ANN

model. One-year data of solar altitude angle and the clearness index ( $\epsilon$ )/sky ratio (SR) were chosen as the input data while global illuminance, global irradiance and diffuse irradiance on horizontal plane are the output targets. The RMSE, MBD and  $R^2$  were used to evaluate the forecast ability simultaneously. Subsequently, the next half year data was used to test the ANN model. The prediction power was summarised in Table 2.6.

Table 2.6 Summary of prediction power of Sine, Novel sine and ANN model to illuminance[74]

Sky condition	Model	Global illuminance			Global irradiance			Diffuse irradiance		
	(%)	Sine	Novel sine	ANN	Sine	Novel sine	ANN	Sine	Novel sine	ANN
SR	MBD	11.6	10.8	0.08	12.8	12.5	3.00	12.2	12.7	7.64
	RMSE	12.5	14.8	10.8	19.3	23.3	15.93	15.5	19.9	8.78
	$R^2$	0.96	0.95	0.98	0.91	0.89	0.92	0.96	0.95	0.98
$\epsilon$	MBD	3.8	4.5	3.7	3.93	4.50	3.79	4.46	5.50	4.33
	RMSE	4.5	11.8	3.8	15.7	19.5	14.52	16	20.4	9.08
	$R^2$	0.96	0.95	0.98	0.92	0.91	0.93	0.96	0.95	0.98

### 2.3.1.2. Internal illuminance prediction

The ultimate goal of predicting external solar illuminance availability is to evaluate if there is enough daylight in interior space and the appropriate daylighting scheme to be used. Navada et al. [75] developed 2 ANN models to predict the external and internal illuminance respectively. There were two different approaches demonstrated in this study. One is

developing the ANN prediction model by using measured interior illuminance data which is similar to most other researches; and the other is utilizing Perez model [73] to convert obtained meteorological data to interior illuminance and then establishing the ANNs model. In Navada's model, a top floor room with dimension of 3.75 m × 3.75 m × 2.35 m and two blinded windows was built (Figure 2.8). The internal illuminance was measured at different blind positions at 0.8 m above the floor. The time series was from 9 am to 5 pm and the blind position changed from 0° to 90° (blind closed) with the increment of 15°. BP algorithm was employed as the learning algorithm. Two input variables were P (blind position) and T (times), while illuminance was the only output. The error of ANN prediction was always below 5%, which means ANN is a strong prediction tool. In the other meteorological method, 2009-2011 hourly solar irradiance from National Renewable Energy Laboratory (NREL) was converted to the outside illuminance by Perez model. Subsequently, according to the known luminance distribution and DF definition (i.e., Equation 1), the interior illuminance was calculated. The next will be the same to the first method, which used 2009-2010 data for training and 2011 data for validation of the ANNs model. The correlation coefficient R was around 0.97 for the ANNs prediction, which is generally good. Moreover, this study compared the performance of various prediction models, which is in order to obtain the most accurate results. The compared results are shown in Table 2.7.

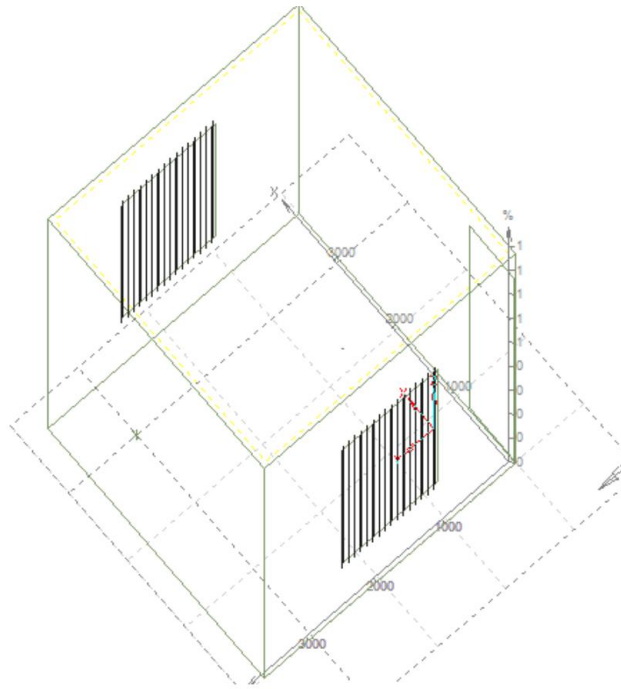


Figure 2.8 The sketch model of simulation room[75]

Table 2.7 Compared results of various prediction methods [75]

Time	% Error				
	Forecast method	Time series prediction	Nero predictor	excel	Matlab code
09:00	24.81	-0.70	0.43	2.15	2.54
09:30	34.86	-0.98	2.68	20.42	2.05
10:00	36.14	-4.03	-0.15	-1.05	-0.93
10:30	-28.43	-1.68	3.31	2.80	-4.98
11:00	-50.32	-6.34	5.91	3.77	1.89
11:30	-69.24	-6.28	3.58	3.68	5.24
12:00	-82.10	-7.46	-0.11	1.83	1.97

12:30	-90.28	-9.02	-2.73	1.06	-0.94
13:00	-86.47	0.07	1.98	3.53	4.23
13:30	-84.71	-3.70	0.26	0.29	1.89
14:00	-75.87	-2.07	2.94	2.18	3.71
14:30	-58.32	-2.05	5.20	2.99	1.13
15:00	-44.41	-1.93	5.47	3.57	-2.21
15:30	42.21	-4.57	-0.67	1.81	-0.19
16:00	42.20	-4.48	-0.28	0.15	-0.01
16:30	50.43	-0.14	4.84	4.45	7.37
17:00	-9.18	-4.04	-2.26	0.56	-1.04

Kazanasmaz et al. [40] developed a more detailed model. This model considered comprehensive parameters, which may affect the illuminance level inside office buildings. The building was located in the Faculty of Architecture of the Izmir Institute of Technology in Izmir, Turkey. It is a 2-story building and both the ground floor and first floor were surveyed in this research. PeakTech lightmeter was used to measure the illuminance value of every point, which 0.5 m away from the boundary and 0.7 m high from the floor. The ANNs model consisted of three layers with 13 input and 1 output variables. Three categories data were chosen as input variables: 6 building parameters (orientation, geometry, windows amount, distance to windows, floor character, sensors' position), 2 time variables (date, hour) and 5 weather variables (solar radiation, UV index, UV dose, temperature, humidity) (Figure 2.9). The only one output was again the illuminance. In the simulation, 80% of the input data was used to train the model and 20% was used to validate. BP was still utilised as the learning algorithm. The innovation of this model was the use of the Excel spreadsheet. defined by

Hegazy and Ayed [76] to optimize the weights in the ANNs structure. It presented the template of the hidden layer in the ANNs model. The model first set 5 or 6 neurons in hidden layers, which resulted in errors of 35.87% and 20.62% respectively. The number of neurons was then increased to 7, 8, 9 and 11 whilst it was found all had 2.20% error. Hence, 7 neurons were the chosen as the best number for the network construction. The forecasting precision is around 98%, which is quite satisfactory. For the sake of simplifying the model, sensitivity analysis was then carried out to identify the most sensible input parameters. It was found that hour, windows' number, orientation and measurement point were the most sensible parameters whilst room geometry, temperature and UV were not. However, neglecting the less sensible parameters would not be a wise decision since it could reduce the accuracy of the ANNs model.

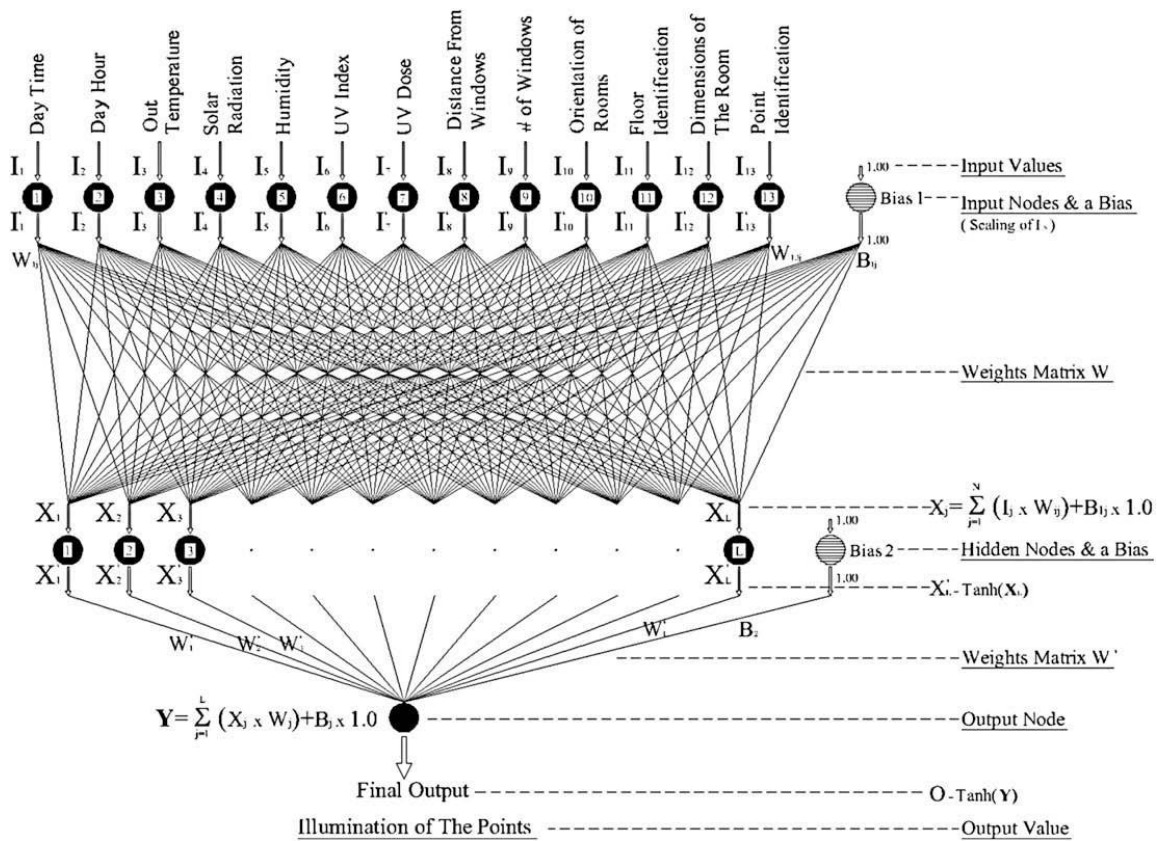


Figure 2.9 A graphic of the best performance ANN architecture [40]

### **2.3.2 Prediction of energy saving due to daylighting**

One of the criteria to assess the daylighting design is based on how much energy could be saved. Fonseca et al. [77] compared ANNs modelling and multivariate linear regression (MLR) in predicting energy saving by employing daylighting. The office simulated was located in Florianopolis climate in Brazil. The data was from 216 parameter groups in 3 types with different room depth (Figure 2.10). Cross-validation (Figure 2.11) was used to train and validate the ANN model due to limited data. The data was simulated by EnergyPlus (energy) and Daysim/RADIANCE (lighting). The ANN network architecture here adopted 6 input variables, 1 hidden layer with 10 nodes and 1 output variable structure. The 6 input parameters include quantitative variables (room depth, room orientation, solar heat gain coefficient, and window-to-wall ratio) and qualitative variables (vertical and horizontal shading coefficient). 90% of parameter groups to train the ANNs model while the rest 10% were for validation. Multifold cross-validation presents an excellent performance to solve the issue of limited data sets. From the comparison of their coefficients of determination, that is,  $R^2 = 0.9867$  for ANN and 0.8028 for MLR, it is clear that ANN can provide much more accurate prediction of daylighting energy saving.

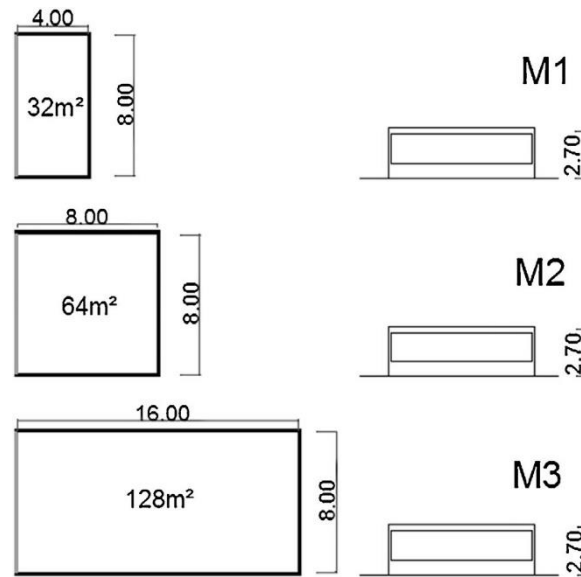


Figure 2.10 Scheme of geometries of test room [77]

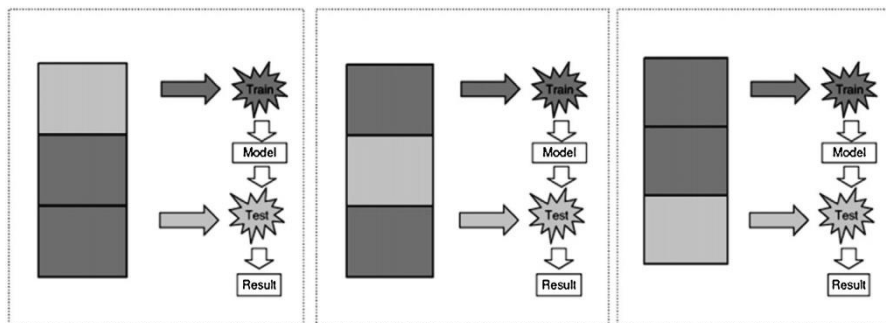


Figure 2.11 A sample diagram of cross-validation method [77]

Electric lighting consumes about 20%~30% of office building electricity [78]. Proper lighting design with utilization of daylighting can directly reduce the lighting energy consumption and also indirectly reduce air conditioning energy consumption which would be used to neutralize the heat released by artificial lighting. Wong et al. [79] used ANNs modelling to develop the daylighting design for an office building in subtropical zone. The daily electricity consumption for cooling, heating, artificial lighting, etc. was the output of the ANNs model (Figure 2.12). In this study, EnergyPlus simulations were first run followed by ANNs modelling – 70% and 30% of the data obtained from EnergyPlus was used to train and validate the ANNs model, respectively. Different from other researches, a commercial software named NeuroShell 2 was

chosen as the prediction tool. A new coefficient Nash-Sutcliffe efficiency coefficient (NSEC) which can be expressed as in Equation 2.7, which is similar to the  $R^2$  and was adopted to access the accuracy of the model.

$$\text{NSEC} = 1 - \frac{\sum_{i=1}^n (x_i - y_i)^2}{\sum_{i=1}^n (x_i - \bar{y}_i)^2} \quad (2.7)$$

where  $x_i$  is the daily electricity consumption obtained in ANNs,  $y_i$  and  $\bar{y}_i$  are the daily electricity consumption and the mean electricity consumption respectively simulated in EnergyPlus,  $n$  is the total number of data used in ANNs training and testing. NSEC was introduced to evaluate the model performance, which were 0.994, 0.940, 0.993 and 0.996 respectively. Logistic sigmoid was chosen as the active function. 3 groups of random input data generated by using Monte Carlo methods were employed to assess the accuracy of ANNs model. Statistical analysis involved MBD, RMSE, NMBE and CVRMSE. It was concluded that ANNs could well describe the non-linear relationship between input and output variables; it is especially useful at mass end use situations (e.g., cooling in summer and heating in winter). Moreover, ANNs model can optimize design parameters without carrying out experiments and avoid considerable time consuming. In order to get the relative minimum consumption of the total electricity, different combinations of input parameters were put into the ANNs model to predict the total electricity consumption value. The minimum energy consumption value can be obtained from the ANNs model in a mesh graphic (Figure 2.13) and the corresponding best input parameters for best design can also be determined.

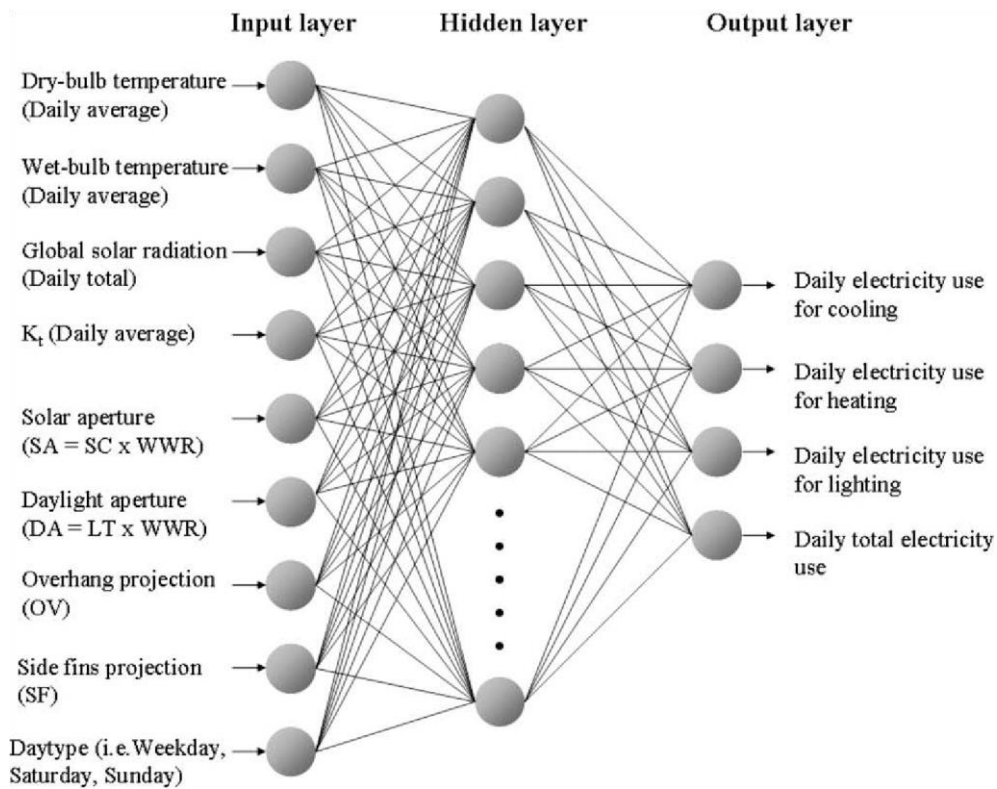


Figure 2.12 The multi-layer perceptron (MLP) ANN structure [79]

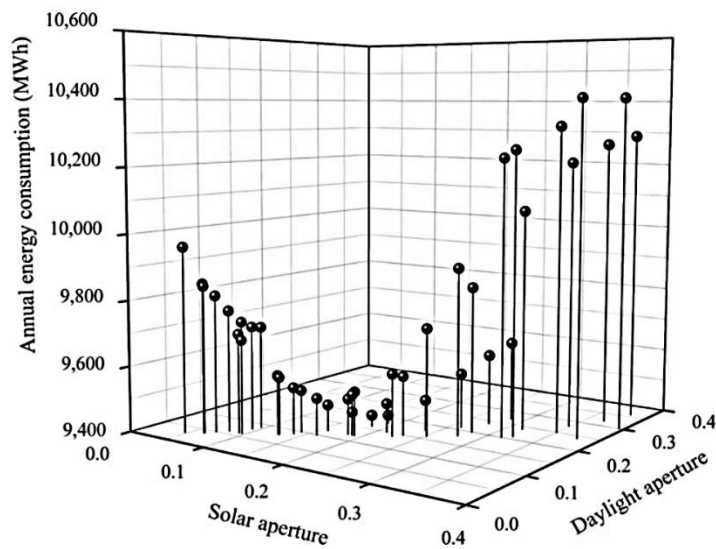


Figure 2.13 A demonstration of optimization using ANN model to determine proper design parameters in application [79]

According to [80], if daylighting and HVAC (heating, ventilating and air conditioning) system are separately considered, it often causes conflicts between energy efficiency and

environmental comfort. Hence, to set up an integrated control process, which could simultaneously satisfy all requirements as mentioned above, is essential. Due to the complex geometrical conditions and complex operations, ANNs would be an ideal option. Daylighting integrated with HVAC system is a nonlinear problem. The integrated daylighting and HVAC (IDHAVC) model (as shown in Figure 2.14) was set by Kim et al. [81] to predict the building energy performance. It was an integrated meta-model (Figure 2.15), which included regression models (indoor artificial illuminance model, lighting energy consumption model) and ANN models (temperature, indoor daylighting illuminance, total energy consumption). The building was located in Seoul, Korea and ANN were trained with data generated from EnergyPlus for three months. The ANNs model consisted of 4 variables for indoor daylighting illuminance and 11 variables for temperature and total energy consumption respectively. Levenberg-Marquardt (LM) algorithm was adopted to train the ANNs model. The number of hidden layers were fixed at three and the neurons in each hidden layers were optimized by Genetic Algorithm (GA). 70% of the data generated by EnergyPlus were used to train the model, 15% were used to test and the rest 15% for validation to avoid overfitting. The prediction accuracy is measured through  $R^2$  which is bigger than 0.98. This optimization model was achieved via minimizing energy consumption but still keeping the same thermal and visual comforts of occupants. It was shown that 13.7% energy could be saved compared with original model.

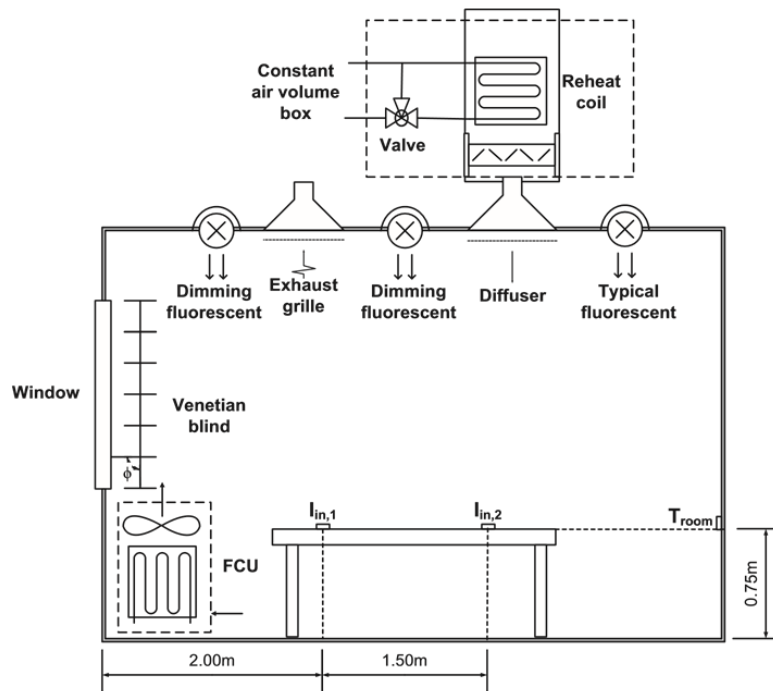


Figure 2.14 The schematic of the IDHVAC system [81]

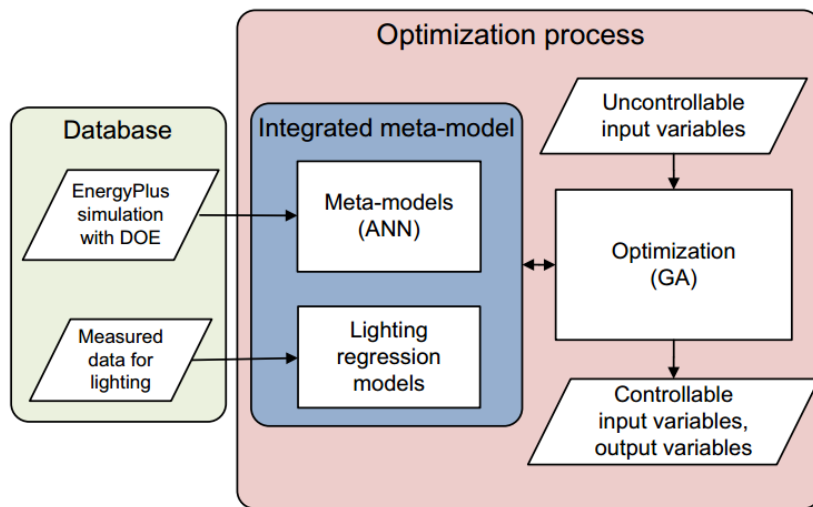


Figure 2.15 Flow chart of the IDHVAC system optimization [81]

### 2.3.3 Daylighting Controls

Excessive daylighting could cause overheating problem in buildings, which increases the consumption of cooling energy. It is essential, in daylighting design, to estimate the daylighting control system to avoid unwanted sun light and thermal discomfort. According to

different strategies for the control of lighting systems, daylight-linked lighting controls can be divided into daylight-linked switching and daylight-linked dimming [82]. Daylight-linked switching can control the light by switching between ‘On’ and ‘Off’ states based on available daylight. There may also be multi-level switching. For instance, based on the level of available daylight in a particular control zone, 33%, 50%, and 66% of light in the zone may be switched off. Dimming system controls the lamp outputs continuously using dimmable electronic ballasts. Dimming requires dimmable ballasts to maintain the illuminance level of the lamps, so it is more expensive than switching system. However, integrating energy efficient lamps with lighting control can significantly reduce electrical energy consumption[83] and also improve vision efficiency [84]. Adding lighting control system is widely common strategies in retrofitting project of lighting. Based on simulation studies, which predict the effect of retrofitting investment save the unexpected money and time. However, traditional simulations need a large number of data and a lot of time. ANN as a surrogate model was developed by Hu et al. to simulate lighting retrofitting in a building located in Chicago [85]. It successfully solves the issue of time wasting and uncertainty retrofitting parameters. This model could predict the lighting and HVAC energy consumption under different combinations of lamp types, control strategies, weather conditions and occupants’ pattern. This created model could save a large number of repeating modelling runs. Surrogate modelling (SUMO) toolbox was firstly introduced into ANNs modelling. Weather condition, LED wattage and occupancy level and control strategies were all considered as input parameters in the modelling. The results of the ANNs modelling showed a reliable relationship between the input building parameters and the output lighting energy consumption. Meanwhile, it has shown that the minimum lighting electricity energy consumption could be achieved by using occupancy plus daylighting control replacing existing manual control and change the T12 lamp to LED lamp. Another advantage

of this model is the HVAC energy consumption could be obtained at the same time, which has 98% precision and considerably saves time.

Venetian blinds is another form of daylighting control, which can significantly control direct solar radiation and glare as well as overheating. Based on ANNs modelling, an illuminance-based slat angle selection (ISAS) model was developed to predict the optimum slat angles of split blinds to achieve the required illuminance [86]. The input variables were the horizontal illuminance and the sun angle while the output was the illuminance level at a sensor point. The automated split-controlled blinds divided the whole blinds into three equal parts from the top to the bottom (Figure 2.16). EnergyPlus was employed to simulate the working plane illuminance at the sensors' positions in an office located in Gainesville, Florida, USA. The illuminance data obtained from the EnergyPlus simulation, combined with weather parameters, were used to train the ANNs model which was subsequently validated. Once the ANNs model was established, the illuminance predicted by the ANNs model was employed to optimise the slats angle and to find the optimum value. Similar to most other researches, a multi-layer feedforward ANNs model with BP learning algorithm was derived. Illuminance at sensor points located at 3 positions of the blind, i.e., top, middle and bottom, were predicted. It was shown that the model prediction performance in terms of comparison between the prediction illuminance and measured value could reach 94.7%, this demonstrated high accuracy in forecasting illuminance level in sensor point. Then the illuminance forecasted by ANNs were input to a mathematical model to optimize the slat angles of blind to achieve the aim of daylighting control (the process is shown in Figure 2.17). Another advantage of ANNs model is that it could solve the real-time blind control problems. Since the external illuminance data could directly feed in the ANN model and determine the optimum slat angle of blinds, this

really solves the difficulties in controlling the daylight in real conditions as a result of the dynamical change nature of solar irradiation.

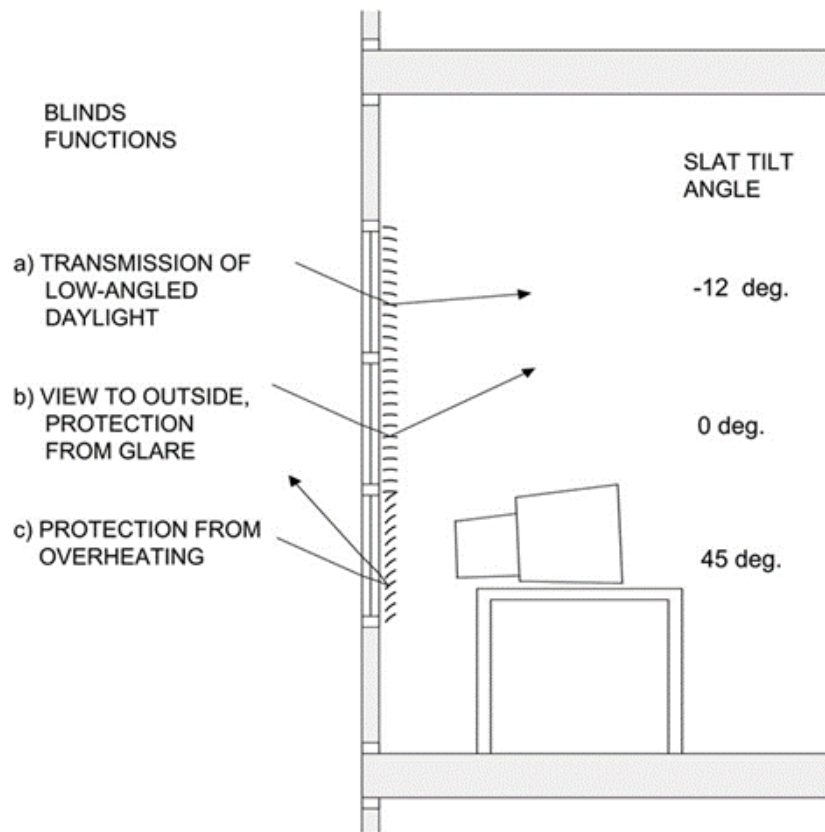


Figure 2.16 The diagram of automated split-controlled blinds [86]

Almost all articles in daylighting prediction by ANNs modeling are searched and reviewed. A summary of ANNs application in predicting daylighting with detailed input and output parameters is presented in Table 2.8. Back Propagation (BP) is the most common training method for an ANN model. It could be applied in almost multilayer non-linear problems and perform consider satisfactory results.

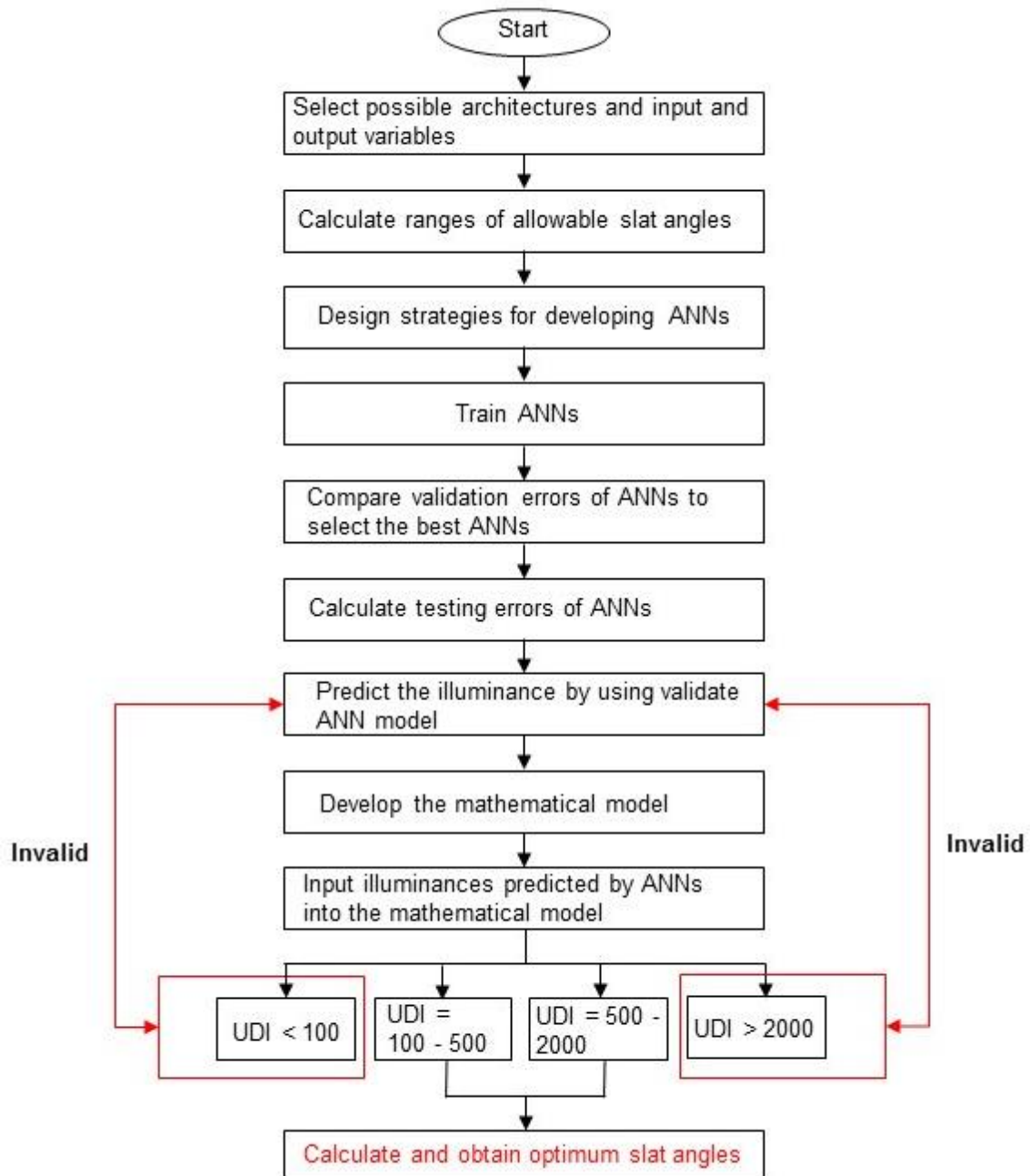


Figure 2.17 The flow chart of ANNs application in daylighting control of blind [86]

\* The UDI is the abbreviation of useful daylight illuminance and its unit is lux.

Table 2.8 Summary of ANN applied to predict daylighting in literatures

Literatures	ANNs models	Input variables	Output variables	Accuracy
<i>External luminance prediction</i>				
Janjai et al. [70]	BP	<ul style="list-style-type: none"> <li>- Solar zenith angle;</li> <li>- Zenith angle of the sky element;</li> <li>- Angular distance between the sky element and the sun</li> </ul>	Sky luminance	Table 3 ANN models better than CIE models
López et al. [71]	BP	<ul style="list-style-type: none"> <li>- Solar zenith angle;</li> <li>- Perceptible water;</li> <li>- Diffuse fraction;</li> <li>- Direct transmittance</li> </ul>	<ul style="list-style-type: none"> <li>- Direct component of luminous efficacy;</li> <li>- Diffuse component of luminous efficacy;</li> <li>- Global component of luminous efficacy</li> </ul>	Table 4 RMSE < 9%
Tíba et al. [72]	BP	<ul style="list-style-type: none"> <li>- Dew point temperature;</li> <li>- Rain precipitation;</li> <li>- Darkness of sky;</li> <li>- Clearness index of Perez;</li> <li>- Index of transmittance</li> </ul>	Hourly luminous efficiency	MBD < 6% and RMSE < 6%
Pattanasethanon et al. [74]	BP	<ul style="list-style-type: none"> <li>- Solar altitude angle;</li> <li>- Clearness index/sky ratio</li> </ul>	<ul style="list-style-type: none"> <li>- Global illuminance;</li> <li>- Global irradiance;</li> <li>- Diffuse irradiance</li> </ul>	More accurate than the empirical models and the novel sinusoidal models

<i>Internal illuminance prediction</i>				
Navada et al. [75]	BP	<ul style="list-style-type: none"> <li>- Blind position;</li> <li>- Times</li> </ul>	Illuminance	%Error <5% The correlation coefficient $\approx 0.97$
Kazanasmaz et al. [40]	BP	<ul style="list-style-type: none"> <li>- Orientation;</li> <li>- Geometry;</li> <li>- Windows amount;</li> <li>- Distance to windows;</li> <li>- Floor character,</li> <li>- Sensors' position;</li> <li>- Date;</li> <li>- Hour;</li> <li>- Solar radiation;</li> <li>- UV index and UV dose;</li> <li>- Temperature;</li> <li>- Humidity</li> </ul>	Illuminance	Precision = 98%
<i>Prediction of energy saving due to daylighting</i>				
Fonseca et al. [77]	MLP Feedforward	<ul style="list-style-type: none"> <li>- Room depth;</li> <li>- Room orientation;</li> <li>- Solar heat gain coefficient;</li> <li>- Window to wall ratio;</li> </ul>	Final electric energy consumption	$R^2=0.9867$

		<ul style="list-style-type: none"> <li>- Vertical shading coefficient;</li> <li>- Horizontal shading coefficient</li> </ul>		
Wong et al. [79]	BP	<ul style="list-style-type: none"> <li>- Dry-bulb temperature (Daily average);</li> <li>- Wet-bulb temperature (Daily average);</li> <li>- Global solar radiation (Daily total);</li> <li>- Daily average clearness index;</li> <li>- Solar aperture;</li> <li>- Daylight aperture;</li> <li>- Overhang projection;</li> <li>- Side fins projection;</li> <li>- Day type</li> </ul>	<ul style="list-style-type: none"> <li>- Daily electricity use for cooling;</li> <li>- Daily electricity use for heating;</li> <li>- Daily electricity use for lighting;</li> <li>- Daily total electricity use</li> </ul>	<ul style="list-style-type: none"> <li>- NSEC = 0.994</li> <li>- NSEC = 0.940</li> <li>- NSEC = 0.993</li> <li>- NSEC = 0.996</li> </ul>
Kim et al. [81]	LM BP	<ul style="list-style-type: none"> <li>- Slat angle;</li> <li>- Outdoor air ratio;</li> <li>- Lighting energy consumption;</li> <li>- Setpoint temperature;</li> <li>- Air handling unit schedule (on/off);</li> <li>- Flow rate;</li> <li>- Outdoor air temperature;</li> <li>- Previous time step room temperature;</li> <li>- Outdoor illuminance;</li> </ul>	<ul style="list-style-type: none"> <li>- Room temperature</li> <li>- Total energy consumption</li> <li>- Indoor daylight illuminance</li> </ul>	$R^2 > 0.98$

		- Azimuth angle		
<i>Daylighting controls</i>				
Hu et al. [85]	BP	<ul style="list-style-type: none"> <li>- Weather condition (overcast, medium, clear);</li> <li>- LED input wattage;</li> <li>- Occupancy level (low, medium, high)</li> </ul>	Energy consumption	Precision = 98%
Hu et al. [86]	BP	<ul style="list-style-type: none"> <li>- Solar altitude angle;</li> <li>- Solar azimuth angle;</li> <li>- Global horizontal illuminance;</li> <li>- Diffuse horizontal illuminance;</li> <li>- Slat angle;</li> <li>- Global horizontal radiation;</li> <li>- Dry bulb temperature;</li> <li>- Zenith luminance;</li> <li>- Relative humidity;</li> <li>- Horizontal infrared radiation intensity from sky</li> </ul>	Illuminance at 3 sensor points of the blind (top, middle, bottom)	Precision = 94.7%

## 2.4 Discussion on research gaps

ANNs has been proved a useful and powerful numerical tool for predicting daylighting performance and optimizing daylighting design. However, according to the comprehensive review, there are still research gaps, which hinder the widespread application of ANNs in daylighting prediction and optimization. In this section, these gaps and problems are summarized and analysed.

(1). Almost all ANNs models in literature used BP algorithm as the training method. However, some improvements have recently been made for the BP algorithm. For instance, advanced techniques such as adding momentum and adaptive learning rate, as well as using more effective optimization algorithm, e.g., conjugate gradient method, LM method etc., should be explored.

(2). Most literature in this topic chose three years data for the input parameters; however, no evidence has been available as why three years is better. Some justification should be provided or some other time scales may be adopted.

(3). In ANNs training procedure, if too large capacity or too many iterations were selected, over training would happen. Prior to running ANNs simulation, considerable high precision or large number of training cycles should always set as priority to define when to stop the training process. However, due to unavoidable uncertainty, some training data obtained from experiments or elsewhere could sometimes be erroneous. Hence, over high precision can also cause over fitting and reduce the prediction accuracy. In order to overcome this problem, the number of training cycles and input data need to be optimized.

(4). Since the data used to train ANNs model sometimes cannot cover the entire range of the data, the extrapolation can become ineffective. When preparing the input data for training ANNs model, the maximum and minimum values should be selected from all the proposed data. Empirical correlations can be applied to some training samples and the selected training data shall be able to represent the entire operating range of the system in order to reduce the extrapolation errors.

(5). Decision on the number of the hidden layers is dependent on empirical trials. Effective methods need to be developed to find out the appropriate number. So far, the number of neurons in hidden layers can be calculated as follows [87],

$$L = \sqrt{m + n} + a, \quad a \in [1, 10] \quad (2.8)$$

where L is the number of neurons in hidden layers, m is the number of neurons in input layer, n is the number of neurons in output layer, and a is an adapting variable, which range from 1 to 10.

(6). Most of the hidden layers tend to be one hidden layer. In fact, two or more hidden layers help return more accuracy. However, more hidden layers cost more time and make the system complex. Therefore, the balance of accuracy and time cost is a key problem. The Bayesian approach can offer selection of optimum number of hidden layers. In addition, under what circumstances a second hidden layer should be chosen needs to be discussed in future research.

(7). Not many researchers in this field have considered the input parameters with respect to the output parameters. In fact, sensibility test should be undertaken to determine the input

parameters in order to remove the irrelative parameters and keep the model as accurate as possible.

(8). For luminance and illuminance, one of the most important factors is local climate. For indoor daylighting level, the sun position is a crucial parameter. These parameters should be considered into the ANNs modelling.

(9). The initial dataset should remove noise before being used. For instance, GA could be used to optimize the input dataset such as variable extraction and selection on measured data.

(10). The outputs of neural networks may not be exactly what expected. The outputs could be corrected by post-processing results, such as fuzzy logic.

(11). ANNs model is a strong simulation tool to solve the problems with large number of input variables data. The input data can be split into training data, testing data and validation data. Improper data splitting can lead to a poor prediction. More quantitative guidance on the data selection is one of the keys to successful ANNs simulation in daylighting performance and optimization.

## **2.5 Summary**

This Chapter has presented a literature review on the research work in daylighting prediction and optimization by using ANNs approach. In the review, the luminance and illuminance prediction, daylighting control and energy saving with daylighting have been extensively discussed. The existing work can be useful for building professionals and researchers to estimate the availability and suitability of ANNs in predicting daylighting performance.

Moreover, the research gaps currently hindering the widespread and effective application of ANNs in daylighting prediction and optimization have been explored and presented. The findings could help architects and practising engineers adopt proper daylighting design schemes and evaluation methods, and therefore promote sustainable developments in architectural buildings.

**Chapter 3 Performance of lightpipes and  
Artificial Neural Network (ANN) model  
development for predicting the  
transmittance of lightpipes**

## **3.1 Introduction**

### **3.1.1 Background**

It was found that electric lighting, one of the major energy demands, accounts for 20~30% of total electricity consumption in commercial buildings [19] and 10% in residential properties [88]. Historically, daylight was used as the primary source of luminance during the day. However, during the development of modern cities, artificial lighting has been substantially used in buildings in the daytime. Such a massive consumption of artificial lighting and hence energy has brought into attention to numerous scientists and engineers as if it could be reduced or replaced by the natural daylighting. For example, Li and Tsang [6] carried out a survey on some open layout office buildings in Hong Kong and found that 20-25% of electric lighting energy could be saved if half of the occupancy time was served by daylighting with proper artificial lighting control.

Compared with artificial lighting, daylighting does not only save the energy consumption, but also improve the visual comfortable and the health of occupancies, which applies “light vitamin” to people living in the buildings. Begemann et al. [7] have conducted a long-term study and found that the occupants in buildings prefer varying levels of natural lighting cycle to the constant artificial lighting. In addition to the direct save on the energy consumption and personal preference, daylighting can save the cooling cost in air-conditioned buildings. This is due to that the Luminous Efficacy (number of lumens per watt) of daylighting is normally higher than artificial lighting. As such, given the same level of illuminance, less radiant power is required. In other words, natural illumination normally dissipates less heat than artificial illumination and therefore it is considered as an efficient illumination. In an office building

with normally extensive use of artificial lighting, significant amount of heat dissipation could be saved by utilizing daylighting instead, which reduce the cooling energy consumption [8].

Most research to date only addressed limited configurations while the design criteria for prediction of daylighting performance is scarce. This chapter attempts to employ the Artificial Neural Network method in the performance prediction of lightpipes.

### 3.1.2 Outline of the principles of Artificial Neural Network

Since the last three decades, Artificial Neural Networks (ANNs) have been used as an alternative approach to these pre-mentioned prediction methods for daylighting. As a numerical method, ANNs can solve complex problems in a number of fields by the means of simulation, identification, prediction, optimization, classification and control.

ANNs was initialled developed in the research of human brain around 50 years ago. There are 10 billion inter-connected neurons in a human brain. As shown in Figure 3.1, each neuron is a cell which can perform biochemical reactions to receive, process and transmit information [88]. The application of ANNs has been extended to other disciplines since two decades ago.

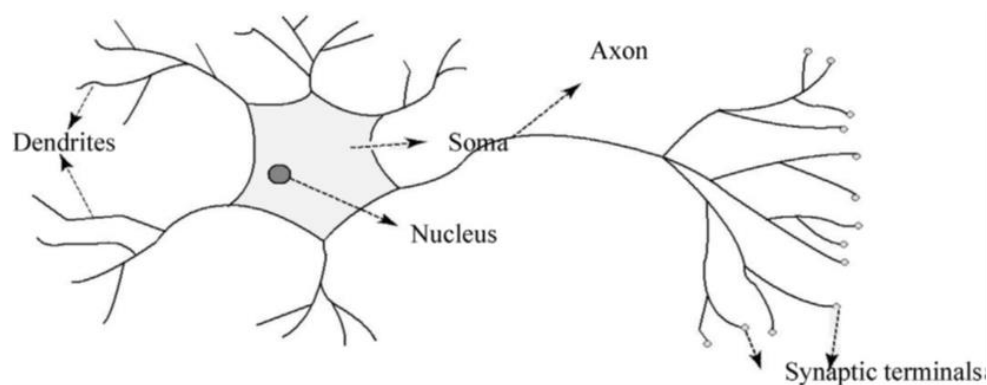


Figure 3.1 Mammalian neuron [89]

ANNs is a self-learning and self-training platform or programme. A typical multilayer neural network is illustrated in Figure 3.2. A neural network is normally composed of three layers. These layers are usually one input layer, some hidden layers and one output layer. Within each layer, there are a certain number of neurons. They are processing elements (PEs) and each connection of them has an associate weight [90]. The process of an ANNs simulation starts with weighted summation activation of the neuron through its incoming connections; it is then followed by passing through an activation function and this activated value is the output of the neuron[14].

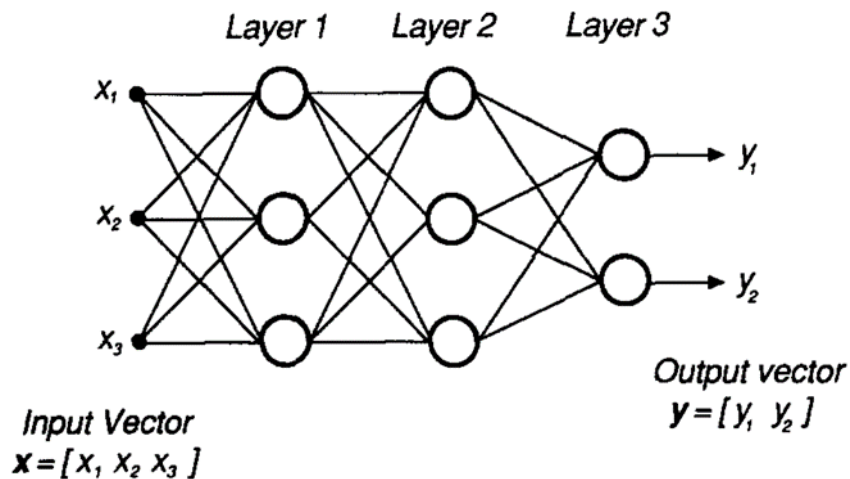


Figure 3.2 The typical sample of a multilayer feed-forward neural networks [61]

The sigmoid function, which is the most common logical transfer function, is an “S” shaped transfer function ranging from 0 to 1, which can be expressed as follows:

$$\text{sigmoid}(x) = \frac{1}{1+e^{-x}} \quad (3.1)$$

where  $x$  is the weighted sum of the inputs. The procedure for developing an ANN model includes 3 phases including modelling, training and validating. First, modelling involves

analysing data, identifying input parameters and selecting network architecture and internal rules. The prepared data can then be trained, for example, by using the back-propagation learning algorithm to establish a model. After the training of data and the establishment of the model, it should be validated before application.

### **3.1.3 Research significance**

The prediction of daylighting in building design is a key part of the whole design process. As is widely accepted, daylight condition is highly dynamic throughout a day and a year, which brings difficulty to the prediction of daylight. Early work about daylighting prediction always employed sensitivity and regression analysis to deal with annual energy using situation. However, such analysis methods considerably relied on well-understood energy consumption data. Due to the non-linear nature of daylight, artificial neural networks (ANNs) had been introduced to daylighting prediction, which has advantages in solving nonlinear problems [9].

The main difficulties in evaluating all underlying factors for the performance of lightpipes poses barriers to assess the efficiency of lightpipes. The complexity in the mechanism of lightpipes transmitting light makes it difficult to appraise the performance by means of physical modelling. Besides, prior to this research, the lack of lightpipes performance data, which include both environmental, and geometrical data make it impossible to predict the performance by using mathematical methods as well.

This Chapter is to develop an artificial neural network model for the prediction of lightpipes daylighting performance. Although the performance of lightpipes has been investigated in a number of studies, no methods could predict the bended lightpipes because the non-linear

relationship between the system parameters and the daylighting performance of lightpipes. Following a logical process from raw data simulated by an optical software photopia collection to evaluation of ANNs models, an artificial neural networks model for predicting the daylighting performance of lightpipess is developed. Although the complexity in the working mechanism of lightpipes makes it difficult to evaluate its performance, with the aid of Photopia, Matlab and high performance computing facility, it is possible to develop a numerical model to predict the performance of lightpipes, especially bended lightpipes, which have non-linear relationship between transmission characters and performance. Moreover, this study aims to produce a reliable research method, and a framework under which further development in daylighting performance modelling can be conducted in a consistent direction leading to the final solution.

## **3.2 Methodology**

In overall, this Chapter consists of two parts. The first part is to study the lightpipe performance by using computer software Photopia. Models have been built in the AutoCAD for the calculation of performance of lightpipes. Data such as lumen output, illuminance flux are then put forward from the simulation of Photopia. Parametric studies are conducted to investigate the influence on the performance by changing length of tube, diameter of dome and tube, reflectivity of mirrored material, and bended angle of the lightpipes. Moreover, solar altitude and solar azimuth are important factors as well. Further, data like transmission of light will be collected to check the efficiency of lightpipes. However, the decision on the lightpipe parameter range is not random which should follow the normal standards of lightpipes. Thus, the size guide given by the manufactory of lightpipes will be referred to in the simulated examples (Monodraught LTD, 2016).

The other part is using the data simulated from Photopia in ANNs modelling. A variety of lightpipe parameters were chosen as input values and efficiency was chosen as output value. In this research, two computer software, i.e., Photopia and Matlab, are used. The following (Figure 3.3) is the brief introduction to the function and operation of the software related to lightpipes.

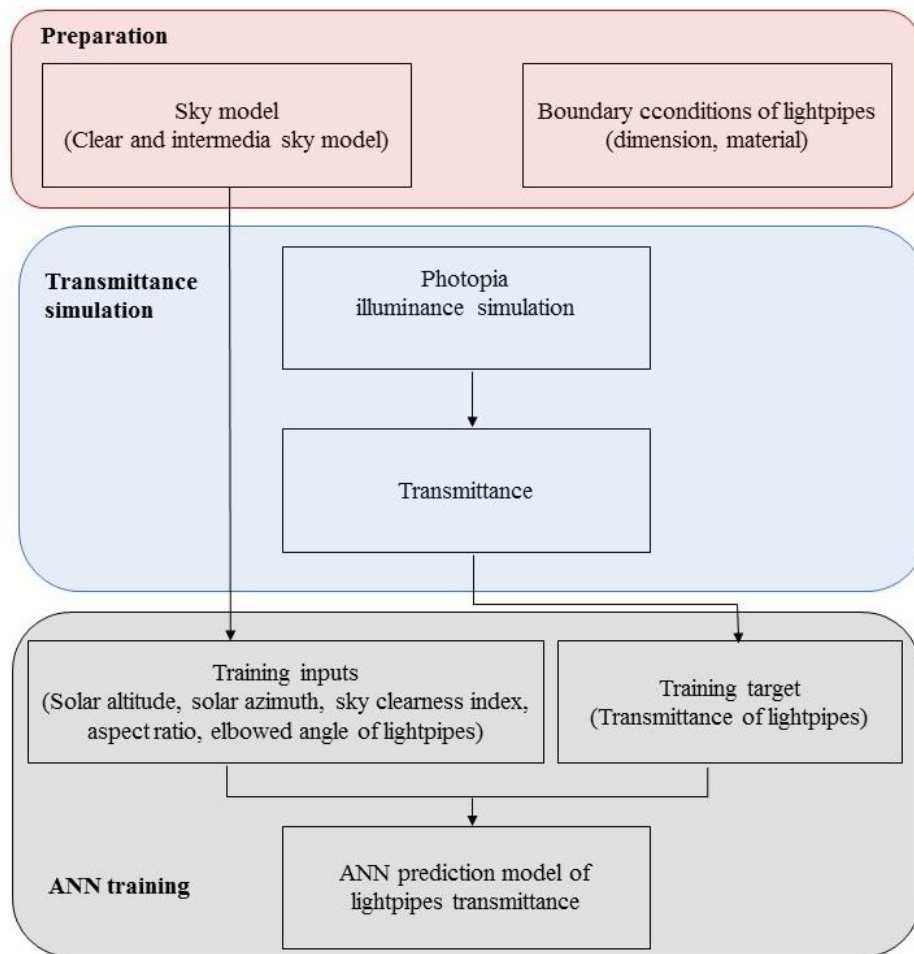


Figure 3.3 Illustration of the process of ANN

### 3.2.1 Simulation data acquisition in Photopia

Photopia contains sun and sky dome models as the lamps for the simulation of daylight collecting and transporting devices. By combining the sun along with the sky dome models, the entire illuminance through the daylighting device area matching the real outdoor

conditions can be produced. The lightpipe model imported from AutoCAD program has layers such as dome, light tube and diffuser lens. They are defined for the layer type as transmitted and reflective. The running process allows for the setting of design properties, photometric output specification and ray-trace settings. The output will cover candela distribution polar plot, illuminance shaded plot, photometric report, etc.

Various models of different lightpipes are built for study initially. The length, diameter, bended angles, solar altitude and solar azimuth are the main parameters to study the lightpipe performance. Table 3.1 lists the brief description of the base lightpipes parameters for simulation. Figure 3.4 is one type of the lightpipes with three components simply, the dome, the reflective tube, and the diffuser lens, in addition, the reference surface.

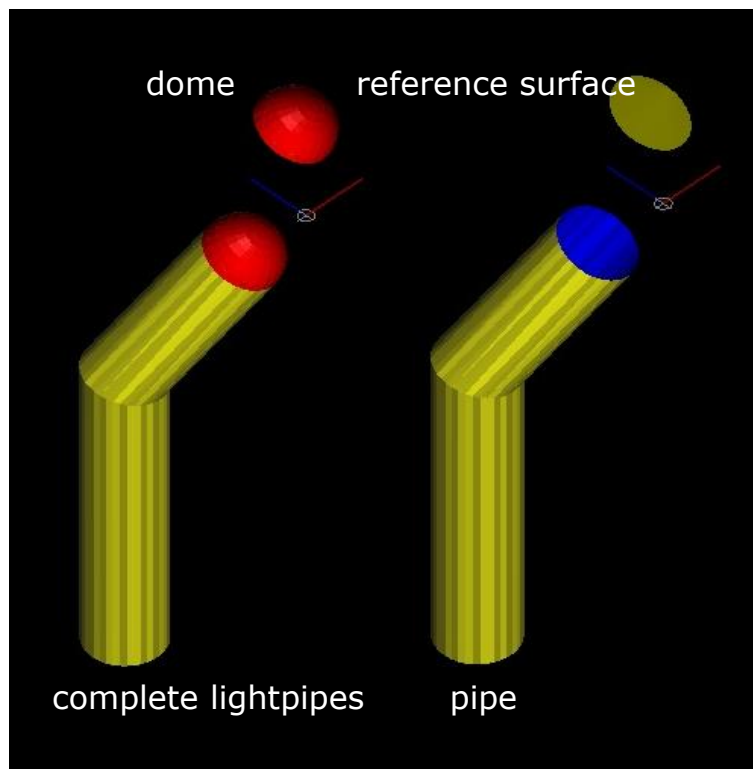


Figure 3.4 A single group of a single type of lightpipes

Table 3.1 Brief description of the basic lightpipe parameters for simulation

	Material	Property
Dome (TRAN - Dome)	Clear acrylic	Transmittance = 92%
Light pipe (REFL – Light Pipe)	Alanod Miro 4 Silver	Reflectivity = 98%
Reference layers (two)	Black layer	Reflectivity = 0
Bended angles of lightpipes		0°, 30°, 45°, 60°
Solar altitude		10°, 20°, 30°, 40°, 50°, 60°, 70°, 80°, 90°
Solar azimuth		0°, 10°, 20°, 30°, 40°, 50°, 60°, 70°, 80°, 90°
Diameter of lightpipes		230mm, 300mm, 450mm, 530mm
Lengths of lightpipes		1000mm, 1500mm, 2000mm
Lengths of tilted upper part		610mm
Sky condition		Clear, intermediate,

In order to define the changeable elements, those three parameters are shown in Figure 3.5. The whole tube consists of a bended part and a joining vertical part to the ground. However, the changing parameter is the length of the vertical part only. An assumption could be made that the bended part is vertical to the pitched roof and the distance between the ceiling and the roof is fixed. Consequently, it makes sense to change the lower straight part of the tube as a design parameter. As such, this scheme of lightpipe design can be seen as deeper transportation of light in the vertical space of the room. The bended angle is defined as the angle between

the bended pipe and the vertical perpendicular line. For example, the 30 degrees' elbow means rotating 30 degrees from the vertical line anticlockwise.

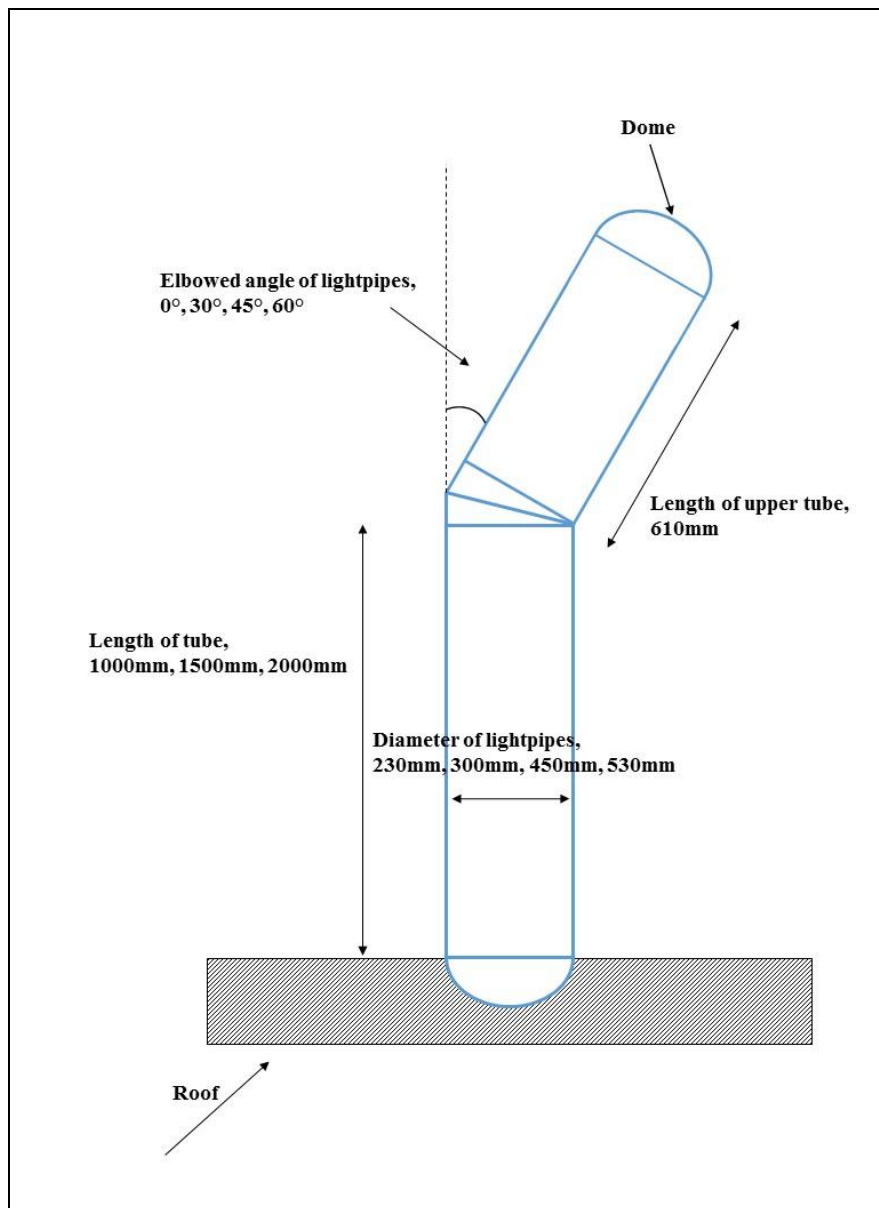


Figure 3.5 Parameter demonstration of single lightpipes

Solar altitude angle and solar azimuth angle need to be determined. Usually solar altitude is defined by Hartmann as the angle between horizon and the central disc of the sun. The larger is number is, the higher the sun will be vertically. Solar azimuth is defined as the angular displacement from south of the projection of beam radiation on the horizontal plane.

In terms of straight lightpipes, the only effect of solar light is solar altitude. So solar altitude from 10 degree to 90 degree were used to do simulation. However, in terms of bended lightpipes, both solar altitude and solar azimuth effect the efficiency of lightpipes. As a result, solar altitude 10 degree to 90 degree and solar azimuth 0 degree to 90 degree were combined to simulate the efficiency of bended lightpipes. Figure 3.6 gives a demonstration of solar altitude and solar azimuth. 10 degrees' gap for each altitude was chosen.

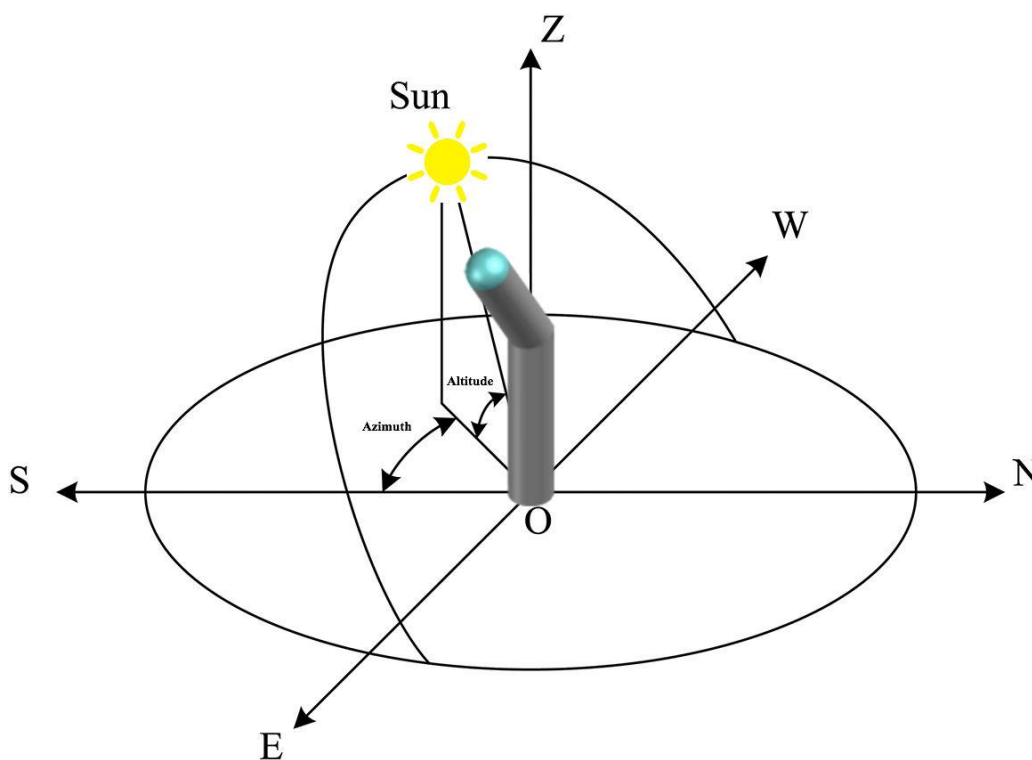


Figure 3.6 Solar altitude and solar azimuth.

Figure 3.7 and Figure 3.8 show lengths range from 1000, 1500, 2000 mm and diameters of 230, 300, 450 and 530mm respectively. The lengths of tilted upper part are all 610 mm. The definition of the length is the distance between the centres of the circles. When doing the parameter study by different diameters, other parameter including length and bended angles will not be changed.

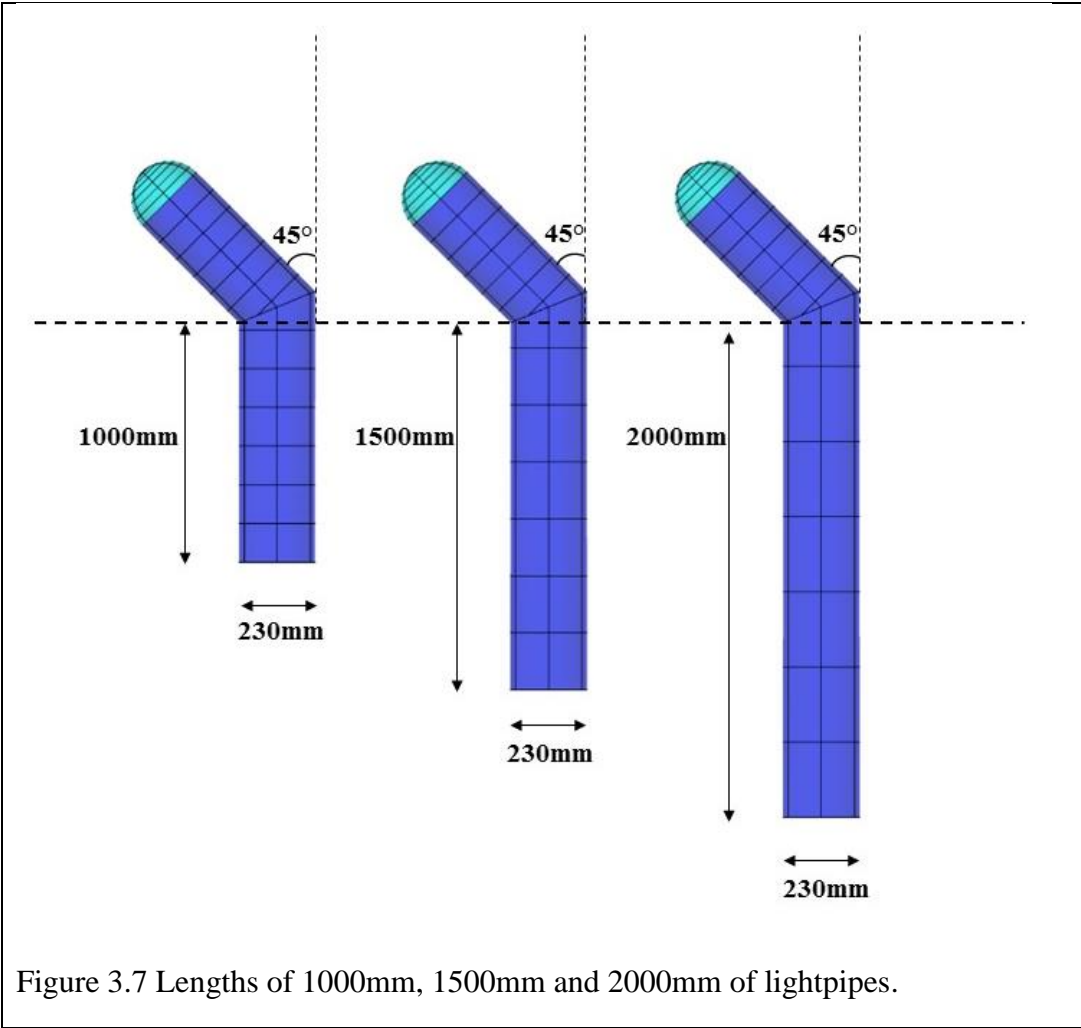


Figure 3.7 Lengths of 1000mm, 1500mm and 2000mm of lightpipes.

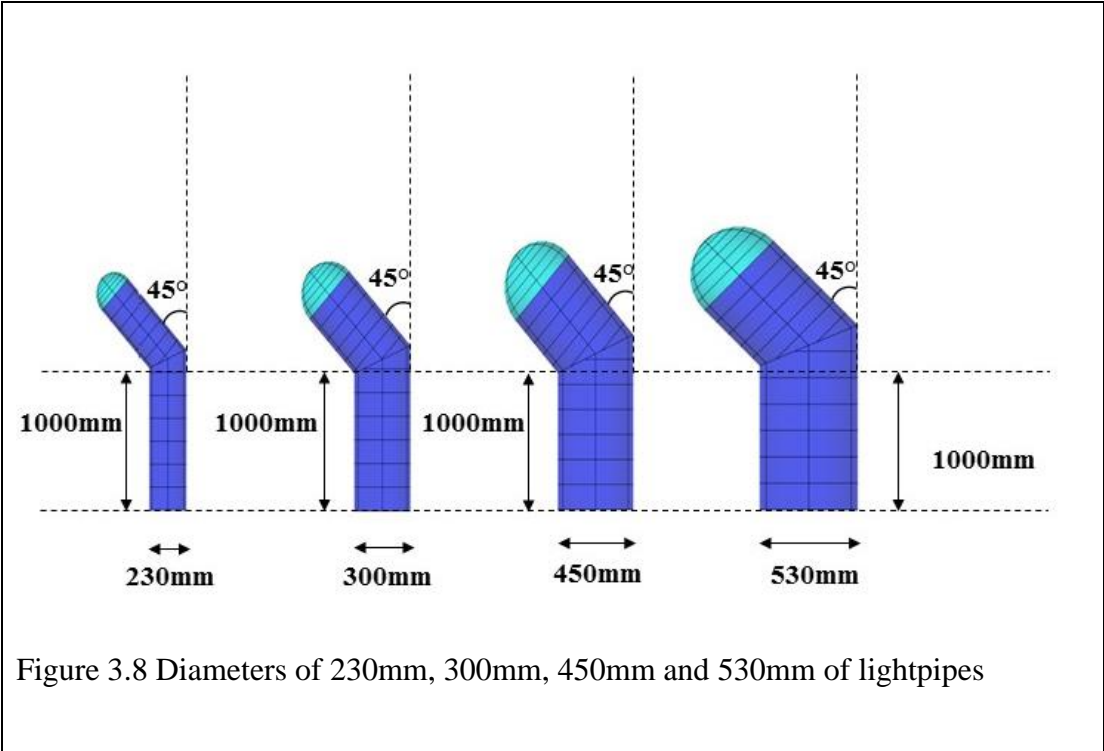
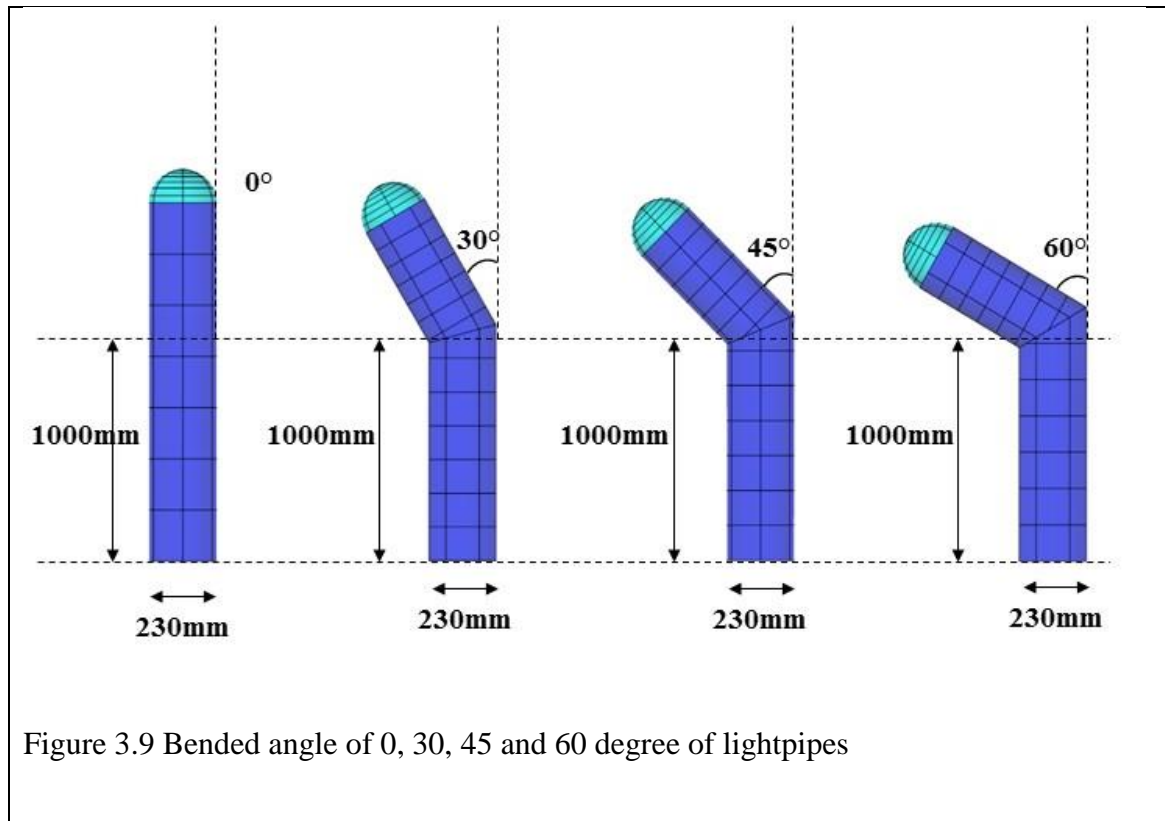


Figure 3.8 Diameters of 230mm, 300mm, 450mm and 530mm of lightpipes

Three types of lightpipes with bended angles of 30, 45, 60 degrees are selected together with the straight one which can be seen as 0-degree elbow. These four lightpipes are arranged below (Figure 3.9). Also, the only variable among them is the elbowed angle, the length and the diameter will be fixed.



After building various types of lightpipes system models, the settings in the photopia should be adjusted for the further calculation. As stated before, the lightpipes models are imported as DXF file from AutoCAD to Photopia. Then, the lamp models of sky and sun are also imported. The location of each component is modified in order to reach the simulation condition. Additionally, the project setting of units are appointed as millimeters initially. Then some surfaces need to be oriented towards the incident light, meaning that their respective layer colours should face the incident light. For instance, for light entering through the top of the dome, the real colour should face outside. For the reflective surface for light to be transported

through the pipe, the real colour should face inside. The two reference surfaces should also have the real colour facing the incident light.

To fulfil the goal of simulating lightpipes system under the condition of only sunlight and sunlight with daylight. The original lamp of sun and sky model should have all the sky layers to be closed if they are supposed to simulate sunlight incident only. In addition, the layer properties of lightpipes model are set as reflective and transmissive. The two reference layers are set as black surface with zero reflectivity because they ought to absorb all the incident light on the surface to represent the inlet and outlet of the lightpipes. Likewise, the coverage layer should block all the incident light so it is also appointed as no reflectivity. The light tube for light transportation system (REFL-Light Tube) is set as 98% reflectivity for the material of Alanod Miro 4 Silver. The material of dome layer (TRAN-Dome) is appointed as clear acrylic with 92% transmittance.

### **3.2.2 Configuration of Artificial Neural Network**

The nature of lightpipe daylighting prediction is non-linear multivariate regression. According to the literature review in Chapter 2, ANN is a useful technique in solving non-linear issues. Thus, ANN was employed here to forecast the performance of lightpipes. “NN Toolbox” in the software MATLAB R2017a was used to train and test the data acquired from Photopia. To create an ANN model should follow 5 steps: definition of training parameters, configuring network architecture, training network, testing network and using the successful network to conduct prediction. Figure 3.10 demonstrates the basic work mechanism and process of neural network.

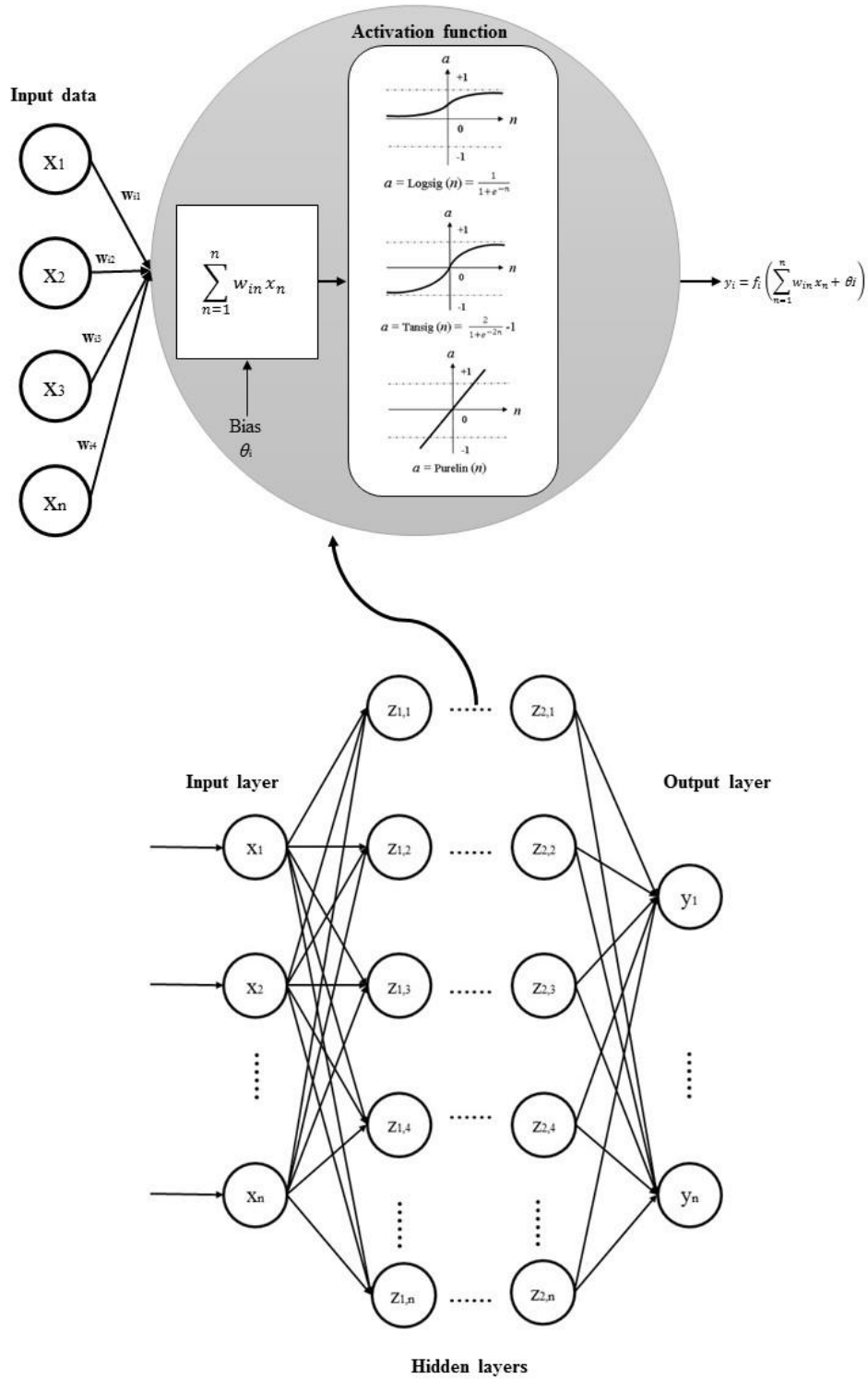


Figure 3.10 The typical network architecture and work mechanism of neural network

In the first step, formatting the integrated simulation data so that the input parameters and output parameters can be read by the ANN model. In this study, the initial direct viewing input variables are ① the elbowed angle of lightpipes (°); ② the lengths of lower part of lightpipe (straight part) (mm); ③ the diameter of lightpipes (mm); ④ the solar altitude (°); ⑤ the solar azimuth (°). Only one output variable is the luminous flux exported from the lightpipe in Photopia (lumen). It could be found that the original parameters have different physical meaning and physical units. It would reduce the readability of the input data of ANN and as well as the accuracy of ANN prediction ability. In this step, normalization the disunion data is essential. Take ① the elbowed angle of lightpipes (°) for example, the Degree Measure (the unit is °) should be transfer to Radian Measure (without unit) as follows.

$$\alpha = \alpha * \left(\frac{\pi}{180^\circ}\right) \text{ rad} \quad (3.2)$$

where  $A$  is the angle with unit as degree (°). All the parameters with degree (°) can be transferred to radians.

Table 3.2 The parameters with Degree Measure and corresponding Radian Measure

Bended angles of lightpipes ( $x_1$ )		Solar altitude ( $x_2$ )		Solar azimuth ( $x_3$ )	
0°	0	10°	0.1745329	0°	0
30°	0.5235988	20°	0.3490659	10°	0.1745329
45°	0.7853982	30°	0.5235988	20°	0.3490659
60°	1.0471976	40°	0.6981317	30°	0.5235988
		50	0.8726646	40°	0.6981317
		60°	1.0471976	50	0.8726646
		70°	1.2217305	60°	1.0471976
		80°	1.3962634	70°	1.2217305

	90°	1.5707963	80°	1.3962634
			90°	1.5707963

Regarding ② the length of lightpipe (straight part) (mm) and ③ the diameter of lightpipe (mm), the ratio of length to diameter is used in ANN simulation.

$$A_p = L/D \quad (3.3)$$

where  $A_p$  is the aspect ratio,  $L$  is the lengths of lightpipe, and  $D$  is the diameter of lightpipes.

All the aspect ratios are listed in Table 3.3.

Table 3.3 The parameters with Degree Measure and corresponding Radian Measure

Diameter	Lengths	Aspect ratio ( $A_p$ ) ( $x_4$ )
<b>230mm</b>	1000mm + 610mm = 1610mm	7
<b>300mm</b>	1500mm+ 610mm = 2110mm	9.173913
<b>450mm</b>	2000mm+ 610mm = 2610mm	11.347826
<b>530mm</b>		5.3666667
		7.0333333
		8.7
		3.5777778
		4.6888889
		5.8
		3.0377358
		3.9811321
		4.9245283

In Su's model [36], the ratio of the actual horizontal global illuminance  $E_{ext}$  to the theoretical value under the CIE clear sky was introduced to instead of using the sky clearness index (defined as the ration of global to the extra-terrestrial irradiance). This variable was adopted in this study as well. It is expressed as  $\lambda$ . The theoretical horizontal global illuminance could be calculated from the given solar altitude. The correlation is given in Figure 3.11.

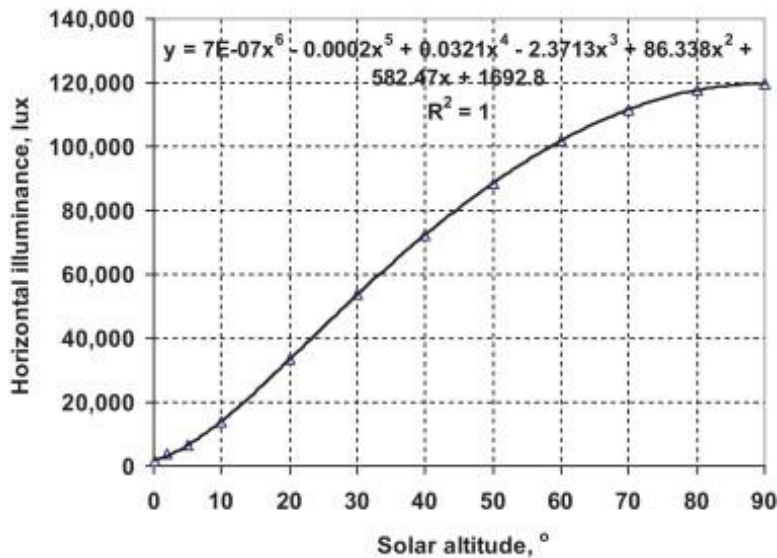


Figure 3.11 Horizontal global illuminance under the CIE clear sky versus solar altitude [37].

Although the “only sun”, “clear” and “intermediate” situations were simulated in Photopia, the “only sun” situation never exists in real sky condition, which do not have practical meaning. Thus “clear” and “intermediate” situations are considered in ANN prediction. The  $\lambda$  is constant 1 under clear sky and variables under intermediate sky. The value of  $\lambda$  is listed in Table 3.4.

In summary, the input parameters in this study are bended angle of lightpipes ( $x_1$ ), solar altitude ( $x_2$ ), solar azimuth ( $x_3$ ), aspect ratio ( $x_4$ ) and sky clearness index ( $x_5$ ). The output parameter of ANN model is the transmittance of lightpipes which is expressed as  $y$ . In total, 6696 values of transmittance ( $y$ ) are obtained from Photopia. All these values are to be used in training and testing the ANN models, as shown in Table 3.5.

Table 3.4 The parameters for the sky clear index

Sky clear index $\lambda$ ( $x_5$ )	
Clear sky index	Intermediate sky index
1	0.5879972
	0.5895754
	0.6438484
	0.6882964
	0.6902739
	0.6263268
	0.5507468
	0.4248583
	0.3156408

Table 3.5 The input parameters and output parameters in ANN models

$x_1$	$x_2$	$x_3$	$x_4$	$x_5$	$y$
0	0.1745329	0	7	1	Total 6696 values
0.5235988	0.3490659	0.1745329	9.173913	0.5879972	
0.7853982	0.5235988	0.3490659	11.347826	0.5895754	
1.0471976	0.6981317	0.5235988	5.3666667	0.6438484	
	0.8726646	0.6981317	7.0333333	0.6882964	
	1.0471976	0.8726646	8.7	0.6902739	
	1.2217305	1.0471976	3.5777778	0.6263268	
	1.3962634	1.2217305	4.6888889	0.5507468	
	1.5707963	1.3962634	5.8	0.4248583	
		1.5707963	3.0377358	0.3156408	
			3.9811321		
			4.9245283		

In the second step, the neural networks architecture is configured. In ANN modeling, the network parameters including the number of neurons in input, hidden and output layers, network architecture, transfer function, learning algorithm, momentum factor, learning rate are the basic but significant ones. The input layer delivers the values to each neuron in hidden layer. The number of hidden layers and optimum number of hidden neurons significantly affect the system accuracy. The number of neurons in the hidden layer, momentum factor and learning rate values are optimized by trial and error method to get accuracy simulation results.

According to the literature review in Chapter 2, decision on the number of the hidden layers is dependent on empirical trials. Effective methods need to be developed to find out the appropriate number. So far, the number of neurons in hidden layers can be calculated as follows [87].

$$L = \sqrt{m + n} + a, \quad a \in [1, 10] \quad (3.5)$$

where  $L$  is the number of neurons in hidden layers,  $m$  is the number of neurons in input layer,  $n$  is the number of neurons in output layer, and  $a$  is an adapting variable, which range from 1 to 10. In this research, the  $L = \sqrt{5 + 1} + a, \quad a \in [1, 10]$ ,  $L$  could take the value from [3, 4, 5, 6, 7, 8, 9, 10, 11, 12, 13].

In the third step, ANNs are trained with a set of known input-output data and suitable learning method to perform a function by adjusting the values of weight coefficient between processing neurons. The Levenberg-Marquardt function is chosen as training function in this study. In terms of medium size of dataset, Levenberg-Marquardt is the fast training method. The weakness is that it occupies lots of memory of the computer. It would be improved by

customizing the parameter as 1, 2, 3, ..., separating the Jacobian Matrix into several submatrix. However, this method is also highly demanding for memory storage of computer. Thus, how to balance them during the network training is essential in the process.

After having successfully trained the neural networks, the rest remaining 30% data are used to test the accuracy of network. The selected data of testing programme is similar to the training programme. Both of them are random. In addition, the feature of tested data should be the same as trained data. The criteria used for measuring the performance of the network are correlation coefficient (R) and absolute fraction of variation (R<sup>2</sup>). These two parameters will be checked in the testing of network to ensure the accuracy.

### 3.2.3 Evaluation metrics

The results from ANN prediction can be evaluated by various evaluation metrics. 12 evaluation metrics are identified in the previously reviewed studies [89], which will not be repeated herein again. Some of the common metrics can be performed from equations shown as follows:

$$RMSE = \sqrt{\frac{1}{N} \sum_{i=1}^N (\hat{y}_i - y_i)^2}$$

$$MSE = \frac{1}{N} \sum_{i=1}^N (\hat{y}_i - y_i)^2$$

$$R^2 = 1 - \frac{\sum_{i=1}^N (\hat{y}_i - y_i)^2}{\sum_{i=1}^N (y_i - \bar{y})^2}$$

$$MAE = \frac{1}{N} \sum_{i=1}^N |\hat{y}_i - y_i|$$

$$MBE = \frac{1}{N} \sum_{i=1}^N (\hat{y}_i - y_i)$$

$$PE = \frac{(\hat{y}_i - y_i)}{y_i} 100\%$$

$$CV = \frac{\sqrt{\frac{1}{N} \sum_{i=1}^N (\hat{y}_i - y_i)^2}}{\hat{y}_i} 100\%$$

where  $\hat{y}_i$  is the predicted illuminance value for times  $i$ ;  $y_i$  is the simulated illuminance value for times  $i$ ,  $\bar{y}_i$  is the average illuminance value; and  $N$  is the number of data points used for evaluation. In this study,  $R$ ,  $R^2$  and  $MSE$  were chosen to estimate the prediction performance of ANN models.

### 3.3 Efficiency of various lightpipes under clear sky

#### 3.3.1 Efficiency of various aspect ratio of lightpipes under clear sky

Different aspect ratio (the length to diameter ratio for lightpipes) of straight lightpipes and bended lightpipes were chosen to compare the influence of various aspect ratio. Efficiencies for each group lightpipes are calculated. Figure 3.12 shows the efficiency viable for each group of lightpipes with same length at solar altitude 50 degrees and solar azimuth 30 degrees. It is straightforward to see that the overall trends for all four groups of lightpipes reducing. In addition, the uptrend improves that the more aspect ratio the lightpipes has, the less efficiency of transporting light will be achieved. For the lightpipes with 30° bended angle, the efficiency reduces from about 90% to nearly 77% when the aspect ratio expands from 0.35 to 11.5. For the lightpipes with 60° bended angle, the efficiency reduces from about 55% to about 15%. However, because the effect of solar azimuth, the transmittance has wave motion. But the total trend is reducing along with the aspect ratio increase. On the other hand, to compare the line

in the chart vertically, if the lightpipes with same aspect ratio, the angles mire close to solar azimuth 30degree, the more efficiency will have. All these findings fulfil the trends within these data used as aspect ratio from 3.05 to 11.5.

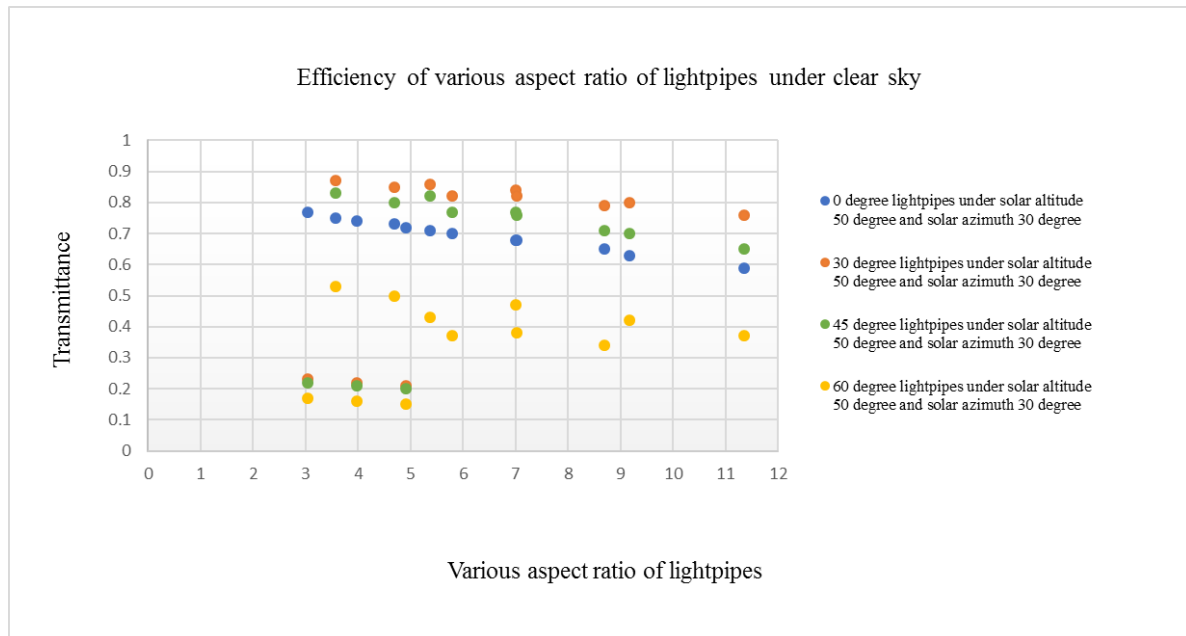


Figure 3.12 Efficiency of various aspect ratio of lightpipes under clear sky

These findings are discussed as follows. The expansion of the width of certain lightpipes may result in more incident light from the dome. The pipe becomes wider, the light transmitted through the dome is multiplied. The larger area of dome will collect more light, though the possibility for having more rays lost may be higher because of wider tube. Thus, the bigger diameter pipe causes more light collected than the loss of reflectivity, and the efficiency can be improved if enlarging the diameter from 230mm to 530mm. For the lightpipes with same diameter, the scene of the ray tracing in the bended part will be the same since lightpipes are same during this part of transportation. When the light become reflected to the vertical straight part, the reflected light angle will also be same because of the same bended angle of those lightpipess. However, the longer the vertical part of pipe is, the more the light will be reflected in the pipe otherwise light will be transmitted through the diffuser lens. Therefore, it is

undoubtedly that making the same type of lightpipes longer will lead to the declined efficiency. Having said that, the same trend could not be observed clearly in bended lightpipes. It will be research in more details in Section 3.5 by using ANNs to deal with the non-linear problems.

### **3.3.2 Efficiency of various bended angle of lightpipes under clear sky**

This stage of simulation is to change the bended angle for each group of lightpipes. The calculated efficiency results are shown in Figure 3.13. The curved lines have similar tendency, as they all increase for bended angle from  $0^\circ$  to  $30^\circ$  and decrease for bended angle from  $30^\circ$  to  $60^\circ$ . However, the larger aspect ratio, the more decrease of efficiency will be caused by bending from  $30^\circ$  to  $60^\circ$ . Furthermore, for the pipe with aspect ratio 3.58, the efficiency drops from 85% to about 55%. The decreased efficiency is about 30%. For the lightpipes with aspect ratio 11.35, the falling efficiency ranges from 75% to about 35%, which is about 40% drop. As such, the larger aspect ratio of lightpipes will have more apparent dropping trend of efficiency. Similar to the aspect ratio influence studied before, the larger aspect ratio pipe will have less efficiency on the whole system. In addition, this finding in trend of efficiency is under the situation of having solar altitude of  $50^\circ$  and solar azimuth  $30^\circ$ . However, when the aspect ratio is very small, meaning the lengths are very short and the diameters are very large, the transmittance is very small. The possible reason may be associated with the fact that the larger area of dome will collect more light, though the possibility for having more rays lost may be higher because of wider tube.

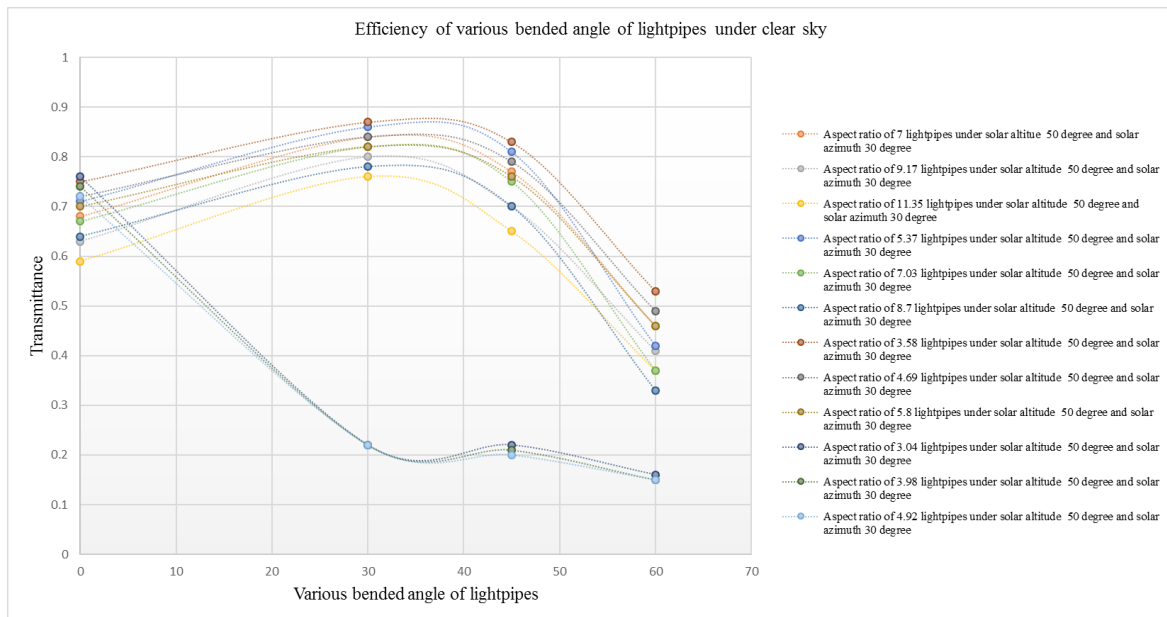


Figure 3.13 Efficiency of various bended angle of lightpipes under clear sky

In order to explain the underlying reasons, the bended angle seems to play a vital role in affecting reflectivity in the pipe. In this part of simulation, the solar position is fixed, so the light orientation is constant. If making upper part of pipe bended from straight to 30 degrees, the incident light of 45 degrees will have the light reflected more. For the straight lightpipes, the reflectivity curve of light in the tube will keep the overall curvature. If the upper part of pipe becomes rotated from the vertical direction, the curvature of reflectivity will be replaced with different reflectivity angle when light entering the lower part of the pipe. From elbow of 30° to 60°, the orientation of light in the pipe from the bended part will be more distinct from the one in the straight part. As a result, the larger elbowed angle will re-orientate light from a more varied angle to vertical angle, and there may be more chance for light to be lost. It is easy to see that the peak point of highest efficiency happens when the pipe is bended at 30° but not 45° though the solar altitude angle is 45°. It may be more appropriate to see 45° bended lightpipes with higher efficiency because more light seems to be incident in the bended part since two angles match. However, the lower straight part of the pipe will also play a role in

redirecting the light; it may be hard for light to be transported from 45° elbow to the vertical part. The reason for larger aspect ratio causing less efficiency is explained hereinbefore.

### 3.3.3 Efficiency of lightpipes with various solar altitude under clear sky

The diagram below shows influence of various solar altitude angles on the efficiency (Figure 3.14). It is straightforward to find that the lightpipes with larger aspect ratio will have weaker efficiency when other parameters remain the same. There are also some regulations that can be found from the chart. In terms of straight lightpipes, the efficiency is increasing from solar altitude 0 to 90 degrees.

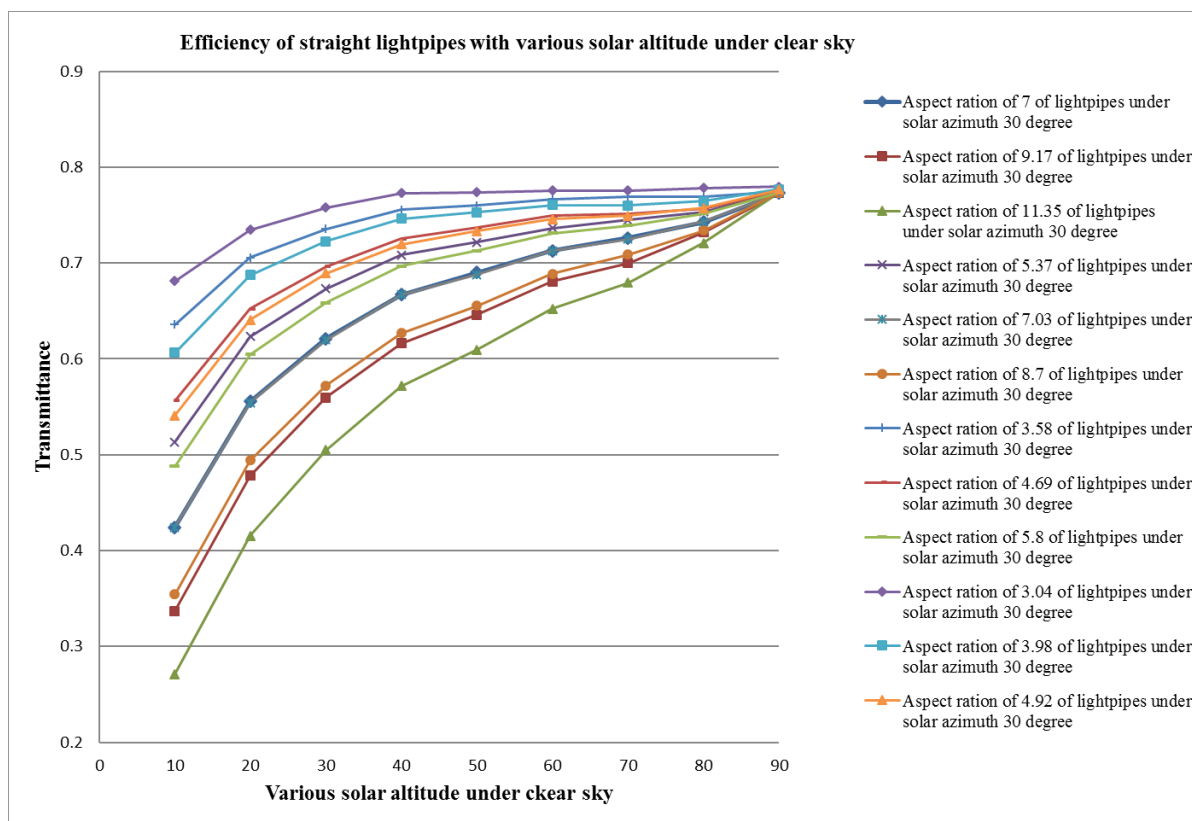


Figure 3.14 Efficiency of straight lightpipes with various solar altitude under clear sky

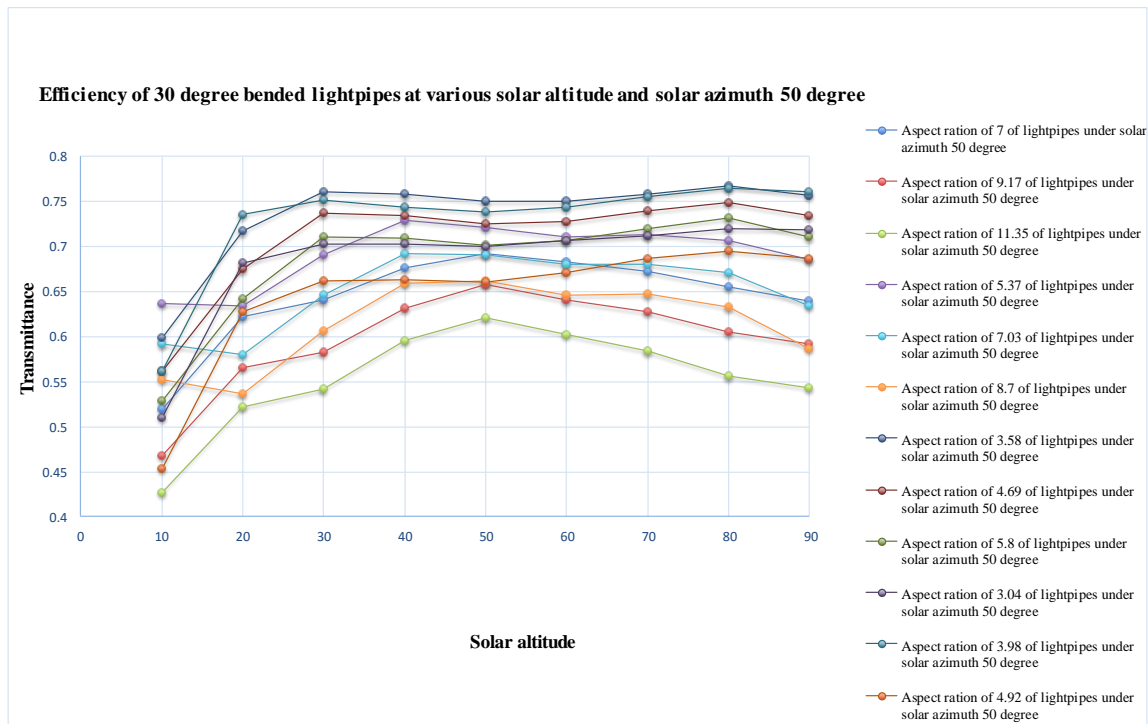


Figure 3.15 Efficiency of 30° bended lightpipes at various solar altitude and solar azimuth 50°

When keeping the lightpipes bending angle fixed at 45°, the increasing angle of solar altitude will have the efficiency to be fluctuated but the curvatures of three types of the lightpipes with different lengths are similar. When having sun raising from 0 altitude to 45 altitude, the efficiency increase fast. When the solar altitude angle becomes larger 45°, there is a slight increase with less than 1% growth.

The influence on the straight lightpipes is clearer than others because the incident sunlight will have uniform reflected pattern in the pipe. When the solar altitude angle becomes larger, the angle of sunlight entering the pipe will be closer to the pipe direction. Therefore, there is less possibility that light will be reflected since the light may go to the end of the pipe straightforward. For other lightpipes with different bended angles, it is hard to foresee the reflectivity trend in the pipe for the different light direction and pipe direction. The 30° bended

lightpipes seems to have better efficiency than the straight ones. The reason may be that the smaller elbow of the pipe and the incident sunlight will not be reflected too much when comparing with other elbowed lightpipes.

The reasons for this fluctuation may be the distinction between solar incident angle and the pipe bending angle in the section plane. When the sun raising from  $0^\circ$  altitude to  $45^\circ$  altitude, the sunlight direction changes from horizontally parallel to tilted direction. The incident angle become closer to the pipe elbow angle, so less light will be reflected in the upper bended part of lightpipes. From  $45^\circ$  to  $90^\circ$  solar altitude angle, though there should be less loss from light reflectivity since the incident angle of sunlight the upper bended pipe match similarly, the light will have to be redirected to from the bended part to the straight part.

### **3.3.4 Efficiency of lightpipes with various solar azimuth under clear sky**

If changing the solar azimuth angles, the viable tendencies exist for each lightpipes with different elbows as shown in Figure 3.16. When it comes to the explanation, the straight lightpipes will not be affected when sun moves from south to west. Nevertheless, the bended lightpipes will be affected by the horizontal movement of sun. The difference between lightpipes elbowed part and the incident sunlight direction may result in the increasing frequency of reflection. As a result, it is difficult to predict the efficiency since the solar azimuth angle and bending angle differ. The severe fluctuation might be brought about by the great distinction of incident light and pipe direction. There will be reflection in the upper bended part of lightpipes and also a lot of reflection in the lower vertical part of the pipe. The high frequency of reflection will cause more light loss. When exploring the influence of various solar azimuth angles on the efficiency in terms of sun altitude, it is also hard to regulate

the findings. Although there might be some fluctuation, the whole trend is from decreasing to increasing.

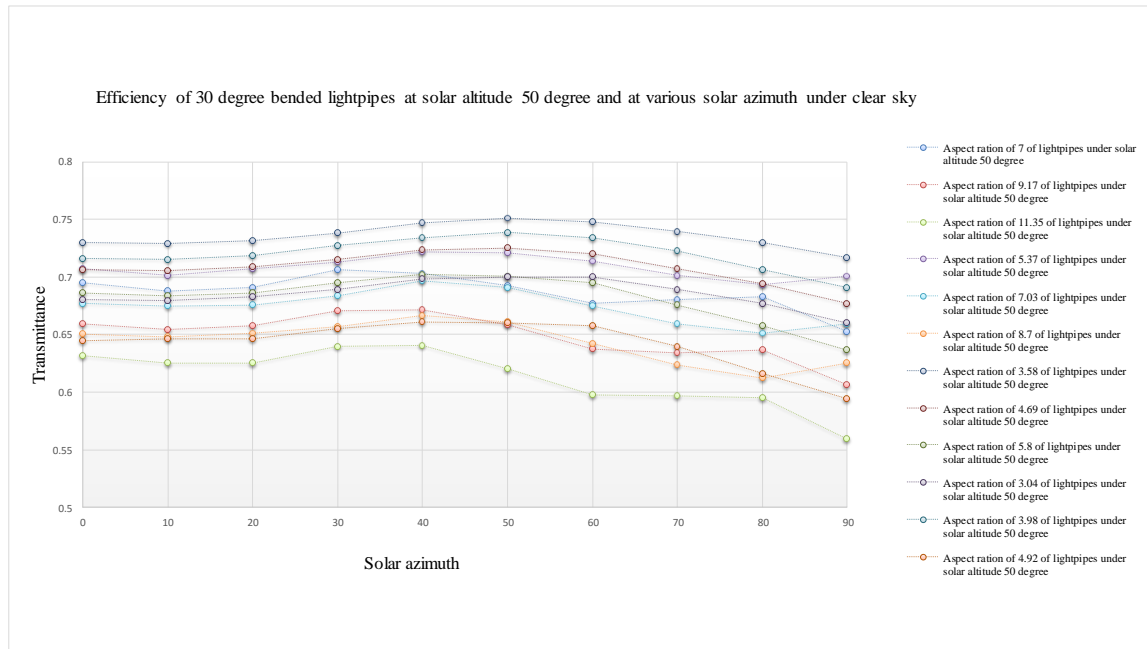


Figure 3.16 Efficiency of 30° elbowed lightpipes at solar altitude 50° and at various solar azimuth under clear sky

### 3.4. Efficiency of various lightpipes under intermediate sky

There are three sky models in Photopia, they are clear sky model, intermediate sky model and overcast sky model. Overcast sky model is not considered in this research due to all the overcast sky models have the same solar altitude. In this study, there is one overcast sky model and the other sky condition is intermediate sky. In this section, the modelling results are not only discussed about the trend under intermediate sky, but also compared with conditions under clear sky model. Some typical angle degree of solar altitude, solar azimuth and measurements of lightpipes are chosen in the discussion.

Elbowed angle of 30° lightpipes with various aspect ratio are chosen to search the change trend. Figure 3.17 and Figure 3.18 shows the efficiency of different aspect ratio and elbowed angle of lightpipes under intermediate sky. Compared with the transmittance under clear sky, it can be see the trend mostly like the condition under clear sky. However, due to the lower solar lighting under immediate sky than under clear sky, the transmittance is a little lower than clear sky.

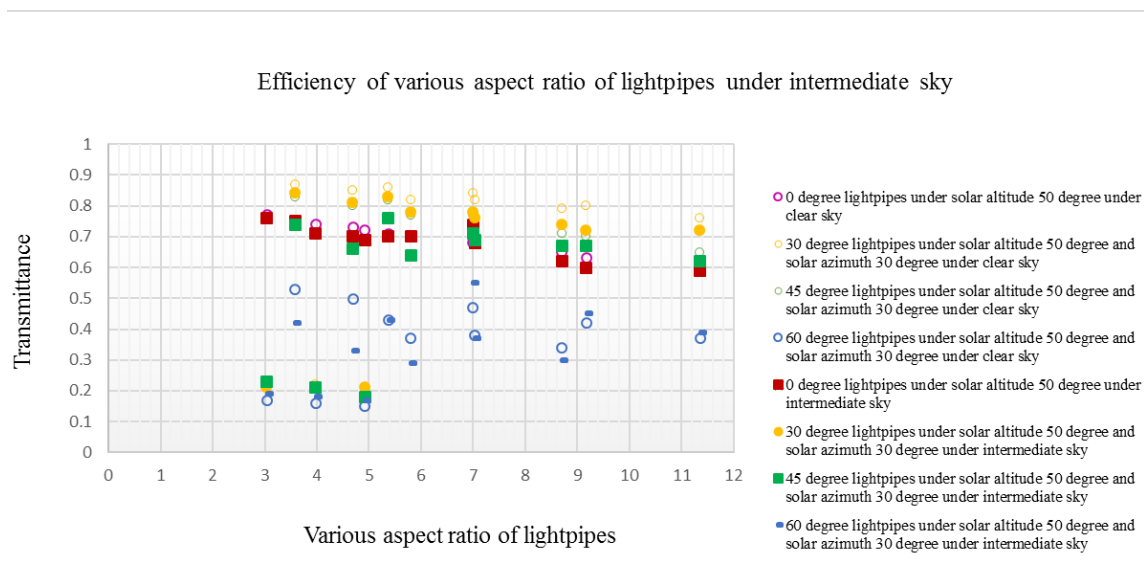


Figure 3.17 Efficiency of various aspect ratio of lightpipes under intermediate sky

Moreover, it can be seen that different aspect ratios lightpipes yield comparable transmittance for straight configuration under various sky conditions but can cause significant difference for different bended angles. Under the same intermediate sky condition, the lightpipe with aspect ratio 8.7 (about 0.75 transmittance) is more than the triple of the lightpipe with 3.98 aspect ratio (about 0.2 transmittance) for the bended angle of 30 degree.

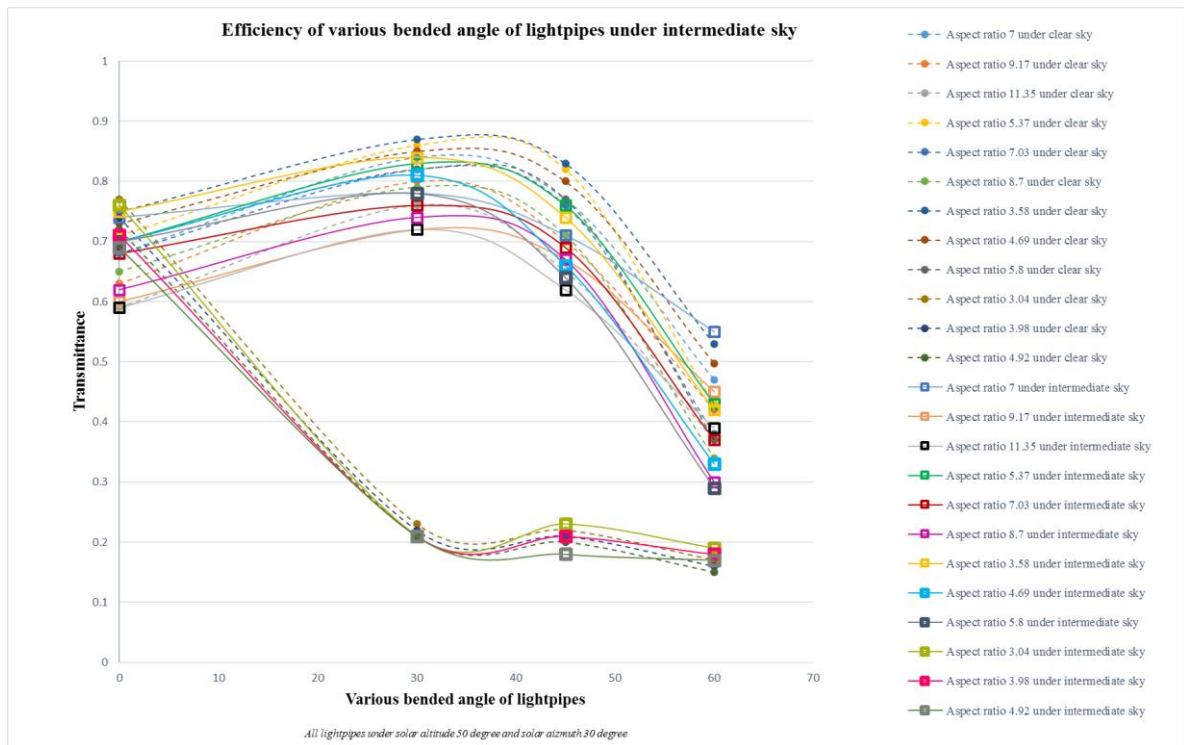


Figure 3.18 Efficiency of various bended angle of lightpipes under intermediate sky

Figure 3.19 and 3.20 illustrate the transmittance performance of lightpipes under various solar altitude and solar azimuth in an intermediate sky condition. It can be seen that transmittance is more sensitive to solar altitude for high aspect ratios while the effect for low aspect ratio is limited. Similar trend has been observed for the solar azimuth. Under various solar altitudes, the highest transmittance occurs around 20 solar altitude while the highest transmittance under various solar azimuth is shifted and not consistent. However, the highest transmittance is concentrated around the low range of solar azimuth and smaller than 30.

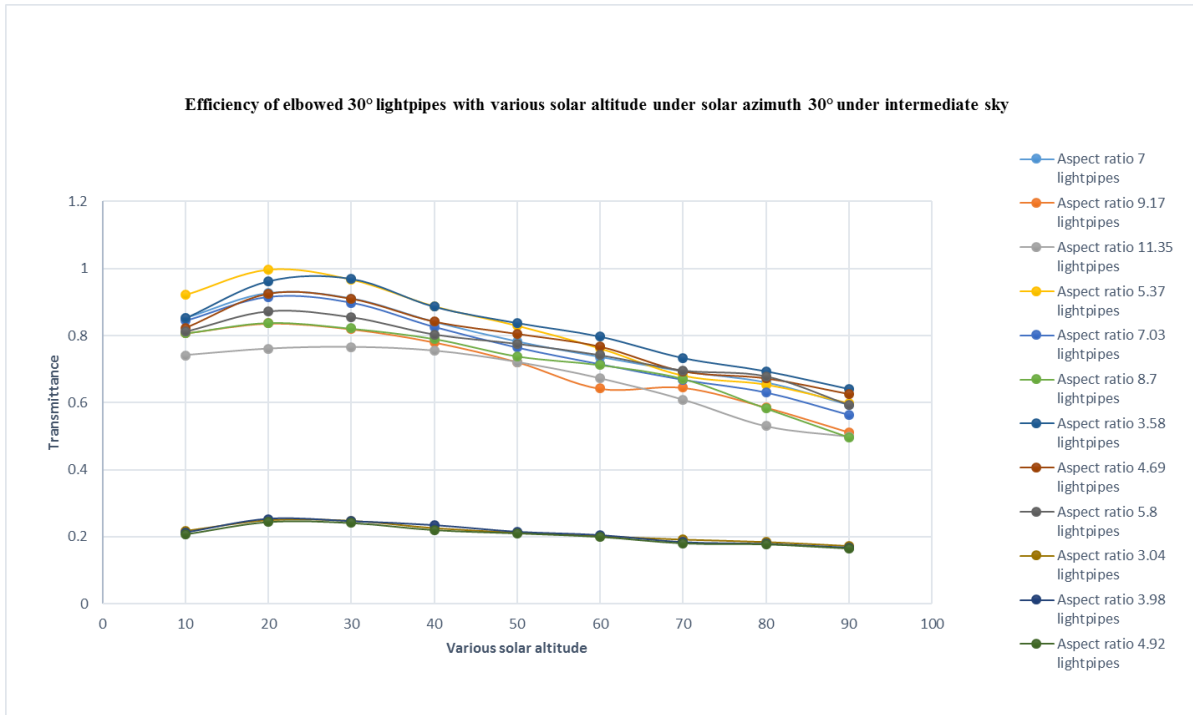


Figure 3.19 Efficiency of lightpipes with various solar altitude under intermediate sky

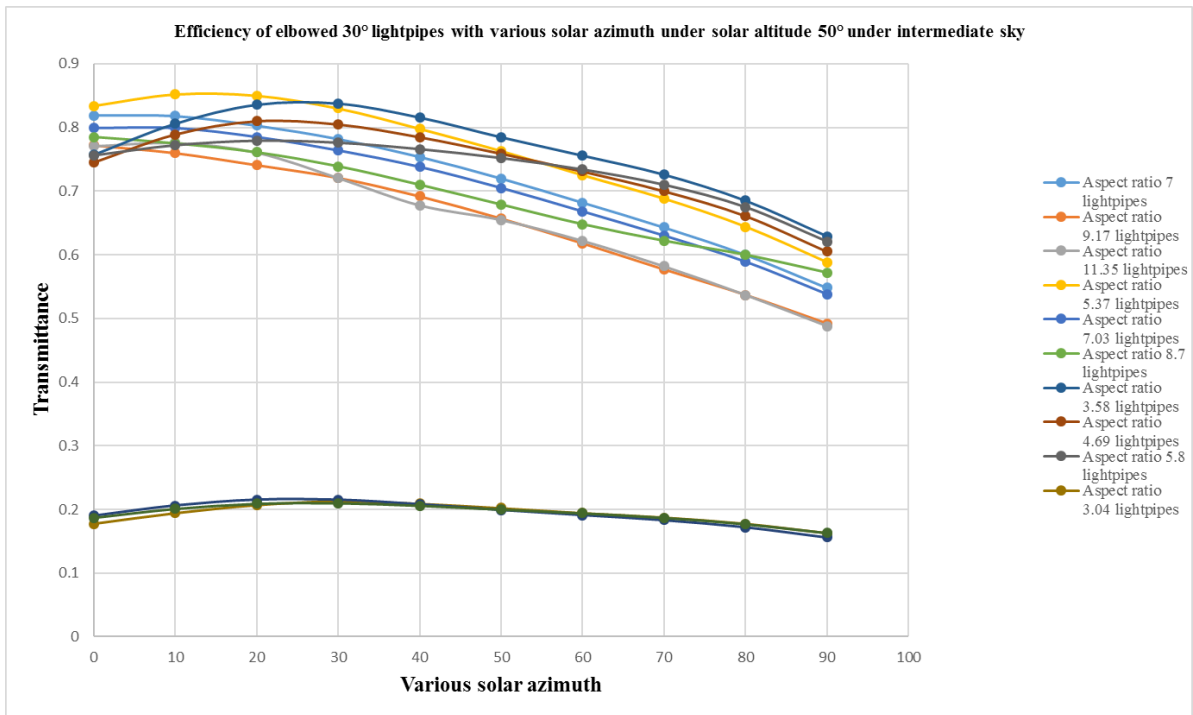


Figure 3.20 Efficiency of lightpipes with various solar azimuth under intermediate sky

### 3.5 Artificial neural network prediction

In this section, ANN network for predicting the performance of lightpipes is configured.

#### 3.5.1 Straight lightpipe prediction by Artificial Neural Network

The ANNs model consisted of one input layer with four input parameters, two hidden layers, one output layer and one output parameter. Four categories of data were chosen as input variables: solar altitude ( $10^{\circ}$ - $90^{\circ}$ ) ( $\alpha$ ), sky clearness index ( $\lambda$ ), tube reflectivity of lightpipes ( $\rho$ ) and aspect ratio ( $A_p$ ). In the simulation, 70% of the input data was used to train the model and 15% was used to validate and testing respectively. Back Propagation (BP) algorithm was employed as the learning algorithm. Nntool was tested in the ANNs modelling. The regression value of them are both close to 0.99 comparing with actual data. A typical configuration is illustrated in Figure 3.21.

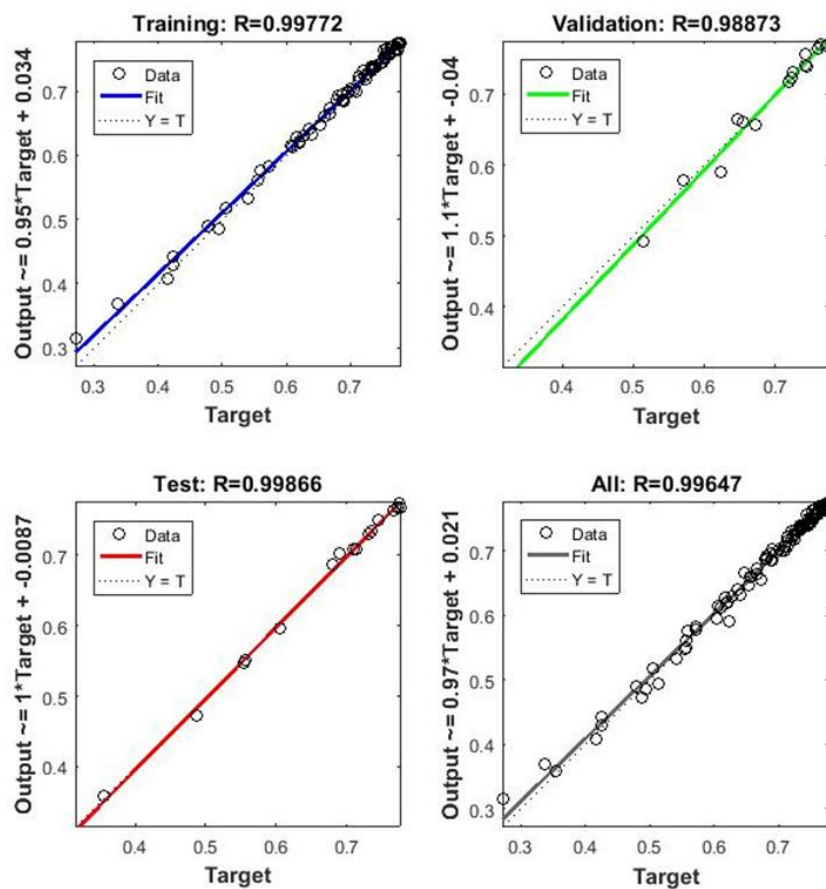


Figure 3.21 ANNs prediction for the efficiency of straight lightpipes

Table 3.6 The correlation coefficients of trained ANN models of straight lightpipes

Lightpipes type	Independent parameters	Dependent parameters	R				R <sup>2</sup>	MSE
			Training (70%)	Validation (15%)	Test (15%)	All (100%)		
Straight lightpipes	$\alpha, \lambda, \rho, A_p$	$\tau$	0.9977	0.9887	0.9987	0.9965	0.9930	0.0005

### 3.5.2 Straight and bended lightpipe prediction by Artificial Neural Network

Training and test sets were prepared for the network initialization. The network was tested with the transfer functions (activation function) logsig and tansig and the results were very similar. The test was carried out completely, with a cross-validation comprising 10 rounds. Table 3.7 compares the results obtained using transfer functions logsig and tansig. It shows the results for the determination and correlation coefficients, MSE and R<sup>2</sup> for the sets using both functions. It can be noted that the correlation and determination coefficients obtained from the two functions are very close, and if rounded to two decimal places they would be equal. Having said that, the MSE and R<sup>2</sup> values of the function logsig group have yielded lower results and as such, the function logsig was selected for the network.

Table 3.7 Comparison between results obtained using transfer functions logsig and tansig.

$N_h$	Tansig function group		Logsig function group	
	R	R <sup>2</sup>	R	R <sup>2</sup>

<b>10</b>	0.8399	0.7054	0.8380	0.7022
<b>20</b>	0.8388	0.7036	0.8496	0.7218
<b>30</b>	0.9190	0.8446	0.9733	0.9473
<b>40</b>	0.8557	0.7322	0.8534	0.7283
<b>50</b>	0.9825	0.9653	0.8495	0.7217
<b>60</b>	0.8519	0.7257	0.8542	0.7297

The configuration parameters of the best prediction capability ANN model architecture is listed in Table 3.8 and also illustrated in Figure 3.24.

Table 3.8 Parameters for the best configuration of ANN model for total lightpipe prediction

<b>Name</b>	<b>TANSIGPURLIN50</b>
<b>Network type</b>	Feed-forward backprop
<b>Input data</b>	$\alpha, \beta, \lambda, \rho, A_p$
<b>Target data</b>	$\tau$
<b>Training function</b>	TRAINLM
<b>Adoption learning function</b>	LEARNGDM
<b>Performance function</b>	MSE
<b>Number of layers</b>	2
<b>Properties for layer 1</b>	Number of neurons: 50
<b>Properties for layer 2</b>	Transfer function: PURELIN
<b>Minimum gradient</b>	1e-07
<b>Epochs</b>	10000
<b>Expected final error</b>	6
<b>Learning rate</b>	0.001

Figure 3.22 shows the MSE results of training, validation, testing and the best modelling. The best MSE performance is 0.0043 when the epoch is 276. The error quickly decreases to smaller than 0.01 with epochs increasing and the errors of testing and validation sets have similar characteristics. Moreover, overfitting does not occur because neither testing nor validation error increased before epoch 276. Figure 23 shows the linear regression of network outputs with respect to targets for training, validation, testing and all sets. The R values of training, validation, test and all are 0.9826, 0.9828, 0.9823 and 0.9825, respectively. So the fit is very good and the output tracks the targets very well for all datasets. Therefore, the established ANN can well predict the target variables.

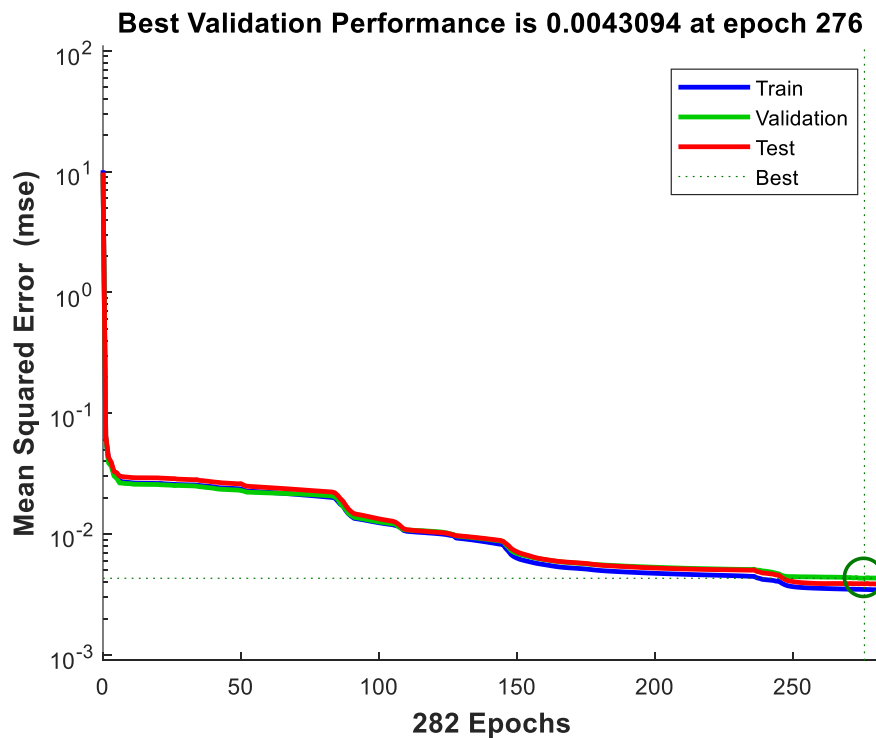


Figure 3.22 The prediction MSE value of ANN model

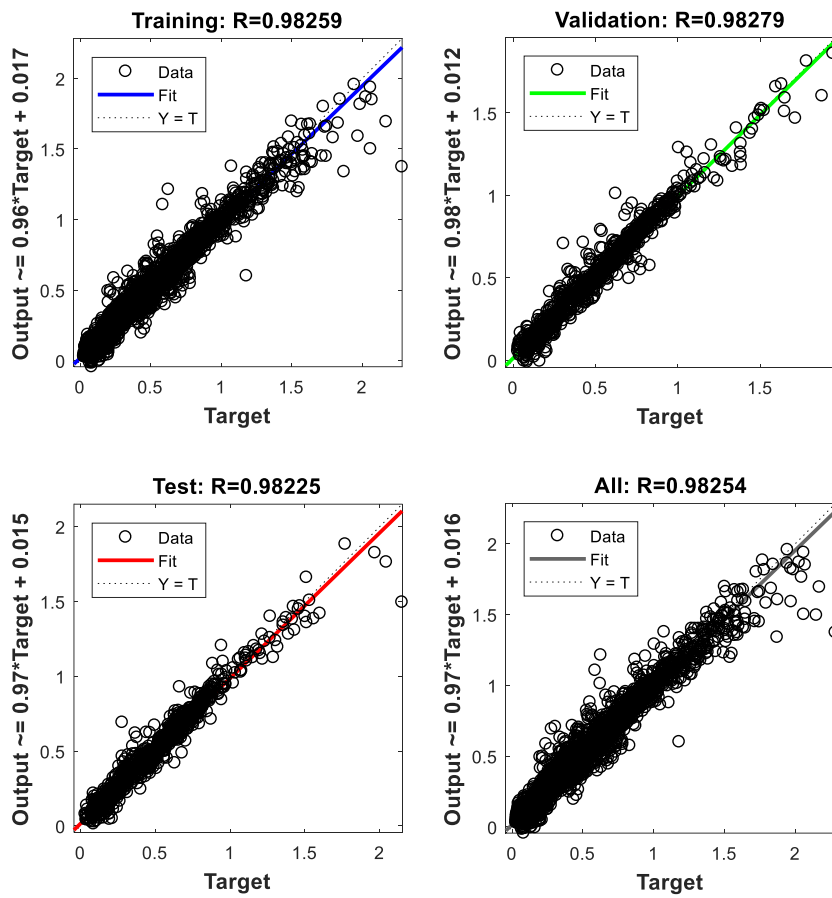


Figure 3.23 The illustration of regression relationship between prediction values and target values in the ANN Training, Validation and Test procedure

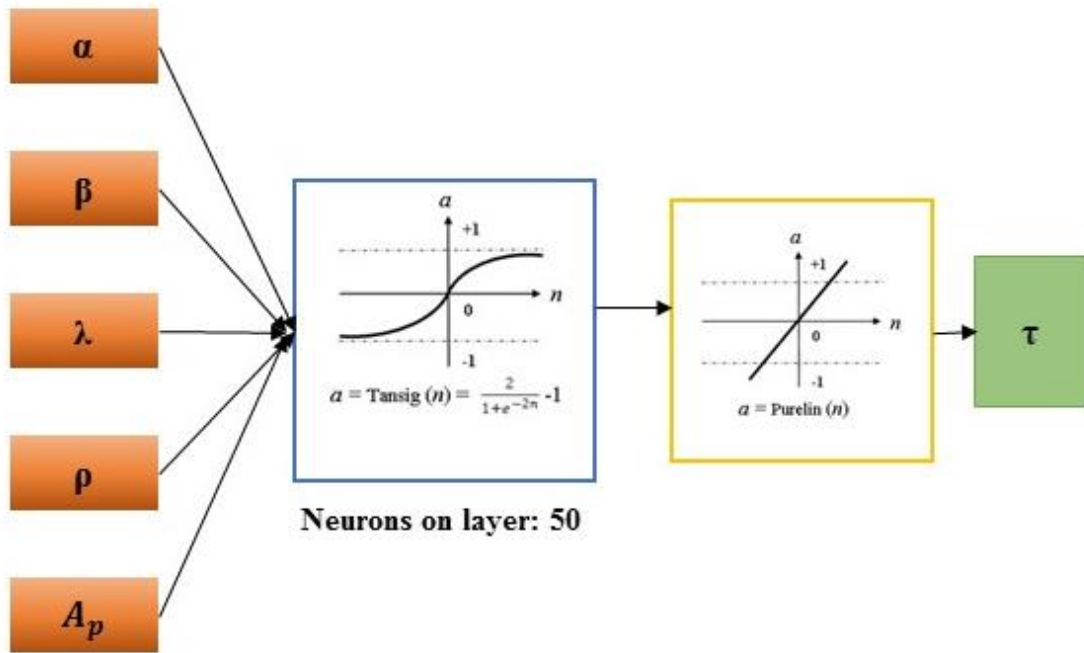


Figure 3.24 A graphic of the best performance ANN architecture (including the input parameters, the output parameters and the neurons number of hidden layer)

In the case of the training function (or learning algorithm), the traingda function was adopted and the results obtained were satisfactory. The network architecture was structured with five input parameters, fifty hidden nodes and one output parameter. The numbers of input and output parameters do not vary since they correspond to the model variables and to the consumption of each one, respectively. However, the number of neurons in the hidden layer may vary through the tests carried out, and fifty neurons was found to be an adequate number.

The following training parameters were defined: minimum gradient 0.0001, maximum number of epochs required for the network to be trained 1000; expected final error 0.000001 and learning rate 0.001.

To determine the number of epochs applied in the training phases, the starting number of epochs was 1000, increasing to 2000, and finally adopting 2000. Despite being slightly more demanding in terms of time, this was considered to be a suitable number of training epochs for this problem. In most cases the best performance reached an average of 276 epochs.

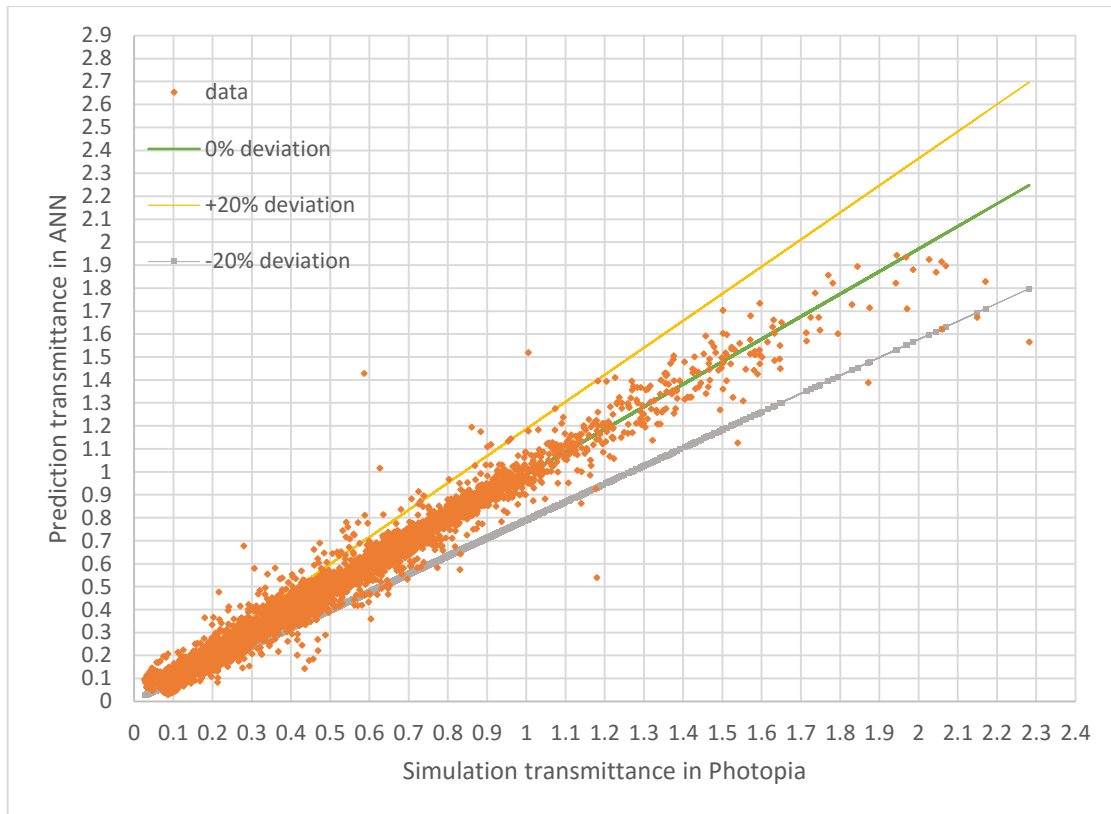


Figure 3.25 Predicted transmittance in ANN versus simulated transmittance of lightpipes in Photopia

It was observed that the network provided a clear representation of the actual results. To verify this, the  $R^2$  and  $r$  values from each set trained, together with the Mean Squared Error (MSE) for the sets, are displayed in Table 3.9. It can be seen that in all cases the training  $R^2$  value was greater than 0.96, which indicates good data prediction. The  $R$  for training, validation, test and all is 0.9826, 0.9828, 0.9823 and 0.9825 respectively. In addition, the average MSE values for the test sets was 0.0043, less than 0.05 as recommended in the literature.

Table 3.9 The correlation coefficients of trained ANN model models of 0°, 30°, 45° and 60° elbowed angle of lightpipes

Lightpipe types	Index	De	R				R <sup>2</sup>	MSE
			Training 70%	Validation 15%	Test 15%	All 100%		
0°, 30°, 45° and 60° elbowed angle of lightpipes	$\alpha, \beta,$ $\lambda, \rho,$ $A_p$	$\tau$	0.9826	0.9828	0.9823	0.9825	0.9654	0.0043

\* Index represents the independent parameters; De represents the dependent parameter.

### 3.5.3 Artificial Neural Network limitations and improvements

The major limitations of ANNs in daylighting prediction include over training, extrapolation errors and network architecture optimization.

**Over Training:** In ANN training procedure, if too large capacity or too many iterations are allowed, over training will occur [91]. Before running ANN simulation, considerable high precision or large number of training cycles are always pre-set to define when to stop training. However, due to the experimental uncertainty, some training data from actual engineering experiment are erroneous. Hence, over high precision will cause over fitting and reduce the prediction accuracy. In order to overcome this problem, the number of training cycles and input data need to be optimized. Wijayasekara et al. elaborated EBaLM-OTR method to reduce the over training error [92].

**Extrapolation ineffective:** Because the data used to train ANN model sometime cannot cover the entire range of the data, the extrapolation is sometimes ineffective. When preparing the input data for training ANN model, the maximum and minimum values should be selected from all the proposed data. Some training samples can be drawn using empirical correlations, which cover the entire range as much as possible. The range of the training data must be representative of entire operating range of the system in order to reduce the extrapolation errors [91].

**Network optimization:** The key point of the ANN accuracy is to choose the best network parameters, such as the number of hidden layers, the number of neurons in hidden layer, momentum factor, learning rate, number of training data and variables. However, the ANN network initialization and architecture are dependent on the experience of the users. In order to get relatively the “best” ANN architecture, repeating trials are needed to optimize the ANN model, which can waste a lot time and the model received may not be the best eventually. Some methods are used to overcome these drawbacks. The number of neurons in hidden layers always use the following equation [6] for optimization [87].

$$L = \sqrt{m + n} + a, \quad a \in [1, 10] \quad (3.7)$$

where L is the number of neurons in hidden layers, m is the number of neurons in input layer, n is the number of neurons in output layer, and a is an adapting variable, which range from 1 to 10. Liu et al. [93] introduced a Genetic Algorithm (GA) and particle swarm optimization (PSO) based ANN approach to optimize the network parameters. The optimum network parameters have been determined using GA/PSO to minimize the time and effort. The GA/PSO component is found to be a good alternative to the conventional trial and error approach to optimize the network configuration quickly and efficiently.

## **Training data requirement**

ANNs model is very strong tool to solve the problems with large number of input variables data. The input data can be split into training data, testing data and validation data. Improper data splitting can lead to a poor prediction ability [94]. Hence, proper selection and splitting of input data is very important in order to attain high accuracy. Experimental uncertainty and theoretical assumptions may influence the reliability of input training data. Hence, the training data would require novel optimization techniques before being used.

## **Improvement in ANNs**

Due to few studies focusing on using ANN models to predict the daylighting, the research in overcoming the limitation of ANNs in daylighting in particular has been scarce. However, other successful examples are worth to be adopted to overcome the limitation in ANN prediction in daylighting. The flow of the ANNs structure, optimizing the input variables data, the number of neurons in hidden layers, the number of hidden layers and the output data could be considered to improve the accuracy of ANN prediction models.

### **(1) Input variables improvement**

Kubota et al. [95] used GA for the variable extraction and selection on measured data, and then fuzzy neural networks were developed for the building energy load prediction. In this method, the variable extraction means translating original variables into meaningful information that is used as input in the fuzzy inference system. Hou et al. [96] integrated rough sets theory and a neural network to predict an air-conditioning load. Rough sets theory was applied to find relevant factors influencing the load, which were used as inputs in a neural network to predict the cooling load. Karatasou et al. [97] studied how statistical procedures can improve neural network models in the prediction of hourly energy loads. The statistical methods, such as hypothesis testing, information criteria and cross validation, were applied in

both inputs pre-processing and model selection. Experimental results demonstrated that the accuracy of the prediction is comparable to the best results reported in the literature.

### (2) Optimization of the neurons number of hidden layer

Hegazy and Ayed [76] defined Excel spreadsheet method to simplify the optimization of the neurons number of hidden layers. The method was then applied in [40] which used 5 or 6 neurons in hidden layers and resulted in 35.87% and 20.62% errors respectively. The number of neurons were then increased to 7, 8, 9 and 11 and they found all had 2.20% error. They finally concluded that 7 neurons was the best number for the network construction.

### (3) Output variables improvement

The outputs of neural networks may not be exactly what we expected. Saxena et al. [98] proposed a fuzzy logic to correct the outputs by post-processing the results of neural networks. The fuzzy assistant allows the user to determine the impact of several building parameters on the annual and monthly energy consumption. Some comparisons between neural network and other prediction models were performed in the research in Chapter 4.

## **3.6 Summary**

This Chapter has simulated a number of commercial lightpipes examples in Photopia. The solar altitude was ranged from  $10^\circ$  to  $90^\circ$ , and solar azimuth was ranged from  $0^\circ$  to  $90^\circ$ . The sky condition was clear and intermediate respectively. Different elbow angles were considered, i.e.,  $0^\circ$ ,  $30^\circ$ ,  $45^\circ$  and  $60^\circ$ . In addition, the length of lightpipes were 1000mm, 1500mm and 2000mm. It can be concluded that lightpipes is an efficient device which functions well in introducing daylight into buildings. Compared with elbowed lightpipes, the straight lightpipes work more efficient than elbowed lightpipes. However, in real practical application, elbowed lightpipes has been more widely used than straight lighpipes. In terms

of bended lightpipes, the small aspect ratio (i.e., short tube length and large diameters) would be most effective. In overall, the contributions of lightpipes include energy savings, visual satisfaction and healthy and improved indoor environment.

A three layers Artificial Neural Network was developed to predict the optical performance of lightpipes. The input parameters included six factors, namely, solar altitude, solar azimuth, sky clearness index, elbow angle of lightpipes, aspect ratio and reflectivity of tube. The output parameter was the transmittance of lightpipes. The  $R^2$  could achieve 0.9653 and MSE reached 0.0043. Almost all the prediction values reached  $\pm 20\%$  deviation compared with target values, which proved the ANN prediction model had strong forecast ability.

**Chapter 4 Predicting the transmittance of  
lightpipes by multiple nonlinear  
regression model and comparing with  
Artificial Neural Network (ANN) model**

## 4.1 Introduction

Lightpipe is conventionally used as an alternative source of luminous energy that can bring natural light to the inside of buildings. The lighting energy transported through the lightpipe is a renewable energy. A literature review on daylight transport systems (DTS) revealed that lightpipes can reduce the total building energy used for electrical lighting in buildings up to 20-30% [99]. The preceding chapters have discussed the prediction methods relative to lightpipes. Physical model, computer simulations or the novel ANN have their own advantages and disadvantages. ANN is outstanding in predicting lightpipes performance. However, it requires numerous simulations and scientific knowledge, which hinders the widespread application to the non-professional users. It is therefore desirable to propose a formula for the performance of lightpipe. Given the location of building and geometric of lightpipe, the establish formula can be used to choose suitable lightpipe orientation and configuration.

To date, several researches have proposed available empirical formula to predict optical performance of lightpipes. However, the prediction results often yield errors due to a variety of reasons, such as lack of adequate data, formulation limitations, etc. Alternatively, some formula are too complicated to be applicable in real projects. In this chapter, based on numerous simulations data from Photopia, several potential mathematical models are proposed by multiple nonlinear regression. It is possible to predict the transmittance of various lightpipes by given solar altitude, solar azimuth, elbowed angle of lightpipes, aspect ratio, sky clear index, reflectivity of the lightpipes' tube. The validation and limitations of the models are proposed to discuss the feasibility and reliability of the models as well. On the basis of the regression models, the transmittance of lightpipes can be calculated in a fast and accurate manner rather than the time-consuming raytracing simulations. As such, the performance of

lightpipes and the choice of suitable lightpipes elbow angle and install position could be determined in a convenient way.

## 4.2 Summary of previous work on mathematical models

### 4.2.1 Straight lightpipe

The first formula of lightpipes was contributed by Zastrow and Wittwer [100] in 1980's. the transmission  $T$  was expressed as follows:

$$T = R^{l \tan \theta / D_{effective}} \quad (4.1)$$

where  $R$  is the reflectivity of the lightpipe,  $l$  is the length of lightpipe and  $\theta$  is the angle of incidence of the illuminating radiation with respect to the lightpipe axis. This formula is validation only in the condition of low ratio of pipe diameter to length, low incident angles and high reflectance.

Swift and Smith [38] proposed an integral equation to calculate the transmission of cylindrical mirror lightpipes. They found relationship between the transmission and lightpipes parameters, reflectivity and aspect ratio, the angle of incidence of the incident radiation by using a HeNe laser light source to ray track through the pipe. The equation can be written as follows:

$$T = \frac{4}{\pi} \int_{s=0}^1 \frac{s^2}{\sqrt{1-s^2}} R^{int[p \tan \theta / s]} (1 - (1 - R)(p \tan \theta / s) - int[p \tan \theta / s]) ds, \quad (4.2)$$

where  $p = l/d$  is the aspect ratio of the lightpipes. This expression shows good agreement with the experimental results and much more straight-forward than Zastrow and Wittwer

[100]. The drawback of Equation (4.2) is it suits for relative parallel light. However, apart from the direct light, the real daylight is mixed of diffuse skylight and sunlight.

#### 4.2.2 Elbow lightpipe

The prediction of elbow lightpipe is much more complex than straight lightpipe. However, it is also necessary to guide because it is widely used on a sloped roof down vertically through the ceiling construction. And in the real condition of sun positions and sky patterns, the efficiency of bended lightpipe is larger than straight lightpipe. Normally it is much more difficult to determine the light flow transport in bended tubes when lightpipe placed on slope roofs as a bend is necessary to adjust the vertical pass through the ceilings.

The predictive technique of Zhang and Muneer [101] is designed for lightpipes with an “opal” or cloudy diffuser. The predictions are largely based on illuminance or daylight factor measurements (taken over four months) of light pipes of diameter 0.21m, 0.33m, 0.45m and 0.53 m, varying between 0.6m and 1.2m in length. Extrapolation is then used for light pipes of other dimensions, although the most reliable predictions will be within the dimensions of the pipes used in the study. By measuring the effects of adding 30° elbow sections, pipe bends were also considered so as to produce two separate models (i.e., for straight and elbowed light-pipes).

The simplified DPF model of Zhang-Muneer is, for straight pipes,

$$DPF = (192.5 - 108.8k_t - 0.3\alpha)\rho^{(132.4+4.4A_{pe}+8.6 \cot \alpha-2.6A_{pe} \cot \alpha)} R^2 \frac{(V/D)^{1.3}}{D^2} \quad (4.3)$$

for elbowed pipes,

$$\text{DPF} = (192.5 - 108.8k_t - 0.3\alpha)\rho^{(132.4+4.4A_{pe}+8.6\cot\alpha-2.6A_{pe}\cot\alpha)} R^2(1 - f_{loss})^N \frac{(V/D)^{1.3}}{D^2} \quad (4.4)$$

where  $k_t$  is the sky clearness parameter,  $\alpha$  is the solar altitude,  $\rho$  is the pipe reflectance,  $A_p$  is the aspect ratio of the straight pipe,  $A_{pe}$  is the ratio of the elbowed pipe,  $R$  is the diameter of the pipe,  $f_{loss}$  is the “energy-loss factor”,  $N$  is the number of 30° bends,  $V$  is the vertical distance from the diffuser to the point of interest and  $D$  is the direct distance from the lightpipe diffuser to the point of interest.

Jenkins and Muneer [102] proposed a series of simplified semi-empirical equations to predict the performance of lightpipes. There is no restriction on the number of bends and the bend angle in the prediction. The essential input parameters needed in this equation are external illuminance, pipe dimensions, elbow configuration and pipe positions and floor area. The luminous flux leaving the pipe,  $\Phi$  is presented as follows,

$$\Phi = E_{ex}\tau\pi r^2, \quad (4.5)$$

where  $E_{ex}$  is the external illuminance,  $\tau$  is the total pipe transmission including diffuser and collector and  $r$  is the cross sectional radius of the pipe. Rather than input the transmission explicitly, an expression was found from measurements as a function of aspect ratio to give,

$$\Phi = 0.82E_{ex}e^{-0.11A}\pi r^2, \quad (4.6)$$

where  $A$  is the aspect ratio of the lightpipe length over the lightpipe diameter.

The internal illuminance  $E_{in}$  is then given by:

$$E_{in} = 0.494\phi \frac{\cos^4 \theta}{V^2}, \quad (4.7)$$

where  $V$  is the vertical distance from the diffuser to the point of interest and  $\theta$  is the angle between the vertical line joining the centre of the diffuser with the point of interest. For each elbow, the elbow factor  $\chi$  is introduced into the straight pipe Eq. (4.7), where

$$\chi = e^{-0.0052\beta}, \quad (4.8)$$

and  $\beta$  is the angle of the pipe elbow.

The shortback of this equation is the solar altitude and sky clearness parameters are not considered in it. So the illuminance prediction results of these equations could only be a design guide, not yielding accurate values.

Kocifaj and Kundracik et al. exploited a semi-analytical model with basic formulae for the purposes to solve the complexity of bended lightpipe [103]. They used theoretical solution to forecast the light transmission of a bended lightpipe. However, due to this complexity and the lengthy derivation and explanations, it is difficult to be applied in practice.

#### **4.2.3 Su et al. regression formula**

Su et al. exploited an empirical formula by monitoring of various sized lightpipes at a purposely built test shed with a pitched roof [37]. By monitoring the lightpipes, numerous of data have been recorded to establish a formula to predict the performance. The relative input

parameters are horizontal global illuminance, the lightpipes' diameter and length, the specular reflectance, solar altitude, solar azimuth. The orientation of elbow lightpipes (for straight lightpipes the degree is 0°).



Figure 4.1 The demonstration of the purposely built shed for testing lightpipes [37]

The basic formula from Zastrow and Wittwer, who conducted the earliest theoretical work on light transmission through a mirror-finished pipe of arbitrary cross section. They established an approximate equation correlating the transmittance of a lightpipe with its geometrical and optical parameters that is:

$$T = \rho^{A_p \tan \theta} \quad (4.9)$$

where  $\rho$  is the specular reflectance.  $A_p = L/D$  is the aspect ratio, i.e., the ratio of length to diameter or equivalent diameter.  $L$  is the length of lightpipes (m).  $D$  is the diameter of lightpipes (m).  $\tan \theta$  is the tangent of the incidence angle (between the incident light and the axis of lightpipes).

$$\tau = \frac{\text{lumen}}{E_{\text{ext}}A} = (a_0 + a_1\alpha + a_2\beta + a_3\lambda + a_4\alpha\beta + a_5\alpha\lambda + a_6\beta\lambda + a_7\alpha^2\beta\lambda + a_8\alpha\beta^2\lambda + a_9\alpha\beta\lambda^2 + a_{10}\alpha^2\beta^2\lambda^2)\rho^{(b_1A_p+b_2(1/\tan\alpha)+b_3(A_p/\tan\alpha))} \quad (4.10)$$

where  $\tau$  is the lumen ratio of output to the external horizontal.  $\alpha$  is the solar altitude,  $0-90^\circ$ .  $\beta = |\text{solar azimuth} - 180^\circ - \text{the orientation of elbow}|$  (where the solar azimuth:  $0^\circ$  (north),  $90^\circ$  (east),  $180^\circ$  (south),  $270^\circ$  (west), the orientation of elbow:  $0^\circ$  (south),  $-90^\circ$  (east),  $90^\circ$  (west)).  $\lambda$  is the ratio of the actual horizontal global illuminance  $E_{\text{ext}}$  to the theoretical value under the CIE clear sky. The theoretical horizontal global illuminance could be calculated from the given solar altitude. The correlation is given in Figure 4.2.  $\rho$  is reflectance of lightpipe, it was assumed to be 0.95 according to the manufacturer.  $L$  is length of lightpipes (m).  $D$  is the diameter of lightpipes (m).  $a_0 - a_{10}$ ,  $b_1 - b_3$  are the coefficients.

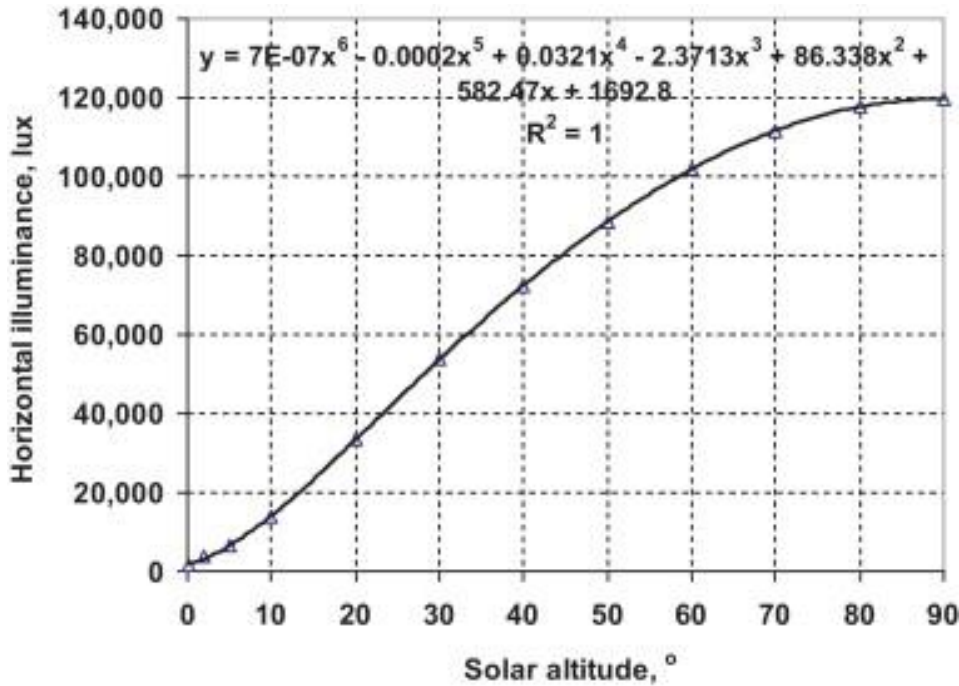


Figure 4.2 Horizontal global illuminance under the CIE clear sky versus solar altitude [37]

The advantage of Su's model is the solar azimuth and the orientation of the elbow are included in the formulation. This is particularly necessary for the bended lightpipes. Moreover, instead

of using the sky clearness index (defined as the ratio of global to the extra-terrestrial irradiance), the ratio of the actual horizontal global illuminance  $E_{ext}$  to the theoretical value under the CIE clear sky was used. Such ratio is more suitable to indicate the level of sky clearness. It was found that a better regression result could be achieved. The regression constants for the elbowed and straight lightpipes are listed in Table 4.1 and 4.2 respectively.

Table 4.1 Regression constants for elbowed lightpipes

$a_0$	0.816107343
$a_1$	0.565594828
$a_2$	-0.001386091
$a_3$	0.002749844
$a_4$	0.005284653
$a_5$	-0.002801175
$a_6$	1.39112E-05
$a_7$	-0.000162761
$a_8$	5.13272E-07
$a_9$	-3.19153E-06
$a_{10}$	5.53944E-08
$b_1$	2.094452
$b_2$	-3.5E-05
$b_3$	0.083696

Table 4.2 Regression constants for straight lightpipes

$a_0$	1.146112964
$a_1$	-0.770250745

---

$a_2$	-0.002965636
$a_3$	0.00053072
$a_4$	0.016810832
$a_5$	0.00637853
$a_6$	2.99647E-05
$a_7$	-0.0001535
$a_8$	-1.18966E-06
$a_9$	-2.78047E-06
$a_{10}$	6.19193E-08

---

The results have shown that the majority of the predicted values fall within  $\pm 20\%$  of the measured data.

## 4.3 Methodology

### 4.3.1 Models of lightpipes

The transmittance is defined as index to evaluate the optical performance of lightpipes. Su's [37] mathematical model has relatively accurately found the relationship between transmittance and given solar altitude, solar azimuth, elbowed angle of lightpipes, aspect ratio, sky clear index, reflectivity of the lightpipes' tube. In this Section, various lightpipes were chosen to demonstrate the correlations between the transmittance and impact factors. As mentioned in Chapter 3, the typical lightpipes configuration includes dome, light tube and diffuser. In this study, the bended angles of lightpipes are from  $0^\circ$  (straight lightpipes) to  $60^\circ$ , the length of lightpipes are from 1000mm to 2000mm, the diameters are from 230mm to 530mm. For the purpose of applying lightpipes to the roof of buildings, different solar altitude

and solar azimuth are chosen in this research as research object. Mass simulation data has been acquired in Chapter 3 by using Photopia simulation. Figure 4.3 is one type of the light pipes with three components, i.e., the dome, the reflective tube, and the diffuser lens; in addition, the reference surface is illustrated.

However, as discussed in Chapter 3, ANNs have advantage in predictions based on limited data. Moreover, Su's regression equation presents strong ability of practical application and relatively good prediction capability. Thus, on the basis of Su's model, this chapter developed a predication formula. Because of the application of Photopia, a large number of dataset could be obtained from simulation. A comprehensive dataset including the three sky conditions (i.e., only sun, overcast and clear sky) were determined via Photopia.

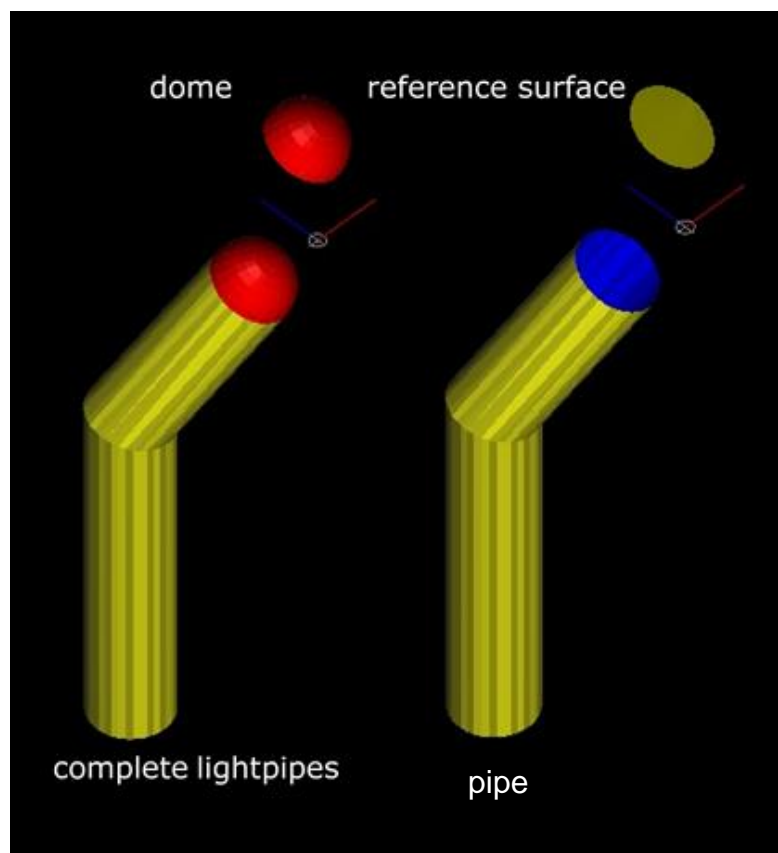


Figure 4.3 A single group of a single type of lightpipes

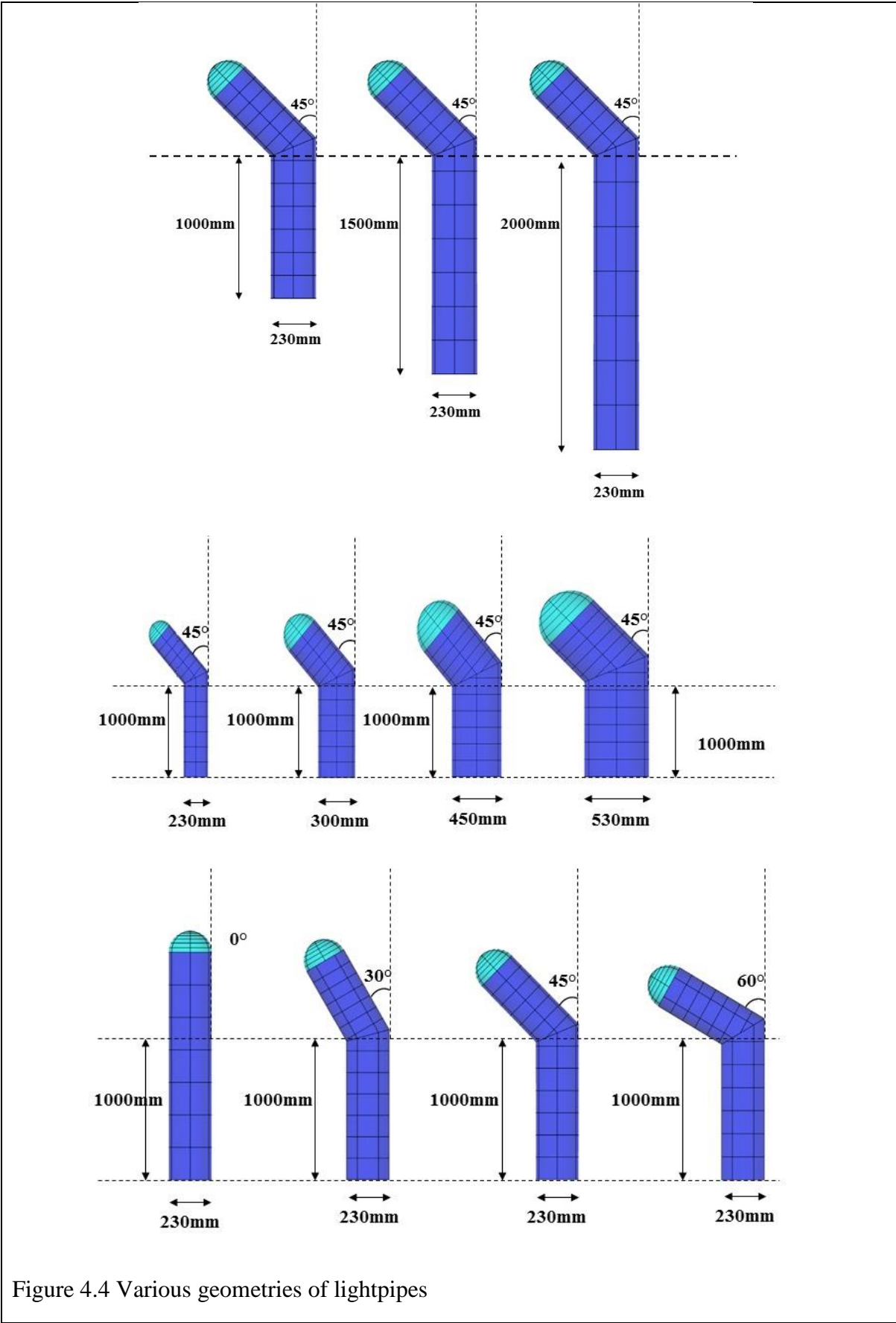


Figure 4.4 Various geometries of lightpipes

### 4.3.2 Multiple nonlinear regression

Multiple nonlinear regression is a kind of regression analysis by which the relationship between observation data can be described using a function. The dependent variable is determined by several independent variables through nonlinear combinations in a multiple nonlinear regression model. Matlab as a strong mathematical tool was used to search the relationship between the independent variables and dependent variables. The function “Fit nonlinear regression model” (fitnlm) in Matlab was used in this study. It can be expressed as follows:

$$\text{Mdl} = \text{fitnlm}(\text{x}, \text{y}, \text{modelfun}, \text{beta0}) \quad (4.11)$$

where the x is a matrix of predictor variables and the y is a response variable.

The goodness of fit always utilizes the coefficient of determination ( $R^2$ ), the Mean Square Error (MSE), the Sum of Square Errors (SSE), and the Root Mean Squared Error (RMSE) to evaluate. In terms of mathematic principle, MSE, RMSE and SSE are related very closely. They all compare the prediction values and target values. However, the R-square compares the prediction value and average of target value. Hence, in this study, the MSE and R-square are chosen to define the goodness of regression. If MSE is closer to 0, it means the model is more accurate. To the opposite, if  $R^2$  is closer to 1, it means the prediction data is closer to the target data and thus the model simulated is more representative and realistic. As shown in Table 4.3, there are four levels for evaluation of accuracy of forecasting.

Table 4.3 Four levels for evaluation of ANNs [61].

<b>MSE≤10%</b>	<b>10%≤MSE≤20%</b>	<b>20%≤MSE≤50%</b>	<b>MSE≥50%</b>
High prediction accuracy	Good prediction accuracy	Reasonable prediction accuracy	Inaccurate prediction

$$MSE = \frac{1}{N} \sum_{i=1}^N (\hat{y}_i - y_i)^2 \quad (4.12)$$

$$R^2 = 1 - \frac{\sum_{i=1}^N (\hat{y}_i - y_i)^2}{\sum_{i=1}^N (y_i - \bar{y})^2} \quad (4.13)$$

where  $\hat{y}_i$  is the predicted illuminance value for times  $i$ ;  $y_i$  is the simulated illuminance value for times  $i$ ,  $\bar{y}$  is the average illuminance value; and  $N$  is the number of data points used for evaluation. In this study,  $R^2$  and MSE were chosen to estimate the prediction performance of mathematic models.

### 4.3.3 Variables settings

Su's mathematical model has been proposed to assess the parametric effects of the transmittance of lightpipes. In terms of independent variables, the angular relationship between the sun and the lightpipes is the most important impact factors to influence the transfer performance of the lightpipes. Hence, as independent variables, the solar altitude, solar azimuth and the elbow angle of lightpipes are the most important impact factors in terms of transmit performance of lightpipes. In order to find the accurate and complete relationship between the sun position and the transmittance performance of lightpipes, in the simulation procedure, various sky models with different sun positions were chosen to include as many incident angles as possible. Figure 4.7 illustrates the schematic of sun positions and lightpipes in this study.

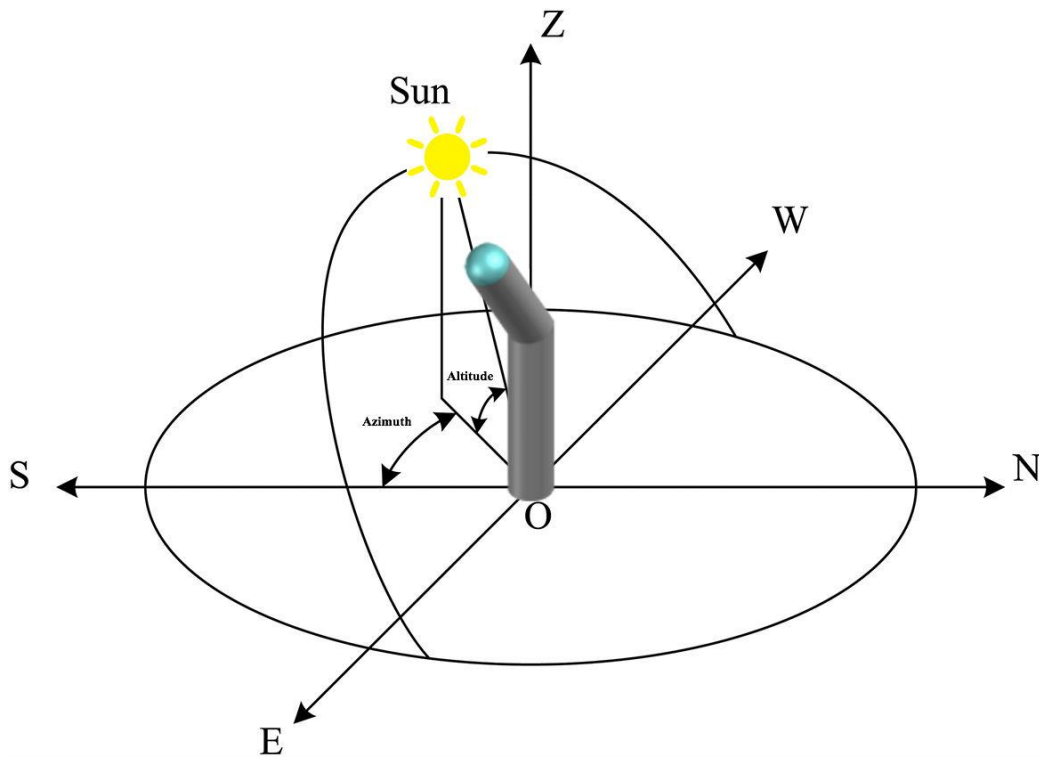


Figure 4.5 Illustration of the schematic of sun positions and lightpipes.

The performance of lightpipes is largely dependent on the sky clear condition. The skylight and sunlight illuminance are also impacted by the sky clear condition. Thus, sky clearness index as an important variable was introduced to the prediction model.

According to the early basic formula of Zastrow and Wittwer [100], the specular reflectance of the light transfer tube and the aspect ratio were applied as another independent variables.

$$T = \rho^{A_p \tan \theta} \quad (4.14)$$

where  $\rho$  is the specular reflectance.  $A_p = L/D$  is the aspect ratio, i.e., the ratio of length to diameter or equivalent diameter.  $L$  is the length of lightpipes (m).  $D$  is the diameter of lightpipes (m).

In this mathematical model, the transmittance is the only dependent variable to evaluate the performance of lightpipes. Transmittance indicates the amount of incident light passed through lightpipes. Optical efficiency reveals how much irradiance is received by the base of lightpipes.

#### 4.4 Results of regression

As shown as Equation (4.15), the formula has been emphasised on the solar altitude ( $\alpha$ ) impact, the included angle of solar azimuth, the elbowed angle of lightpipes ( $\beta$ ) and sky clearness index ( $\lambda$ ) to the transmittance. Compared with the previous mathematical model, the significant contribution of this formula is considered the solar azimuth and the orientation of the elbow of lightpipes. It can achieve a better regression in large degree. In addition, the sky clearness index was replaced by the ratio of the actual horizontal global illuminance to the theoretical value under the CIE clear sky, which is more suitable to express the level of sky clearness.

$$\tau = \frac{\text{lumen}}{E_{\text{ext}A}} = (a_0 + a_1\alpha + a_2\beta + a_3\lambda + a_4\alpha\beta + a_5\alpha\lambda + a_6\beta\lambda + a_7\alpha^2\beta\lambda + a_8\alpha\beta^2\lambda + a_9\alpha\beta\lambda^2 + a_{10}\alpha^2\beta^2\lambda^2)\rho^{(b_1A_p+b_2(1/\tan\alpha)+b_3(A_p/\tan\alpha))} \quad (4.15)$$

The data simulated in Photopia was substituted into Equation 4.15, together with the constant value shown in Table 4.4.  $\rho$  is the reflectivity of the light tube, according to the data from Monodrught company, it is a constant here and value is 0.98. The total is 6696 sets of data.

Table 4.4 values of the constants

$a_0$	0.816107343
$a_1$	0.565594828
$a_2$	-0.001386091
$a_3$	0.002749844
$a_4$	0.005284653
$a_5$	-0.002801175
$a_6$	1.39112E-05
$a_7$	-0.000162761
$a_8$	5.13272E-07
$a_9$	-3.19153E-06
$a_{10}$	5.53944E-08
$b_1$	2.094452
$b_2$	-3.5E-05
$b_3$	0.083696

Equation 4.15 can then become:

$$\begin{aligned} \tau = & [ 0.816107343 + 0.565594828\alpha + (-0.001386091)\beta + 0.002749844\lambda + \\ & 0.005284653\alpha\beta + (-0.002801175)\alpha\lambda + 0.0000139112\beta\lambda + \\ & (-0.000162761)\alpha^2\beta\lambda + (0.000000513272)\alpha\beta^2\lambda + (-0.00000319153)\alpha\beta\lambda^2 + \\ & 0.0000000553944\alpha^2\beta^2\lambda^2]\rho^{[2.094452A_p+(-0.000035)(1/\tan\alpha)+0.083696(A_p/\tan\alpha)]} \end{aligned}$$

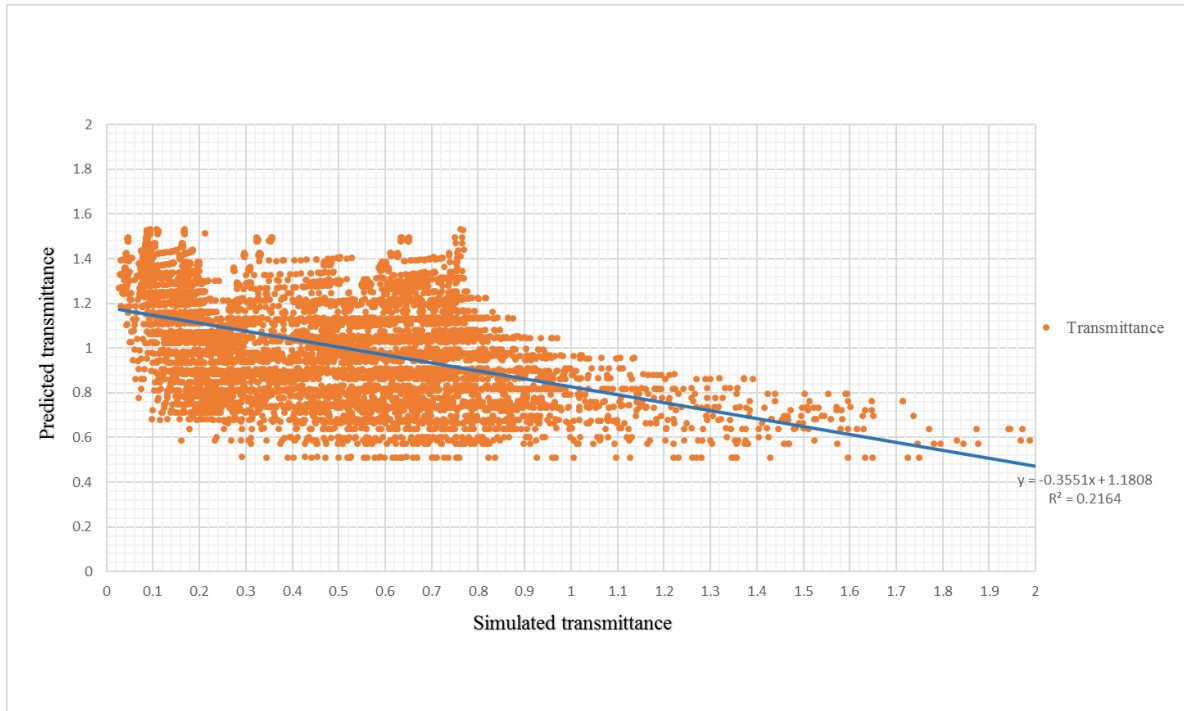


Figure 4.6 Comparison between simulated transmittance and predicted transmittance of lightpipes based on Su’s regression mathematical model.

It can be found that, based on Su’s prediction model, the ability of prediction is quite low. The  $R^2$  is only 0.2164 by regression formula. When mass and various elbowed lightpipes are needed to predict, the format of model needed to be changed and the constants needed to be redefined.

Table 4.5 Options for regression for lightpipes

<b>Fit-1</b>	$\tau = (a_0 + a_1\alpha + a_2\beta + a_3\lambda + a_4\alpha\beta + a_5\alpha\lambda + a_6\beta\lambda + a_7\alpha^2\beta\lambda + a_8\alpha\beta^2\lambda + a_9\alpha\beta\lambda^2 + a_{10}\alpha^2\beta^2\lambda^2)\rho^{(b_1A_p)}$
<b>Fit-2</b>	$\tau = (a_0 + a_1\alpha + a_2\beta + a_3\lambda + a_4\alpha\beta + a_5\alpha\lambda + a_6\beta\lambda + a_7\alpha^2\beta\lambda + a_8\alpha\beta^2\lambda + a_9\alpha\beta\lambda^2 + a_{10}\alpha^2\beta^2\lambda^2 + a_{11}\sin\alpha)\rho^{(b_1A_p + b_2(1/\tan\alpha) + b_3(A_p/\tan\alpha))}$

<b>Fit-3 (best)</b>	$\tau = ( a_0 + a_1\alpha + a_2\beta + a_3\lambda + a_4\alpha^2 + a_5\beta^2 + a_6\lambda^2 + a_7\alpha\beta + a_8\alpha\lambda + a_9\beta\lambda + a_{10}\alpha^2\beta\lambda + a_{11}\alpha\beta^2\lambda + a_{12}\alpha\beta\lambda^2 + a_{13}\alpha^2\beta^2\lambda^2)\rho^{(b_1A_p+b_2(1/\tan\alpha)+b_3(A_p/\tan\alpha))}$
<b>Fit-4</b>	$\tau = ( a_0 + a_1\alpha + a_2\beta + a_3\lambda + a_4\alpha^3 + a_5\beta^3 + a_6\lambda^3 + a_7\alpha\beta + a_8\alpha\lambda + a_9\beta\lambda + a_{10}\alpha^2\beta\lambda + a_{11}\alpha\beta^2\lambda + a_{12}\alpha\beta\lambda^2 + a_{13}\alpha^2\beta^2\lambda^2)\rho^{(b_1A_p+b_2(1/\tan\alpha)+b_3(A_p/\tan\alpha))}$
<b>Fit-5</b>	$\tau = ( a_0 + a_1\alpha + a_2\beta + a_3\lambda + a_4\alpha^2 + a_5\beta^2 + a_6\lambda^2 + a_7\alpha\beta + a_8\alpha\lambda + a_9\beta\lambda + a_{10}\alpha^2\beta\lambda + a_{11}\alpha\beta^2\lambda + a_{12}\alpha\beta\lambda^2 + a_{13}\alpha^2\beta^2\lambda^2)\rho^{(b_1A_p+b_2\tan\alpha+b_3(A_p\tan\alpha))}$
<b>Fit-6</b>	$\tau = ( a_0 + a_1\alpha + a_2\beta + a_3\lambda + a_4\alpha^2 + a_5\beta^2 + a_6\lambda^2 + a_7\alpha\beta + a_8\alpha\lambda + a_9\beta\lambda + a_{10}\alpha^2\beta\lambda + a_{11}\alpha\beta^2\lambda + a_{12}\alpha\beta\lambda^2 + a_{13}\alpha^2\beta^2\lambda^2)\rho^{(b_1A_p+b_2(1/\sin\alpha)+b_3(A_p/\sin\alpha))}$

where  $\tau$  is the transmittance of the lightpipes;  $\alpha$  is the solar altitude, 0-90°.  $\beta = |\text{solar azimuth} - 180^\circ - \text{the orientation of elbow}|$  (where the solar azimuth is: 0°-90°, the orientation of elbow: 0°, 30°, 45°, 60°).  $\lambda$  is the ratio of the actual horizontal global illuminance  $E_{ext}$  to the theoretical value under the CIE clear sky.  $\rho$  is reflectance of lightpipe, it was assumed to be 0.98 according to the manufacturer.  $A_p$  is the ratio of length of lightpipes to the diameter of lightpipes. a and b are the coefficients.

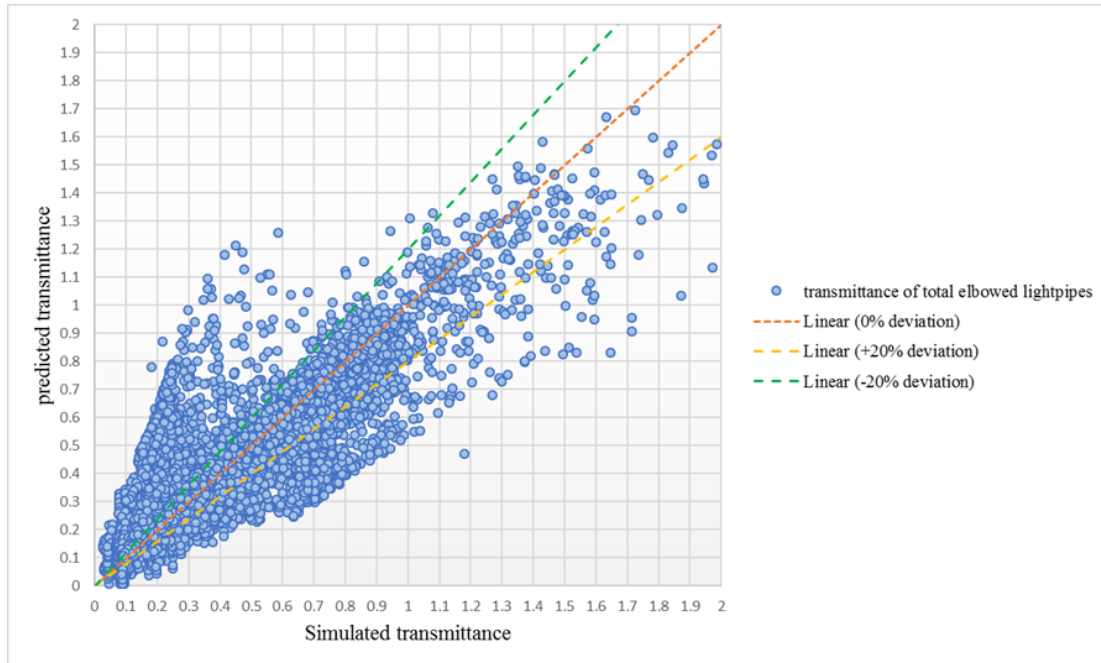


Figure 4.7 Predicted transmittance versus simulated transmittance for total elbowed lightpipes

**RMSE = 0.04**

**R-Squared: 0.77**

According to the analysis of data, some invalid values were removed. The condition at solar altitude  $10^\circ$ ,  $20^\circ$ ,  $80^\circ$ ,  $90^\circ$  and solar azimuth  $10^\circ$ ,  $20^\circ$ ,  $80^\circ$  and  $90^\circ$  are rare in real practical situation and these unexpected simulation value impact the accuracy of performance of prediction model in large degree.

Six mathematic models are developed in Matlab by utilising “fitnlm” function, as shown in Table 4.5. This function tried to find the significance linear relationship between the variables and their respective variables. It can include the cross terms, quadratic terms in the settings. This function is suit for the model installed in this study. Every equation includes the independent variables, solar altitude ( $\alpha$ ), the included angle of solar azimuth and the elbowed angle of lightpipes ( $\beta$ ), sky clearness index ( $\lambda$ ), aspect ratio ( $A_p$ ) and reflectivity of tube ( $\rho$ ) and the dependent variable is transmittance ( $\tau$ ). Regression started from Su-model because it

has acquired reasonable accuracy in field experiment. Considered the Su-model may be limited due to the lack of enough large amount of original data because of the limited of field test. However, in this study massive data has been obtained from Photopia simulation; hence more accuracy model can be derived from regression.

The fitting results in terms of coefficient of determination  $R^2$  and the mean squared error MSE for the 6 regression fits presented in Table 4.5 is shown in Table 4.6. For Fit-1,  $R^2$  is as low as 0.381 and hence, there is no need to discuss this form forward. It is found that the exponential of  $\rho$  affects the prediction capability dramatically. Moreover, Fit-2 is not any better with low  $R^2$  value as well. The trigonometric is only affecting the exponential but not the polynomial function ahead of  $\rho$ . Fit-3 keeps the original form of exponential of  $\rho$ , the polynomial function ahead of  $\rho$  was add in with the sum of  $\alpha$ ,  $\beta$  and  $\lambda$  squares. The accuracy is improved significantly and  $R^2$  can achieve nearly 0.8 and MSE reach 0.04. The prediction is considered as a good prediction. It is then continued to find more fits but  $R^2$  is not increasing; instead,  $R^2$  is as low as 0.699 and the cubic form is not valid in the polynomial function ahead of  $\rho$ . Then Fit-4 and Fit-5 are changed in the exponential term of  $\rho$ . The Su-model used the tangent of  $\alpha$  denominator form. Fit-5 tries the numerator form and found  $R^2$  is 0.543069. Fit-6 keeps the denominator form but changes the tangent to sine form. The result is still not satisfied. In overall, Fit-3 is chosen as the best form to define the prediction model. Accordingly,  $R^2$  is 0.77 and MSE is 0.04 which can be considered as a reasonably good prediction model.

Table 4.6 Regressing equations attempted for the correlations of altitude, azimuth and sky clearness factor to the transmittance of lightpipes

Equation number	R <sup>2</sup>	MSE
Fit-1	0.381	0.064
Fit-2	0.599	0.053
Fit-3 (best)	0.77	0.04
Fit-4	0.699	0.049
Fit-5	0.543069	0.0448
Fit-6	0.506	0.051

R<sup>2</sup>: coefficient of determination

MSE: mean squared error

In fact, in the commercial market, the elbowed lightpipes usually only have some common angles, i.e., 30°, 45° and 60°. By separating the unnecessary data, we can re-evaluate the prediction ability of mathematical model proposed. With the same equation form, the constants have been redefined accordingly as shown in Table 4.7.

Table 4.7 The regression constant of 30°, 45° and 60° elbowed lightpipes respectively and assessment of each model

Constants	30° lightpipes	45° lightpipes	60° lightpipes
$a_0$	-1.619	-1.9698	-0.70013
$a_1$	0.005124	0.005115	0.003646
$a_2$	0.01651	0.017294	0.008946

$a_3$	6.3634	6.5208	2.3474
$a_4$	0.000118	0.000122	3.1E-05
$a_5$	-7.7E-05	-8.5E-05	-5E-05
$a_6$	-2.6419	-2.701	-0.77861
$a_7$	-4.7E-05	-5.2E-05	-6.9E-05
$a_8$	-0.03151	-0.03235	-0.01517
$a_9$	-0.02624	-0.02519	-0.01187
$a_{10}$	-8.5E-07	-7.3E-07	7.83E-07
$a_{11}$	1.25E-06	1.2E-06	1.33E-06
$a_{12}$	0.000241	0.000204	2.65E-05
$a_{13}$	-5.6E-09	-2.4E-09	-7.3E-09
$b_1$	1.2844	-0.25412	-3.0312
$b_2$	-0.72828	-0.3324	7.2734
$b_3$	0.056565	-0.0408	-0.86234
<b>Prediction accuracy</b>			
$R^2$	0.953	0.849	0.773
<b>RMSE</b>	0.0446	0.108	0.137

After redefining the constants in the mathematic formula proposed, it can be seen that the prediction accuracy is considerably improved. Different from the total prediction accuracy, the accuracy value, e.g.,  $R^2$ , are 0.953, 0.849 and 0.733 respectively for the elbowed angle 30°, 45° and 60° lightpipes. Compared with the total prediction accuracy value is 0.77, the elbowed 30° lightpipes is improved by nearly 20%. The elbowed 45° can increase 10% and the worst case, elbowed 60° lightpipe, is also slightly better than the total prediction accuracy. The MSE value of total prediction formula is 0.04, which equals to RMSE 0.2. For the redefined mathematical formula, the RMSE values are 0.0446, 0.108 and 0.137 corresponding to 30°,

45° and 60° elbowed lightpipes respectively. These values for RMSE are significantly smaller. This proves the strong potential of the refined mathematical formula in practical applications. Especially, the elbowed 30° lightpipe is the most widely used lightpipe.

Figures 4.8 – 4.10 describe the deviation of predicted transmittance versus simulated transmittance of elbowed 30°, 45° and 60° lightpipes. In Figure 4.8, nearly all the predicted transmittance for 30° lightpipes fall within the  $\pm 20\%$  deviation. As discussed, 30° lightpipes are the most commonly used in the commercial market. However, elbowed 45° and 60° deviate a bit more from the  $\pm 20\%$  ranges. More errors appear at both the very low transmittance and very high transmittance which are the extreme conditions. It has been explained before, these conditions are associated with very small/large solar altitude and solar azimuth. In real situation, it is common and has less implication on the performance and design.

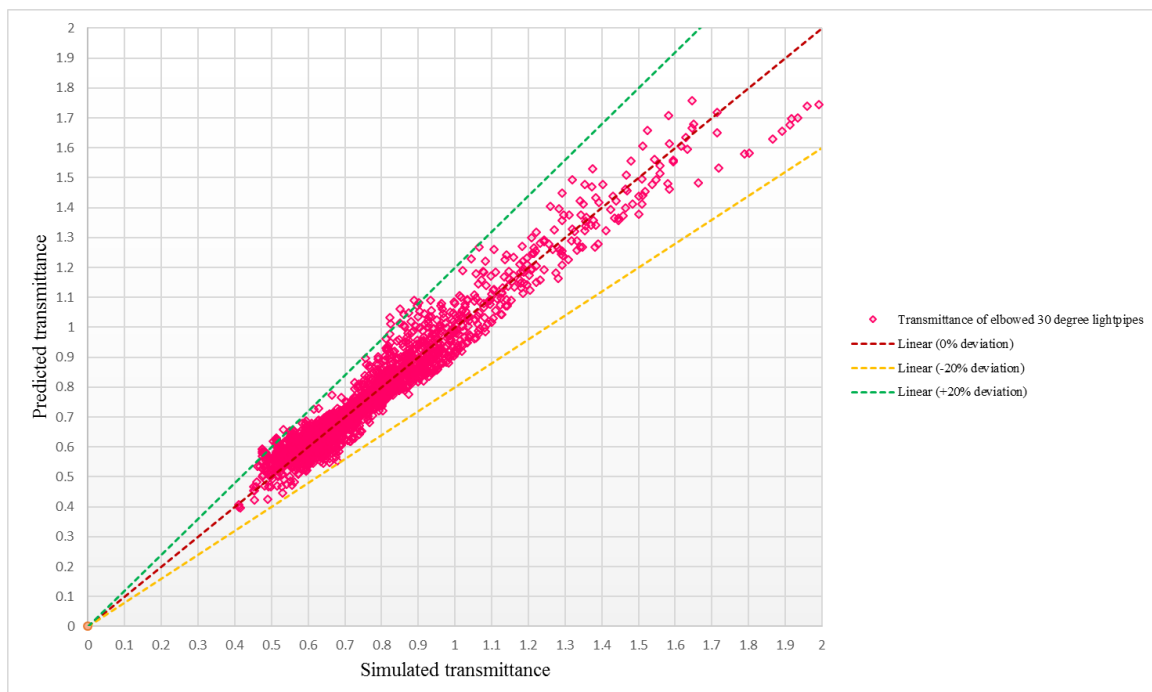


Figure 4.8 Predicted transmittance versus simulated transmittance of elbowed 30 degree lightpipes.

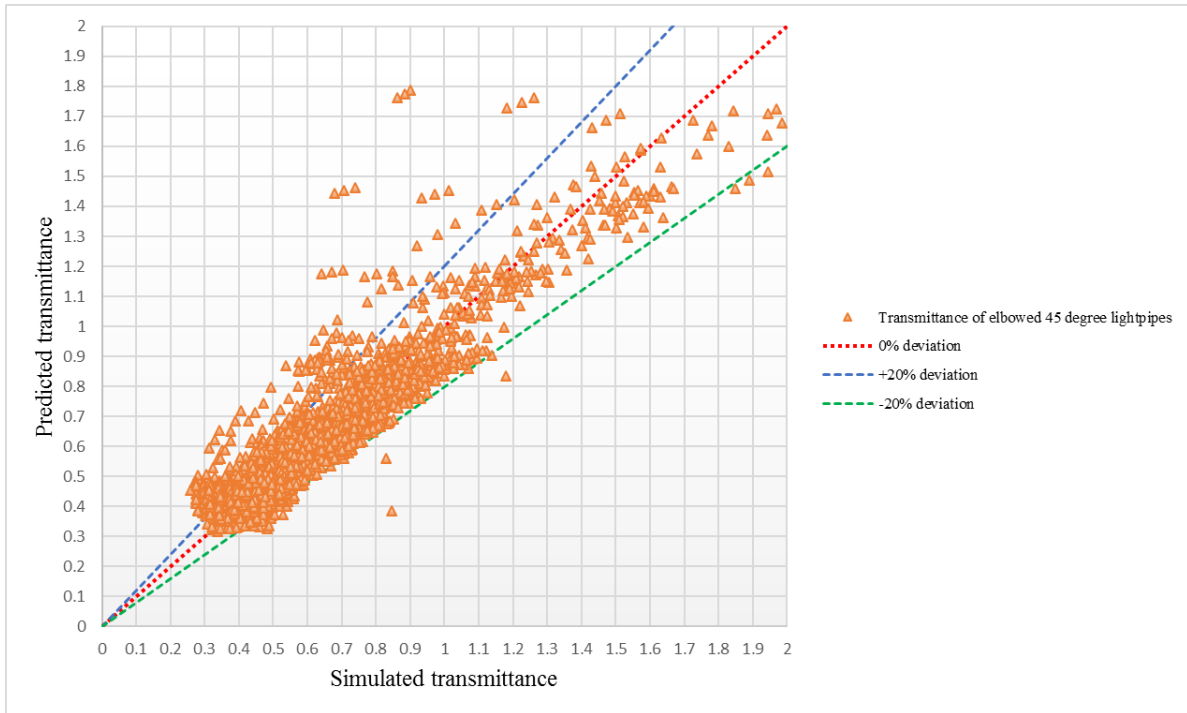


Figure 4.9 Predicted transmittance versus simulated transmittance of elbowed 45 degree lightpipes.

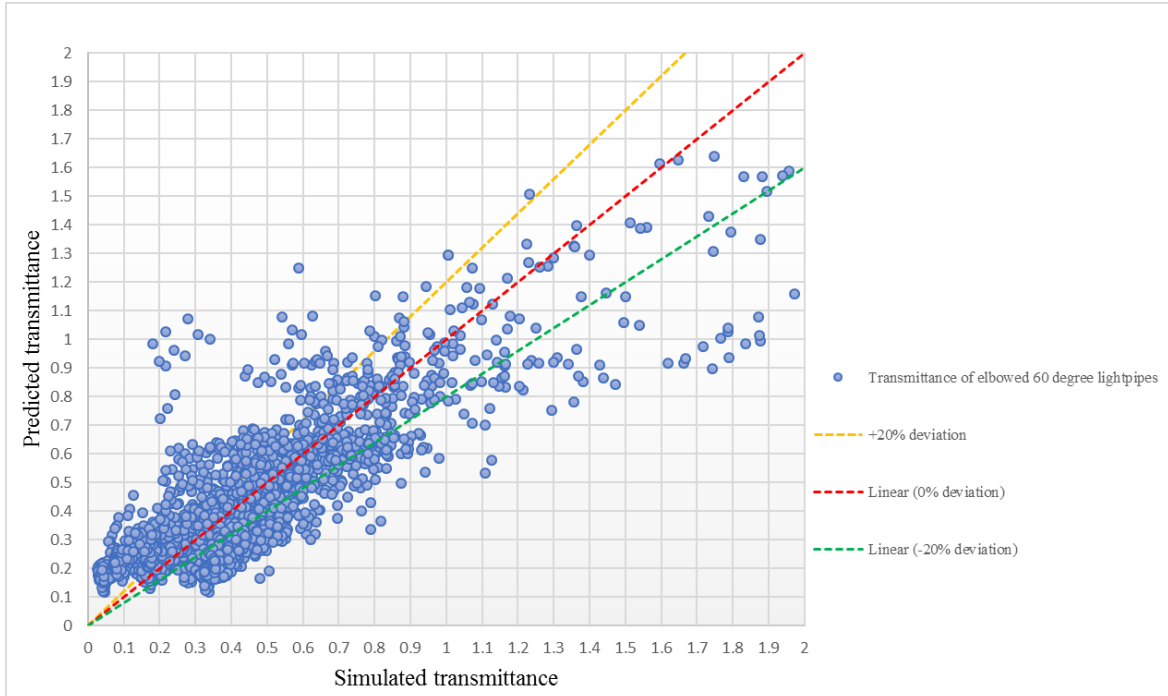


Figure 4.10 Predicted transmittance versus simulated transmittance of elbowed 60 degree lightpipes.

#### **4.5 Comparison between multiple nonlinear regression and ANN model for predicting the transmittance of lightpipes**

The ANN model proposed can be compared with mathematical model. As discussed earlier, the ANN model and MNLN can both be used to predict the transmittance of lightpipes and both of them have good prediction capability. However, ANN is considered better than MNLN. The two models have the same independent parameters solar altitude ( $\alpha$ ), the include angle of solar azimuth and elbowed angle ( $\beta$ ), sky clearness index ( $\lambda$ ), tube reflectivity ( $\rho$ ), aspect ratio ( $A_p$ ) and the dependent parameters transmittance ( $\tau$ ). Although the prediction ability of ANN is much higher than MNLN, interesting finding is that the large error exists in very low transmittance and very high transmittance. The reason for that is because it is in extreme conditions, i.e., the very low solar position (at solar altitude  $10^\circ$ ,  $20^\circ$  and/or solar azimuth  $0^\circ$ ,  $10^\circ$ ,  $20^\circ$ ) or very high solar position (at solar altitude  $80^\circ$ ,  $90^\circ$  and/or solar azimuth  $80^\circ$ ,  $90^\circ$ ). On the other hand, the result is also affected by the parameters of lightpipes; when the diameter is very large such as 530mm, or the length is very long, or the elbowed angle is very large, such as  $60^\circ$ , the prediction error is dramatically affected. Table 4.6 lists the comparison between the prediction accuracy of the multiple nonlinear regression prediction and ANN model. The  $R^2$  is 0.965 for the ANN model and 0.77 for the MNLN model, respectively. The accuracy can raise 20% compared with the MNLN model by using the ANN model. About MSE evaluation, it is 0.0043 for the ANN model and 0.04 for the MNLN model. This means, by comparing with the target simulation values in Photopia, the ANN model yields smaller variation and stronger prediction capability.

Table 4.8 Comparison between the MNL model and the ANN model

<b>Model type</b>	<b>Independent parameters</b>	<b>Dependent parameters</b>	<b>R<sup>2</sup></b>	<b>MSE</b>
<b>ANN</b>	$\alpha, \beta, \lambda, \rho, A_p$	$\tau$	0.965	0.0043094
<b>MNL</b>	$\alpha, \beta, \lambda, \rho, A_p$	$\tau$	0.77	0.04

Figure 4.11 shows the comparison of the results from the multiple nonlinear regression prediction model and the ANN model, in predicting the transmittance of lightpipes, versus simulation values in Photopia, respectively. The top figure in Figure 4.11 compares the predicted transmittance from MNL with the simulated transmittance and the bottom figure compares the predicted transmittance from ANN with the simulated transmittance. It clearly demonstrates the correlation accuracy of the different prediction methods; ANN model predicts better than MNL as almost all data were covered within the  $\pm 20\%$  ranges for the ANN model.

Having said that, ANN and regression can both be considered as effective tools to predict the performance of lightpipes. However, due to different working principles, they have different strengths and weaknesses. The main contribution of regression is to propose a visualized mathematical equation. Given values for the parameters, the results can be calculated directly from the analytical equation. It can obviously save the computational time and cost. Moreover, the mathematical relationship between independent parameters and dependent parameters can be directly found by the equation established. Besides, the advanced technique allows various energy simulation software combined equipment to model the energy consumption together. The equation could be a customized option to be added into the simulation procedure without

setting the physical models of lightpipe or virtual models in software with vast number of parameters.

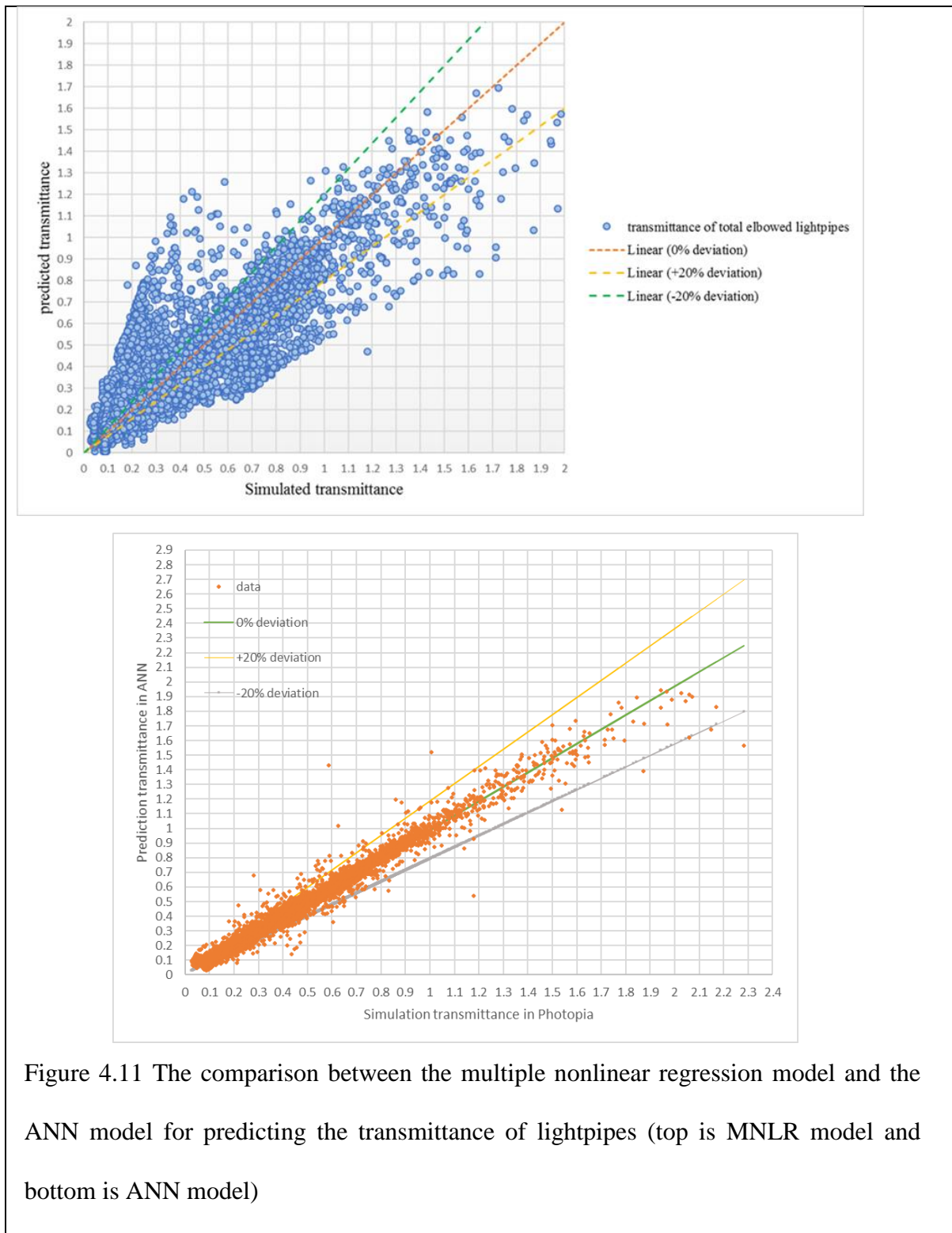


Figure 4.11 The comparison between the multiple nonlinear regression model and the ANN model for predicting the transmittance of lightpipes (top is MNL model and bottom is ANN model)

Though ANN performs more accurately than MNLR, as a kind of black box embedded in Matlab, it is not straightforward or direct as MNLR in terms of understanding and especially not easy to use for non-professional personnel. Moreover, to combine ANN with other energy simulation software is very difficult. It needs to write massive coding scripts in programming software to set the plug-in with the energy software. In overall, both ANN and MNLR are the available tools to forecast the performance of lightpipes. They should be selected depending on the specific conditions according to their characteristics.

## 4.6 Summary

Based on numerous simulation results in Photopia, some different forms of mathematical models have been proposed to predict the transmittance of lightpipes with various elbowed angles. The multiple nonlinear regression method is used in this study. In the model, the independent parameters are solar altitude ( $\alpha$ ), the included angle of solar azimuth and the elbowed angle of lightpipes ( $\beta$ ), sky clearness index ( $\lambda$ ), aspect ratio ( $A_p$ ) and reflectivity of tube ( $\rho$ ) and dependent parameter is only the transmittance of lightpipes. A goodness of fit regression has been obtained with  $R^2$  0.77 and MSE 0.04, which proves the reasonable accuracy of the prediction model. Due to the practical application, most commercial lightpipes are straight,  $30^\circ$ ,  $45^\circ$  and  $60^\circ$  elbowed lightpipes. The prediction model was then used to evaluate each elbowed angle and the regression constants were updated respectively. These specific angles yield greater accuracy with  $R^2$  reaching 0.953, 0.849 and 0.773 for  $30^\circ$ ,  $45^\circ$  and  $60^\circ$  elbowed lightpipes, respectively. Almost all predicted data fall within the  $\pm 20\%$  deviation from the simulated data, which demonstrates the practical application capability of the proposed model. However, because Photopia only includes three standard sky model, which are clear, intermediate and overcast sky models. As such, the amount is much less than CIE standard 14 sky models. Hence, this mathematical model is not suitable for

application in some sky conditions. In the future work, more sky conditions should be considered in the predication model.

Moreover, the ANN model proposed in Chapter 3 has been compared with multiple nonlinear regression (MNLN) in this chapter. The prediction accuracy of ANN is obvious higher than MNLN model, where  $R^2$  can reach 0.9653. However, the mathematical model has significant application potential in practical projects. The mathematical equation can express the relationship between the performance of lightpipes and their parameters directly in an analytical form. The mathematical equations can also be easily combined and implemented in other BIM simulation software for wider application scenarios.

**Chapter 5 Integrating Artificial Neural  
Network (ANN) and BIM Revit via  
Application Programming Interface (API)  
to predict the daylighting performance  
of lightpipes**

## **5.1 Introduction**

In preceding chapters, it has addressed the significance of using daylighting in buildings and its impact on the global energy sustainability development [104]. However, the daylighting performance in buildings is difficult to forecast which poses significant challenge in the wide-spread application of the daylight system or lightpipes [105], [106]. Recent development of new analysing platform or tools, such as BIM (Building Information Modelling) and Artificial Neural Network (ANN), are fashionable applications in their individual scope. However, rare research considers to combine these two systems and develop their strength to solve complex engineering issues, in particular, in daylighting performance in buildings. Integrating ANN and API (Application Programming Interface) in BIM as a hybrid system could be an inspiring attempt with considerable impact. The novel system not only promotes the prediction of the performance of lightpipe in BIM, but also exploit the potential of BIM in daylighting simulation combined with building design.

### **5.1.1 BIM**

Building Information Modelling (BIM) can simply be defined as a process, which include creating an intelligent 3D model and enable document management, coordination and simulation during the whole lifecycle of a project (plan, design, build, operation and maintenance). BIM rapidly promotes the development of design and construction management integrating and collaboration. Last generation 2D drawing systems is based on quickly finishing “drawing” than traditional manual processes. In terms of interoperability, there are no real strength. In order to save building cost and time, the technology of accessing and controlling information needs to be developed. Accordingly, it requires to access and edit the project information in various platforms and devices. Integrating essential information,

including specification, models, point clouds, drawings, reports, etc., can lead to easy access at any stage and any time. Different design teams can be involved in accessing and revising whenever necessary. Novel BIM technology is a revolution in Architecture, Engineering and Construction (AEC) industry. Different from the conventional design process, change for one point will make the whole project updated automatically, including full 3D model, drawing, construction etc [107].

In the AEC industry, BIM has completely upended the traditional drawing-intensive Computer Aided Design (CAD) method. In a typical BIM project, massive information can be implemented to a building. This information is called n-Dimensional (nD). Typical dimensions involve time, cost, accessibility, sustainability, maintainability, acoustic,

thermal requirements, health and safety [108]. Figure 5.1 shows the analysis indexes of the 3D to nD modelling project. However, incorporating these various lifecycle information relies on the external application in creating additional functionality through BIM-enabled tools such as Application Programming Interface (API) [109]. Thus, this Chapter will investigate the implementation of API in BIM-enabled environments.

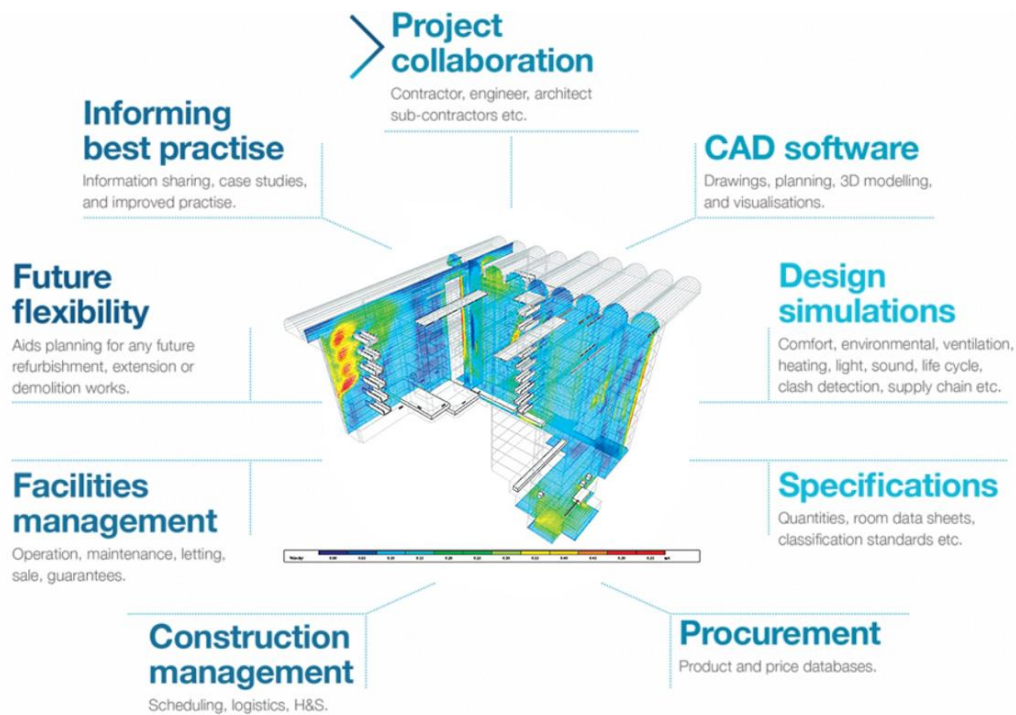


Figure 5.1 Analysis indexes of the 3D to nD modelling project [108]

### 5.1.2 Autodesk Revit API overview

Autodesk Revit is a typical and perhaps the most widely accepted BIM platform in the AEC industry. API is a software development kit, which can provide the operational possibilities to explore the BIM in accounting for different needs [110]. API, as an intermediary platform, is used to exchange information between software and application [111]. API is developed based on programming source codes and a high level interface between computer programmes and operating system. The Revit API platform can be accessed by computer language compatible with the Microsoft .NET Framework, such as Visual C#, Visual Basic .NET.

The Revit API system is implemented in the daylighting domain of the open Revit Platform API. Two class libraries are utilised, i.e., RevitAPI.dll and RevitAPIUI.dll. The RevitAPI.dll is responsible for accessing Revit's application, documents, elements and parameters at the

database level while RevitAPIUI.dll controls all API interfaces related manipulation and customization of the Revit user interface [112] . As shown in Figure 5.2, Revit elements include three categories and they are Model elements, Datum elements and View-specific elements. The windows elements considered in this study belong to the Model elements. It can be mapped into the Revit Interface as RevitElement belonging to RevitAPIObject. The associated BIM API mapping is shown in Fig. 5.3.

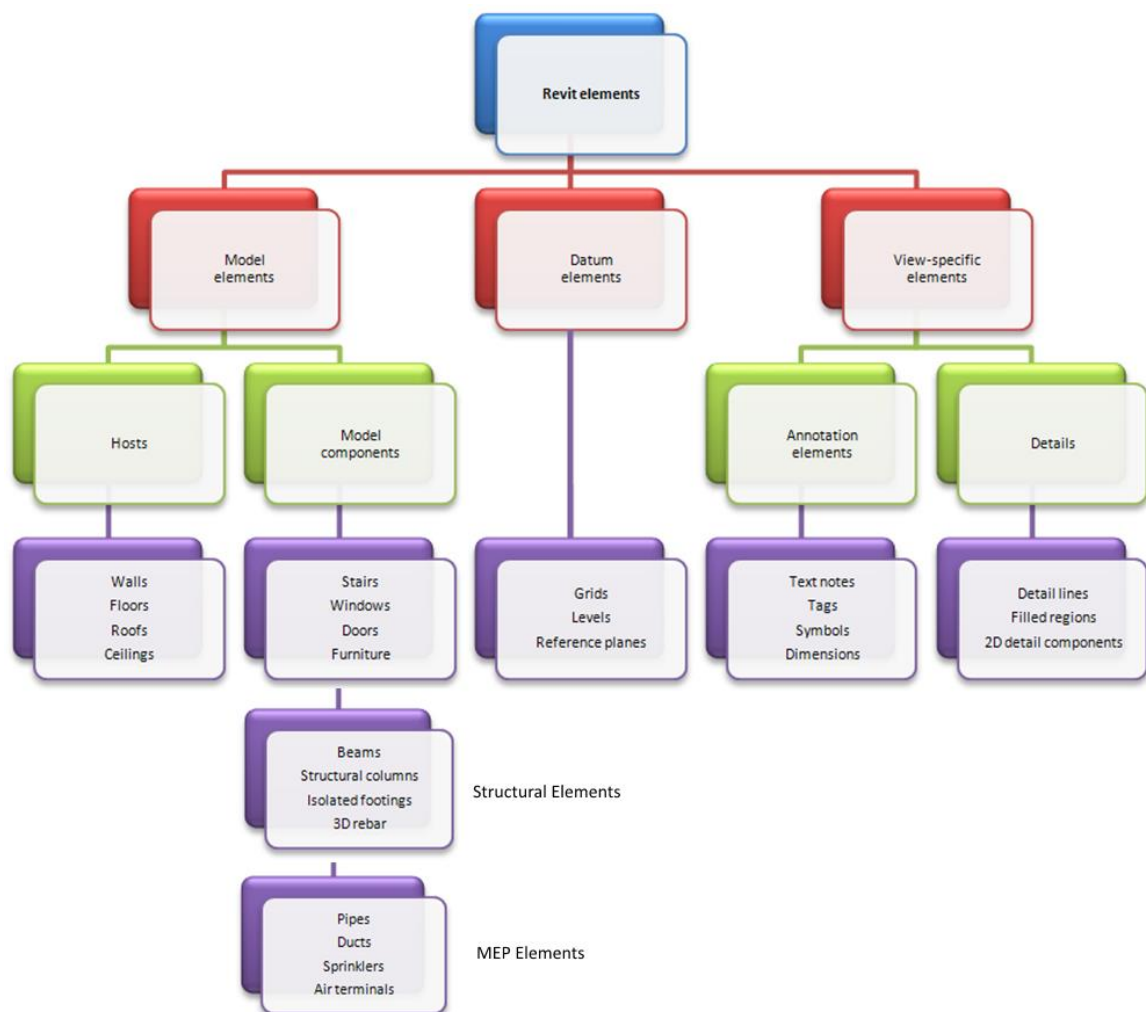


Figure 5.2 The summary of Revit elements

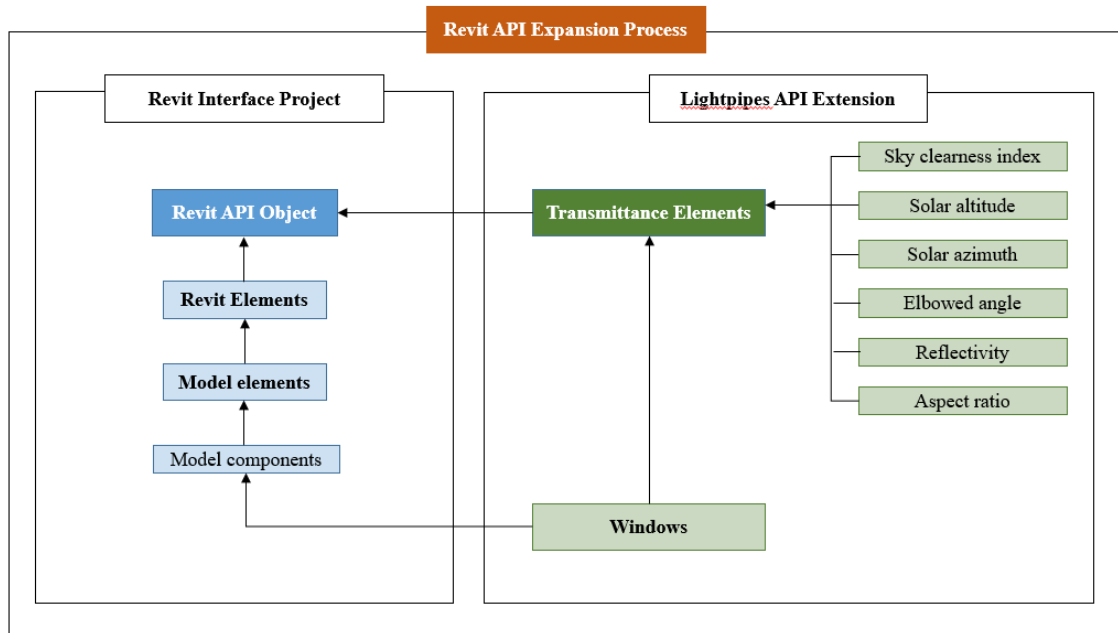


Figure 5.3 Possible mappings linking extension to BIM project (Revit Daylighting)

## 5.2 Fundamentals of hybrid ANN and C#.NET

ANN as a parallel computer model, which normally does not need the input parameters structures or dynamic characteristics, but only needs the input data and target data. Moreover, because the property of non-linear mapping, through the neural network self-study ability can achieve reasonable accuracy in predicting the target. The .NET is an internet facing and supports various terminals of development platform with friendly interface, high operating speed and easy maintenance features etc. Especially, the .NET system can leave the programming platform and form plug-in files. However, comparing with Matlab, the engineering mathematics performance is inferior. Thus, hybrid Matlab and .NET system can have strong performance with wider application. Recently, deep learning neural network is of the trend in AEC industry. However, ANN is chosen in this research rather than deep leaning neural network to save computational cost because the data in daylighting sector usually owns

relative regulation. Accordingly, ANN is sufficient to perform the training of data and generate the prediction model. On the other hand, comparing with the deep learning multi-layers, ANN can significantly save time. Autodesk Revit is developed by .NET C# language; choosing the C# language keeps the system largely stable and compatible.

Matlab, as an advanced programming language and platform, is strong and stable in performance, efficacy and interacting numerical computing and visualization. It integrates numerical calculation, signal processing and image analysis. However, Matlab is not good in the interface development. The program is limited running in Matlab environment and cannot be used in other software developers. However, C#. NET owns the significant excellent features, such as friendly user interface, fewer running time, easy to maintain and update. The file produce from C#. NET could protect the algorithm and data efficiency. Moreover, the file can run without the programing environment. However, the engineering mathematics is difficult and complex. Thus, hybrid the Matlab and C#. NET can largely improve the performance of either of them [113].

### **5.2.1 Artificial Neural Network in the simple retrospect**

ANN achieves the accurate forecasting by iterative method. Sigmoid function is chosen as the transfer function because of the reliable biology basic. The forward neural network with one hidden layer can largely approach any form function. In fact, in order to reduce the number of the nodes in the hidden layer, the account of hidden layers can be raised. However, up to the present, there have been no method or theory to determine the nodes of network and the number of hidden layers. The experimental method of the error of learning sample and test

sample cross trying to define the hidden layer and the nodes number in the hidden layer. The functions used are presented as follows.

Stage 1: The transfer function `tansig ()` is S (Sigmoid) transfer function. It is used to mapping the node value (-M, +M) to (-1, +1), which is always used in training the ANN hidden layer.

Stage 2: Establish the forward neural network by using the function `newff ()`.

Stage 3: `Train ()` function is used to train the ANN.

Stage 4: `Sim ()` function is used to simulate the already used ANN.

### **5.2.2 An overview of integrating ANN and C#.NET methods**

There are four methods to hybrid ANN in Matlab and .NET.

(1). Use the Compiler of Matlab to connect the ANN in Matlab and .NET.

The Compiler in Matlab could transfer the .m file of Matlab as C or C++ source code to configure individual application program without running in Matlab environment. When adding parameters `-e (mcc e *.* )` or `-p (mcc p *.* )` in Matlab compiler `mcc` it could transfer the .m file to specify C or C++ source code. This function can be implemented by using the code “`deploytool`”.

(2). Use the COM component technology

COM (Component Object Model) is a type of software architecture, which let different software combined to configure new software. From Matlab R2006a edition, Matlab Builder for .NET is introduced. It is the expansion of Matlab Compiler. It allows the Matlab function code automatically produce individual .NET assembly Class library or COM Object. The produced Class library .NET assembly can be compatible with C#, VB. NET or any CLS

(Common Language Specification). The COM Object can be run in any COM compatible environment. The Matlab Builder for .NET application could hybrid the Matlab function with desktop and Web application programme. By the standard call for interface, the function could be shared in users group.

### (3). Mideva platform

Mideva is a compile development platform by Mathtool Company, which is a strong development environment for .m file. This platform has various editions for Borland C++, Visual Basic and Delphi etc. programme language. Mideva support thousands of basic functions, including basic operations, orders etc. Mideva has the compile and transfer function, which could transfer Matlab function or code to Dynamic Link Library (DLL) file in the form of C++, then call for the DLL file in the .NET, which could call for the Matlab toolbox.

### (4). Using Matlab engine technology

Matlab engine allows the user to call for the Matlab function in separate application program. Matlab as a compute engine runs in the background. When the users work on this engine, Matlab is progressed in background. Matlab engine works as a bridge between the user interface and the Matlab processing, exchanging the data and transferring the order. In Windows operational environment, Matlab engine is implemented by Active X. Active X is an agreement independent of program language and also not limited to developing environment. Active X could be used in Visual C, Delphi, C++ builder etc. Matlab support the technology of Active X component group and Active X automatic service. When using the .NET program to run the Matlab Active X engine, the engine works just like a server. First, the program transfers the data and command to the Matlab engine. Then the engine exchanges

data and command to Matlab server. Finally, the results feedback to the application program by computer engine.

### 5.2.3 The process of calling for Artificial Neural Network (ANN) in C#.NET

(1). Write .m file.

The ANN function in BpNeuraNet. M process use the function as below. Function BpNeuraNet is used.

*Function [Result] = BpNeuralNet (TrainIn, TrainOut, Test In, Test Out, Par)*

The data in the brackets are the input parameters. TrainIn is the input matrix for training and TrainOut is the target matrix for training. TestIn the input matrix for testing and the TestOut is the target matrix for testing. Par is the parameters matrix for network architecture. The [result] means the prediction target matrix.

Pre-process the simulation data from Photopia. 75% of the data is used to train and 25% is used to test the network. The training data is used to upgrade the net weight and bias. The testing data is used to test and evaluated the accuracy of the network. The data could be a 4800\*6 matrix. Generally, the initial data should be use mapstd to transfer between (-1, 1).

The main code is:

```
[TrainIn 1, ps 1] = mapstd (TrainIn 2); % pre-processing the data
```

(2). Establish the neural network architecture and adjust the parameters.

Establish the BP neural network and the transfer function in hidden layer and output layer are tansig() and purelin() respectively. The count of hidden layers and output nodes and learning rate could be written in interface.

The main code is:

```
net = newff (minmax (TrainIn 1), [Par (2), Par (3)], {'tansig', 'purelin'}, 'traingd'); % set up  
network architecture
```

```
net. TrainParam. mu = Par (1); % learning rate
```

The number of nodes in hidden layer and learning rate is the most impress of the forecast results. The iteration method is used to adjust the node number and learning rate. It keeps one variable, then change the other variable from large to small. Every time after training, testing and modelling, find the best architecture.

### (3). Training and modelling

Use the prepared data to train and simulate. Then the forecast results also need to anti-normalization (mapminmax). The main code is as following:

```
[net, tr] = train (net, TrainIn 1, TrainOut 1); % training the network
```

```
Result 1 = sim (net, TestIn 1); % simulation
```

```
Result = mapstd ('reverse', Result 1, ps 4); % anti normalization
```

### 5.3.4 Embedding Matlab engine in .NET

When Matlab is installed in computer, the Active X engine would be automatically register in computer system. Before using the Active X engine of Matlab in Visual Studio .NET develop environment, need add COM reference “Matlab Application (Version 7.0 Type Library)”. Then the object could be instantiated in the program. The program could start in the interface. The interface Active X engine offer are Execute, PutFullMatrix and GetFullMatrix. They could run the script, add matrix in the Matlab Server and read matrix from the Matlab Server. Some of the ANN parameters could be set up in .NET interface layer. The main code in C# is:

```

MLAppClass matlab = new MLAppClass();

Matlab. PutFullMatrix (“TrainIn”, “base”, TrainInput, TrainInput Im); % add matrix to the
Matlab Server

matlab. Execute (@ “[Result] = BpNeuralNet (TrainIn, TrainOut, TestIn, TestOut, Par)”);

matlab. GetFullMatrix (“Result”, “base”, refReArr, refReArrIm); % read the matrix from the
Matlab Server. The ReArr and ReArrIm is the pre define System. Array object

ReArr. CopyTo (yc, 0); % record the prediction results in the double yc

Matlab. MinimizeCommandWindow (); % minimize the Matlab command window

matlab. Quit(); % close Matlab Sever

```

### **5.3 Methodology**

In this study, a research methodology called prototype is introduced into this research. This prototype is validated in a building model. In order to achieve the information interaction between ANN and Revit. A prototype named ANNREVIT is developed through API. The prototype ANNREVIT packages the ANN model which has been successfully trained in Chapter 3 and can be further transferred as the input file to be used directly in Revit. This prototype is developed in the Application Programming Interface (API) by using C# programme language in .NET platform. This prototype can utilize the ANN prediction strength and generate the transmittance values which can involve the daylighting simulation process in Revit. This generated transmittance value can directly involve daylighting simulation. The objective to exploit such a prototype to seek for an application which transfer the ANN prediction model to Revit add-in file, set the ANN model as a plug-in function and run the prediction model in background without training the ANN model in Matlab manually. It aims to avoid the multi-entering input parameters caused errors. Moreover, in case that users are

lack of professional Matlab knowledge, such a plug-in is more efficient and convenient. Therefore, this design is very friendly to users who require optical simulation software or programme development. Moreover, due to the large quantity of data to input, this plug-in can potentially reduce the errors induced by repeated manual operation. In this ANN-Revit model, the prototype can transfer the add-in which includes all the trained ANN prediction model information. When the add-in is implemented in Revit, the prediction results will be run in the back platform. Thus, the resulting values can involve in the simulation process directly in Revit. Figure 5.4 shows the complete work flow of combining ANN within Revit.

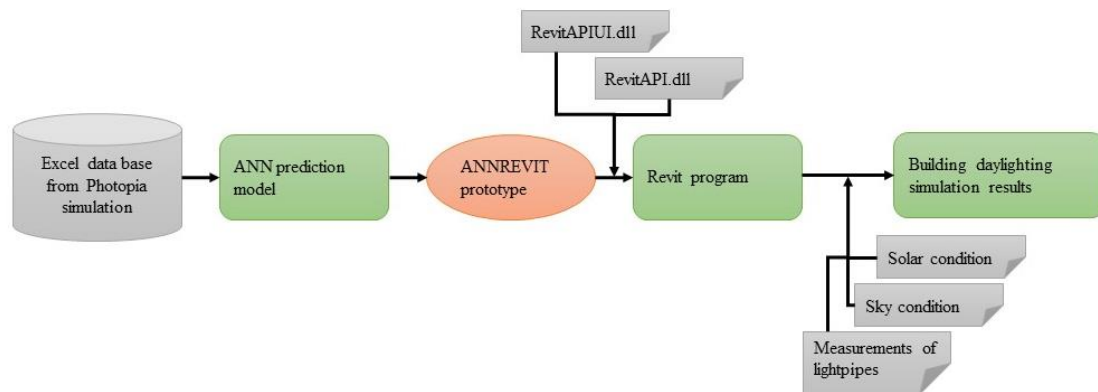


Figure 5.4 Combining ANN with Revit workflow

The hybrid system can be divided into three blocks: integrating ANN and C#; embedding as plug-in; inserting into Revit by API.

### 5.3.1 Define valid parameter file

All building construction such as wall, roof, windows etc. have existing database in Revit called “family”. However, there is no lightpipe family in the database. Therefore, it is needed to custom define the lightpipe model. This research chooses a round window model instead of

new build lightpipe. The aim is to acquire the transmittance of lightpipes, which is used to involve the illuminance simulation of daylighting. However, the transmittance is independent of the form or parameters of windows. Hence, only revising the transmittance instead of changing any other parameters extremely saves time and reduces the compilation of work. In order to change the transmittance of chosen window glass, it is found that the transmittance of glass is calculated by two parameters “color” and “tint” in the rendering. The change of the tint value does not affect the transmittance. Therefore, it needs to change the custom color parameter, which can be achieved by setting the RGB value. In the simulation procedure, the value of RGB is fixed as “EQUAL”. It means that the R, G and B parameters have the same value. It has advantage in simplifying the simulation, because the RGB value only affects the quality and colour of the light instead of the quantity of the light. It will not affect the illuminance while rendering the model hence not affecting the analytical results.

In the optical mathematical equation, the transmittance can be calculated by the equation as follows,

$$\tau = 0.9216 \times 10^{(\text{thickness\_in} \times \log_{10}((\text{RGB} / 255)^2))} \quad (5.1)$$

$$\text{Hence, RGB} = 255 \times \sqrt{10^{((\log(\tau/0.9216^p))/(p \times d/100))}}$$

where,  $\tau$  is the transmittance,  $d$  is the thickness of glazing (mm). In this study, the thickness is defined as 3mm,  $p$  is the number of glazing pane, it is defined as 1.

Moreover, the transmittance equal to relative weight of R, G, B:

$$\text{RGB (R, G, B)} = 0.2126 R + 0.7152 G + 0.0722 B \quad (5.2)$$

The thickness of single glazing round window is default defined as 3mm, the transmittance is assumed 70%, and RGB will specify R50, G50, B50.

In order to achieve the aim to revise the transmittance of lightpipes, only the RGB value in glass material parameters is required to be changed. In order to iterate the RGB values and add into glass material property automatically, Eqs. 5.1 and 5.2 will be exploited and edited in the API programme – utilizing the API programme to achieve this function. Hence, the add-in shall create a shared parameter file through API and add this add-in into Revit modelling platform.

### **5.3.2 Hybrid programme with ANN and C#.NET**

The ANN prediction model has been trained and validated in Chapter 3. It can be used directly in this study. Revit API is an interface which can allow the external programme procedure to visit and operate the Revit modelling process. The type of interface applied in the API is of the type of .NET. Any language that can be edited in .NET framework can be used in the API, such as C, C++, C#, VB etc. However, partially because Revit itself is developed by C# language, C# language is chosen by the author in this study to develop the API. In fact, the interfaces packaged in the Revit API are encapsulated by AutoDesk technicians, not the application of the lowest level functions. Packaged functions and classes need to be called in order to develop a secondary development tool for Revit that meets the design requirements. Revit API has a total of 23 namespaces, and each namespace packs the corresponding tool category. When calling the classes in it, it needs reference and to declare the namespace in the program. The classes in Revit API cover many types and complete majors which can meet almost all requirements in Revit API secondary development process.

As the programme platform, .NET supports a visualization environment. C# is designed for the .NET platform and it is widely suitable for development software. It would be ideal to integrate Matlab and C# language to create a mathematical calculation, powerful function and friendly interactive interface. There are three main methods to achieve this purpose. First, using Matlab engine; second, calling Matlab workplace and sending command directly and; last, using Matlab builder to build the .m file and then pack it into COM component. The computer environment in this research is Microsoft Visual Studio 2018 (project style: Windows Forms Application) and Matlab R2017b.

Amongst the methods introduced, Matlab engine is used in this study to call for the Matlab ANN toolbox in .NET. The diagram below, i.e., Figure 5.5, shows the process of calling for the Matlab ANN toolbox by using C#. NET with Matlab engine. Moreover, Figure 5.6 demonstrates the programme environment and the C# language code selection in writing ANNREVIT prototype.

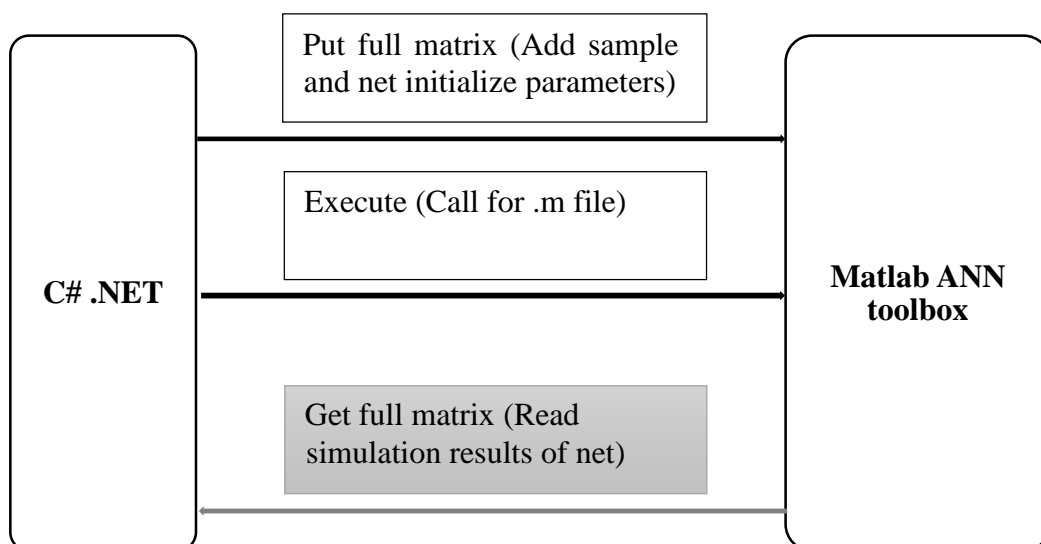


Figure 5.5 The demonstration of C# .NET call for the Matlab ANN toolbox

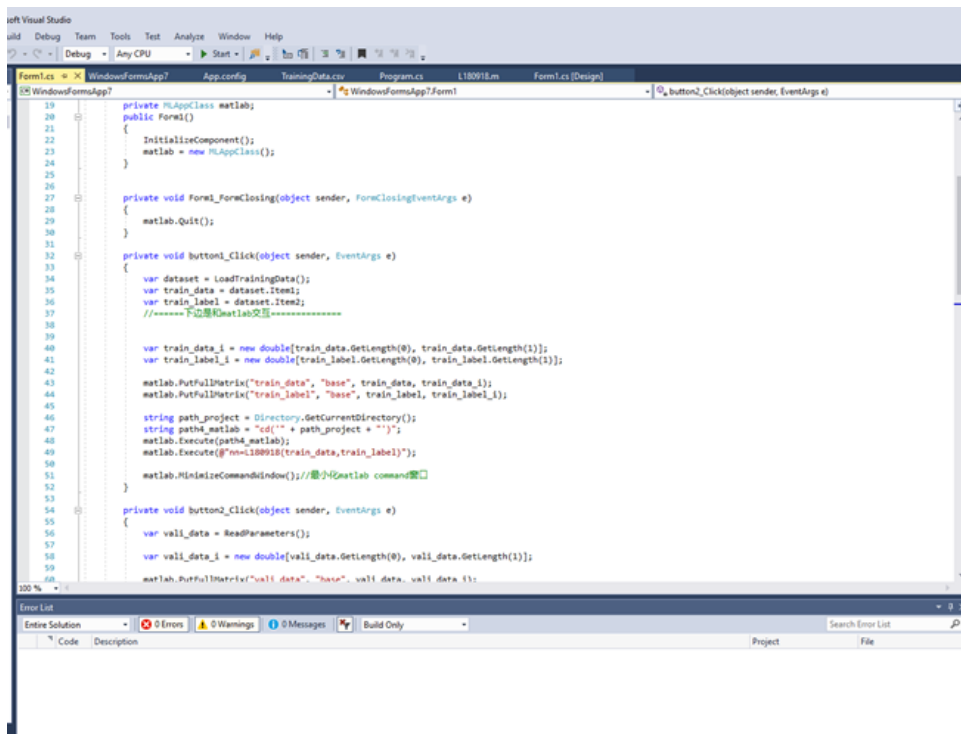


Figure 5.6 The demonstration of C# code in .NET interface when writing ANNREVIT prototype

### 5.3.3 Edit the model translator

There are mainly six parameters affecting the performance of lightpipes, namely, the elbowed angle of lightpies, solar altitude, solar azimuth, the sky clearness index, the reflective value of tube and the respect ratio of lightpipes. All information should be add into the prototype by the model translator programme with initial values for these parameters. It translates all the information of lightpipes into Revit input file. However, there is no existing lightpipe equipment model in Revit. Hence, the double-layer round window in the windows library has been chosen to represent lightpipes. The glass layers of window are defined as the diffuser of lightpipes. An existing window model was chosen from Revit Window Families. The window has the name of NBS\_GlazingVisionLtd\_FrmdRflights\_FlushglazeC. Double glazed 1200mm

diameter 6-16-6mm was chosen because it is of round shape; it is closer to the cross section of lightpipes (shown in Figure 5.7).

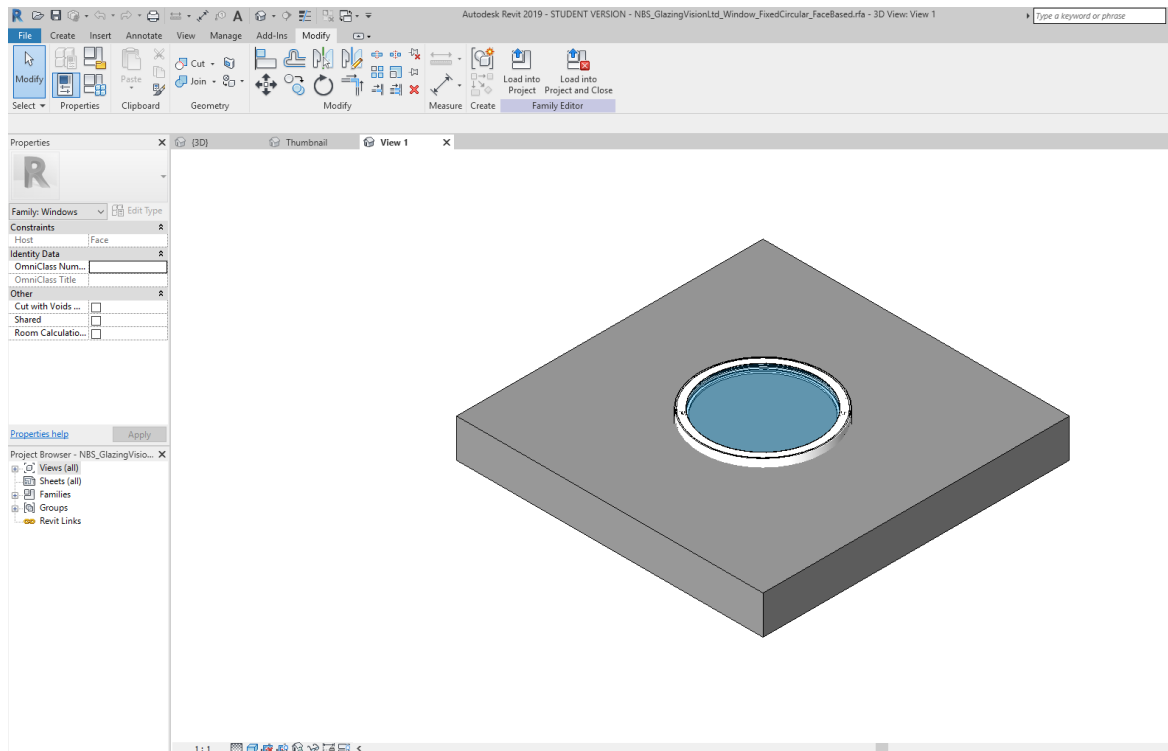


Figure 5.7 Demonstration of window model choice in Revit

The transmittance of lightpipe is controlled by the glass properties of the window. In Revit, there is no ready secularity and roughness values which are used to define the specified material in Revit material library. These values must be custom stored in the material database. In the Revit system, the transmittance of window glazing is controlled by the RGB of glazing. The specific procedure is as follows. First, find the “Properties editor” of glass pane to change the material properties, as shown in Figure 5.8.

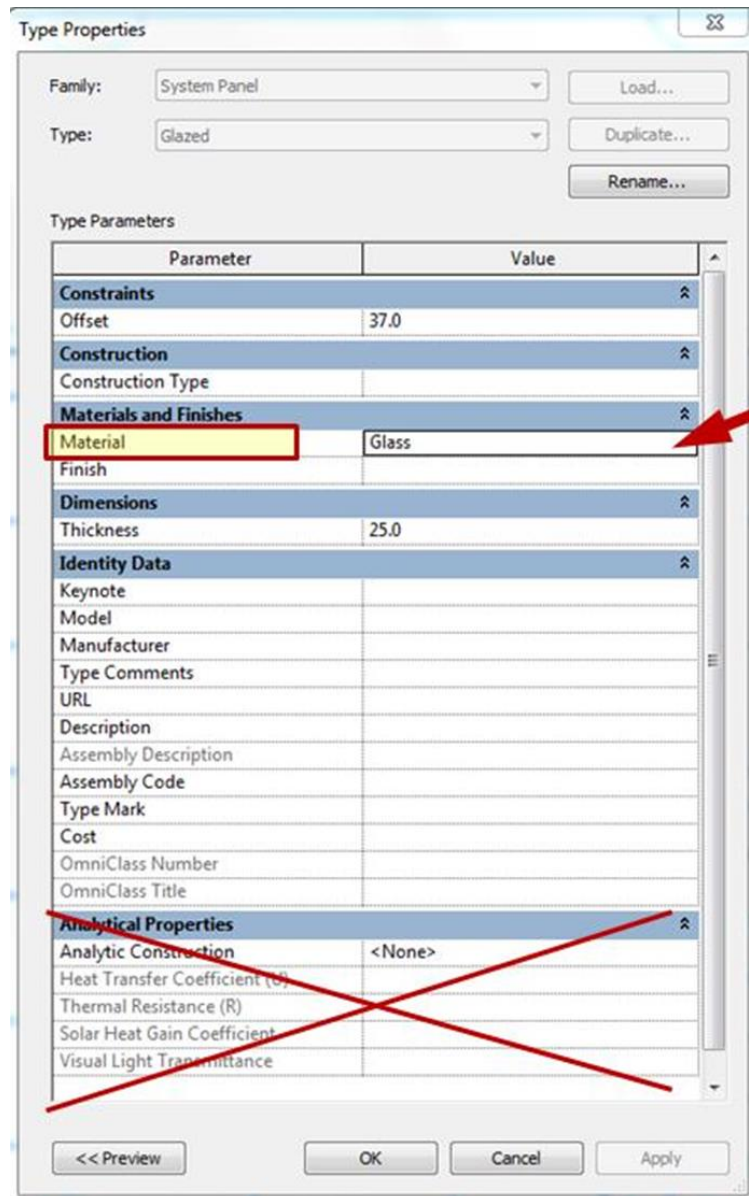


Figure 5.8 The location of "Glass" material in "Type Properties"

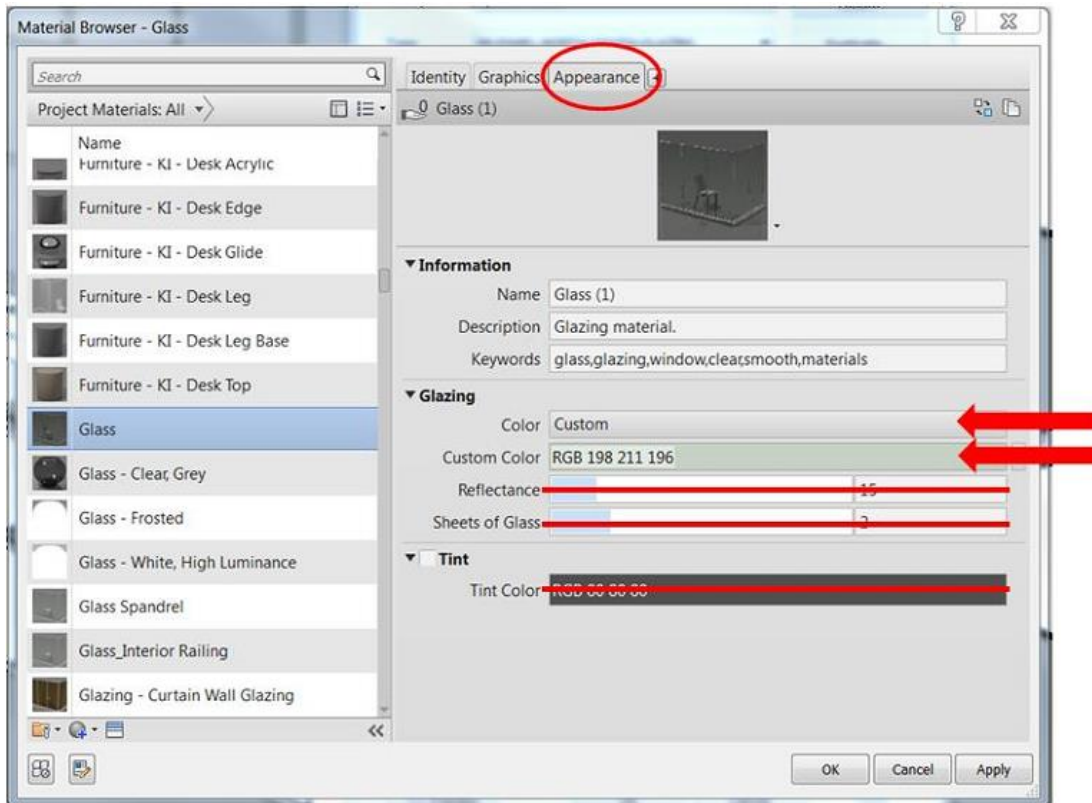


Figure 5.9 The location of RGB values edited panel in Revit

When the valid parameter is found, i.e., the RGB of glass color of in window (Figure 5.9), the relative code can be edited in the .NET environment by using C# language. A series of files should be added in the lightpipes folder structure created by Model Translator. These files include:

- The ANN prediction model file, which has been created and validated in Chapter 3. The completed ANN network configuration and structure should all be included in this file, including the six input parameters and the output parameter.
- Transmittance calculation formula Eq. 5.1 and standard Radiance RGB formula Eq. 5.2 should be included in the file. The transmittance value predicted by ANN model should be reflected into the property of material of glass of window which has been chosen.

- Two batch files, which have ANN model and Revit commands to sequentially execute the ANN model and Revit routines to produce the results.

When the programme coding is finished in .NET, all the code can be packed as .addin file which can be debug in Revit software. It is named as ANNREVIT file. After entering these files into the model translator, the model translator will run the batch files automatically and launch them into Revit programs.

#### **5.3.4. Running the prototype programs in Revit**

In order to simulate the daylighting performance of lightpipes in Revit, the ANNREVIT add-in program must be loaded under the “External Tools” menu. Figure 5.10 shows the loading procedure of all the add-in program into the add-in manager. It also illustrates the execution order of loading steps and perform steps in the add-in manager. Once clicking the main program, the ANN training will run in the background and the transmittance of lightpipes will automatically appear in the blank of dialogue box.

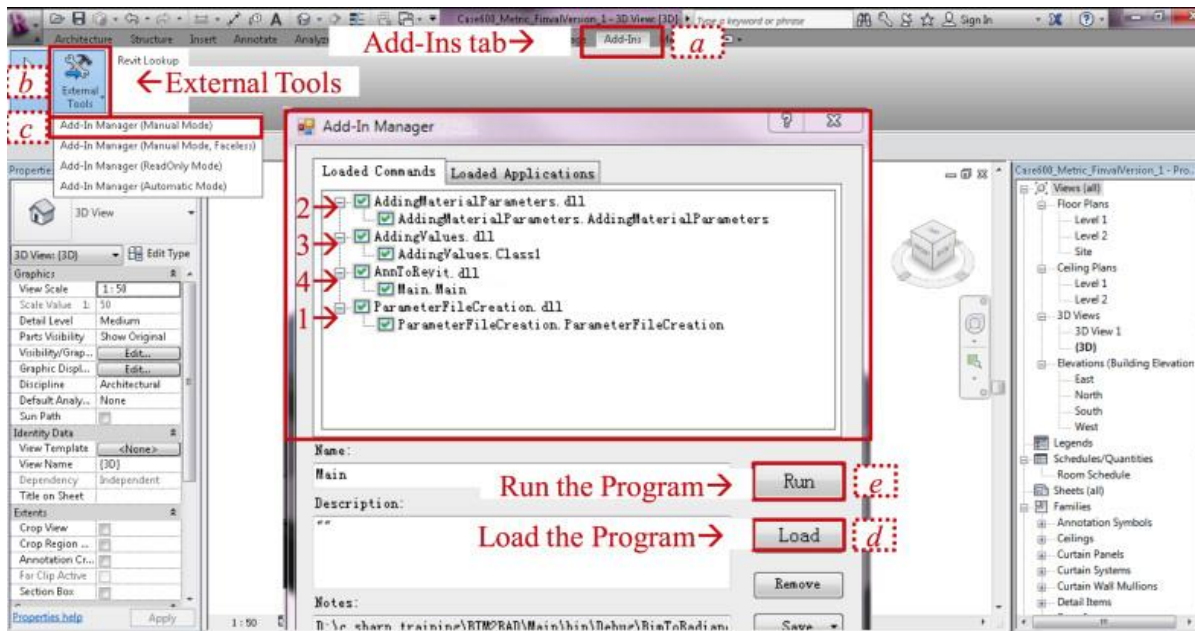


Figure 5.10 Loading the ANNREVIT prototype in Revit

## 5.4 Case study and validation

Once Revit is opened, the Add-ins can be found in the toolbar and the ANNREVIT add-in can be accessed in the drop-down menu of “External Tools”. By evaluating the six input parameters, the transmittance of lightpipes can be returned. The interface is demonstrated in Figure 5.11. After inputting all the values, clicking “train” in the interface as shown in the figure. ANN toolbox will automatically run in the background. Different from the typical ANN interface in Matlab, only result will show in the interface.

A typical house with slope roof was chosen as a case study to validate the prototype. At the beginning the house model should be built in Revit and was named as TEST. Figure 5.12 shows the 3D view of the TEST model and illustrates the lightpipes position in the slope roof (it is presented as round window as justified earlier). Table 5.1 describes the values for material parameters and Table 5.2 lists the values for the ANN parameters, both used in TEST example of the prototype.

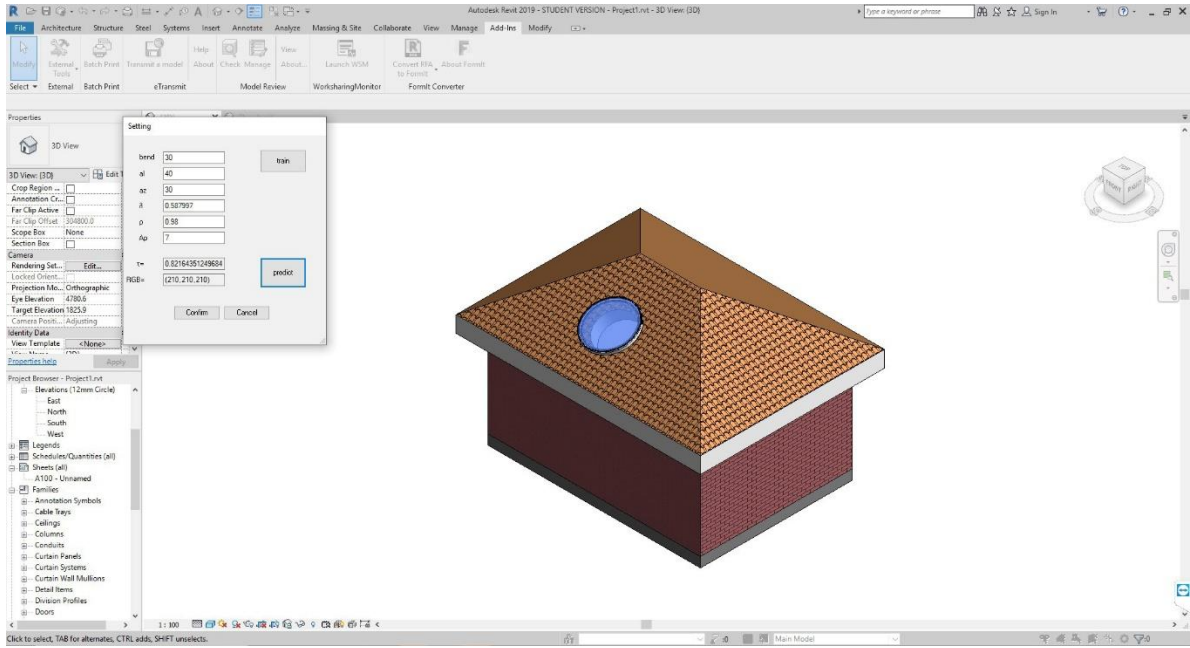


Figure 5.11 Input and output interface in Revit by adding in ANNREVIT prototype

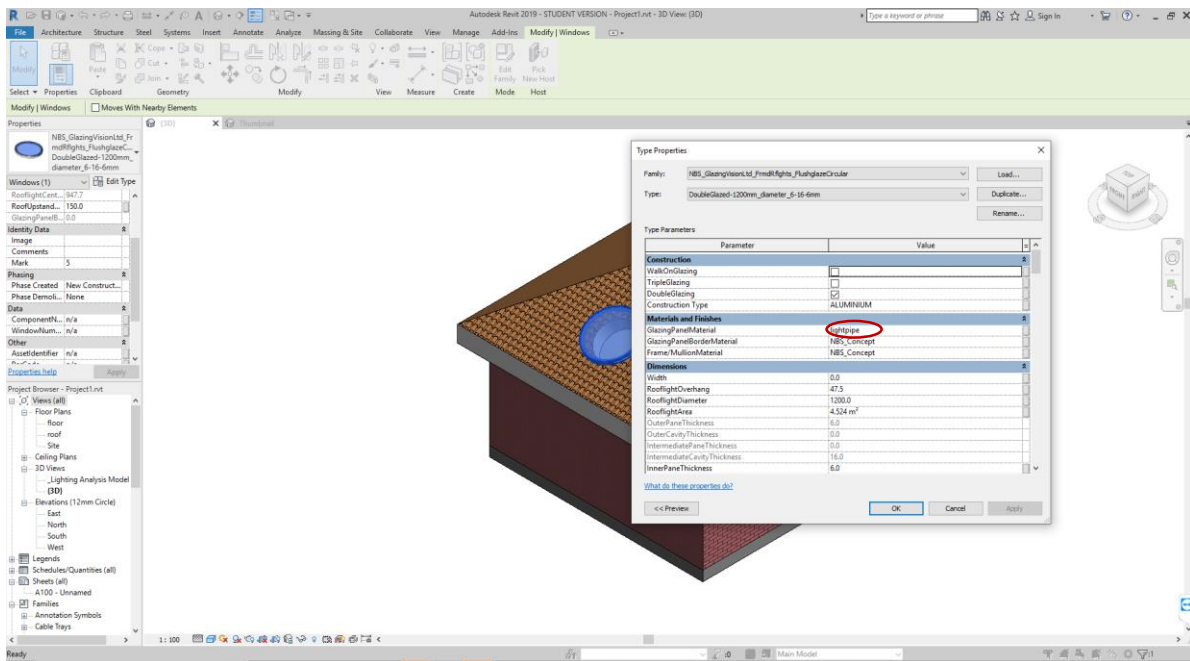


Figure 5.12 Revit information for “lightpipe” in “Type Properties”

Table 5.1 Values for material parameters used in TEST example of the prototype

<b>Building paramaters types</b>	<b>Values</b>
<b>Length of the room</b>	5000mm
<b>Width of the room</b>	3500mm
<b>Number of the lightpipes</b>	1
<b>Wall reflectance</b>	0.5
<b>Floor reflectance</b>	0.2
<b>Ceiling reflectance</b>	0.8

Table 5.2 Values for ANN parameters used in TEST example of the prototype

<b>ANN model parameters</b>	<b>Values</b>
<b>Solar altitude</b>	40°
<b>Solar azimuth</b>	30°
<b>Sky clearness index</b>	0.587997
<b>Bend angle of lightpipes</b>	30°
<b>Aspect ration of lightpipes</b>	7
<b>Reflectivity of tube</b>	0.98
<b>Predicted transmittance</b>	0.8216

In this validation part, the method is using the mathematical equations to manually calculate the results and then comparing with the result calculated from the ANNREVIT prototype. The

transmittance displays from the add-in tool ANNREVIT is 0.8216, while in the Photopia simulation, the transmittance is 0.8210 which are almost the same to the result from ANNREVIT prototype plug-in. It can be postulated that the ANN model has been successfully transferred to the Revit model/platform.

Other than the direct comparison between the plug-in yielded result and the real analytical value, the data flow from the Photopia, to the ANN prediction and to the Revit plug-in calculation is also verified. Figure 5.13 shows the material properties for “lightpipe” in Revit and the transmittance is reflected by R, G and B value. It can be seen that this ANNREVIT plug-in automatically custom-defines the glass value by using Revit RGB with values of 210 for R, G and B respectively, in the lightpipe glazing setting. The average reflectance value is then calculated using Eqs. 5.1 and 5.2, which is 0.8234. The calculation results are shown in Table 5.3. In Figure 5.11 the transmittance is 0.8216, which is nearly same with the prediction value. This is a sample comparison that validates the accuracy of the material translation.

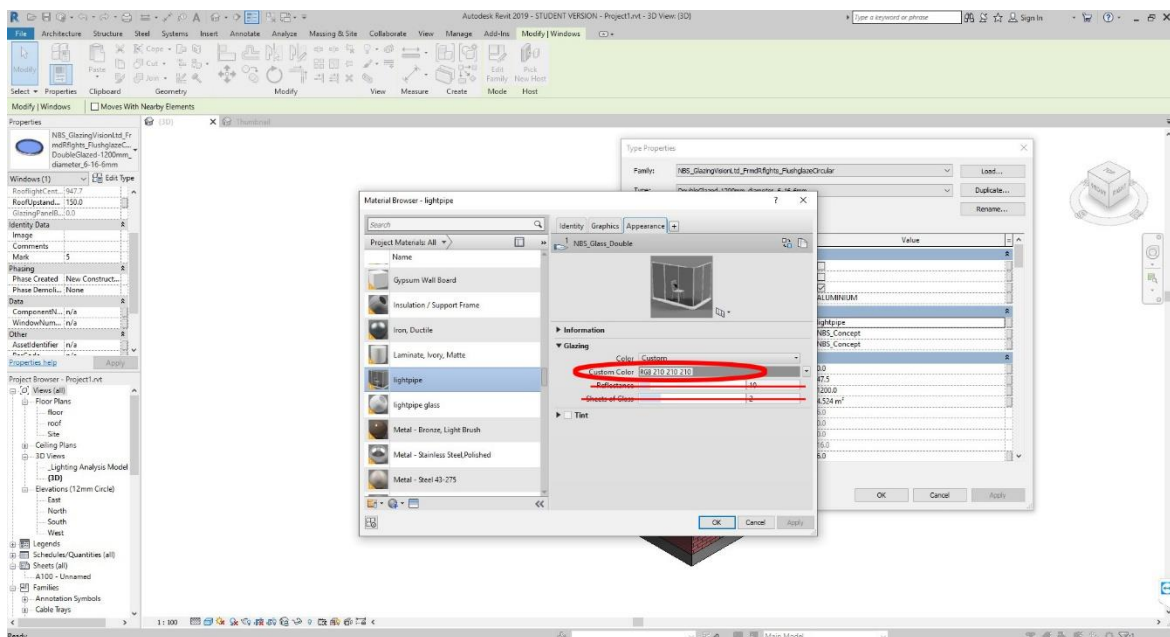


Figure 5.13 Revit material information for “lightpipe” with custom parameters “Custom Color”

Table 5.3 Mathematics calculated the average reflectance of the material “lightpipe” (set as the transmittance of lightpipes in this modelling)

<b>Color channels</b>	<b>Red</b>	<b>Green</b>	<b>Blue</b>	<b>Average reflectance</b>
<b>Value</b>	210	210	210	
<b>Normalized value (value/255)</b>	0.8235	0.8235	0.8235	
<b>Color coefficients (from Eq. 2)</b>	0.265	0.670	0.065	
<b>Normalized value × coefficients</b>	0.2182	0.5517	0.0535	0.8234

## 5.5 Summary

The contribution of this study is extending the scope of Revit application in the area of daylighting modelling. As discussed, ANN presents outstanding prediction ability in the performance of lightpipes. However, there is no available lightpipe model library in the Revit system. Hence, utilising API technique to develop a prototype for predicting the optical performance of lightpipes in Revit is attempted in this Chapter. Moreover, the prototype has been implemented in Revit system as a plug-in. Without running Matlab ANN toolbox, this prototype can predict the transmittance value of lightpipes directly. It helps the users choose the optimized lightpipe system and achieve the best illuminance effect. Further, the approach presented in this Chapter can be extended to other sustainable equipment development in Revit. Other useful applications can be achieved by using API technique to develop add-in extensions. A key contribution of this study is that the designers and/or practising engineers will not need

to do the complicated modelling from scratch. Meanwhile, it encourages the development of programme and eventually promotes the widespread application of BIM.

## **Chapter 6 Conclusions and Future Work**

## 6.1 Conclusions

This thesis has presented a study by using artificial neural network intelligence in simulating and optimizing the transmittance of lightpipes and implemented the developed model in BIM platform. Comprehensive and critical literature review is first provided on the research work in daylighting prediction and optimization by using ANNs approaches. The luminance and illuminance prediction, daylighting control and energy saving with daylighting have been extensively discussed. The research gaps currently hindering the widespread and effective application of ANNs in daylighting prediction and optimization have been explored and discussed. The findings could help architects and practising engineers adopt proper daylighting design schemes and evaluation methods, and therefore promote sustainable developments in architectural buildings.

Numerous simulations in Photopia are conducted to form the data sets for the performance of various lightpipe configurations and structures. Different and independent parameters are considered in the simulation including solar altitude, angle of solar azimuth, elbowed angle of lightpipes, sky clearness index, aspect ratio and reflectivity of tube. Based on the simulated results, some different forms of mathematical models have been proposed to predict the transmittance of lightpipes with various elbowed angles. Based on data obtained from Photopia simulations, ANN model was trained and validated with satisfactory accuracy.

Moreover, the ANN model proposed has been compared with multiple nonlinear regression (MNL). The prediction accuracy of ANN is obvious higher than MNL model, where  $R^2$  can reach 0.9653. However, the mathematical model has significant application potential in practical project. Different from widely used raytracing simulation in computer, mathematical model can be used directly by acquiring the given solar position, sky clear

condition and parameters of lightpipes. The analytical equations for the illuminance performance of lightpipes have been established based on a number of underlying parameters.

This study has further extended the scope of Revit application in the area of daylighting modelling. API is utilised to develop a prototype to predict the optical performance of lightpipes in Revit. First of all, it well fills the gap that there is no lightpipe library in Revit platform, and also the prototype is implemented in the Revit system as a plug-in. A detailed procedure is presented for the implementation process of ANN model into Revit platform. It helps the designers and practising engineers choose the optimized lightpipe systems for the best illuminance effect. The prototype proposed can be an advanced inspiration to other sustainable design performance evaluated in BIM environment. The significant strength is it can apply an approach to interact information between model prediction and parametric assessment.

## **6.2 Limitations and future work**

Matlab is an outstanding computing platform which has a strong toolbox of ANN implemented. To combine ANN in Matlab with BIM modelling software Revit could significantly increase the working efficiency and add tremendous benefits. However, a limitation of this hybrid system is the requirement of installing Matlab software which is expensive and occupies large amount of memory in the computing system. Next development of this research is to use the deep learning system directly from the computer. C#. NET could train the deep learning neural network as well. On the other hand, directly editing the code in C#. NET is considerably complex and a large amount of coding work is needed.

In addition, an extension of the present work could be to further develop the mathematical model proposed in Chapter 4 and embed it in the custom define solar simulation procedure. It would simplify the simulation programme and bring more choices to community and industry.

The next stage could be integrating the daylighting performance and thermal analysis together into Revit platform, to achieve the multi-objective simulation. So far, only single lightpipe system can be handled in the proposed prototype. The further work can attempt more complex lightpipes types, such as lightpipes combined with ventilation system, lightpipes with DCPC system etc. Moreover, based on API technique, combining ANN with Revit and building energy simulation software such as EnergyPlus all together in order to get a comprehensive and streamlined simulation flow for illuminance and energy consumption model of lightpipes would bring tremendous advantages and convenience.

## REFERENCES

1. Hobley, A., *Will gas be gone in the United Kingdom (UK) by 2050? An impact assessment of urban heat decarbonisation and low emission vehicle uptake on future UK energy system scenarios*. Renewable Energy, 2019. **142**: p. 695-705.
2. Paraschiv, S. and L.S. Paraschiv, *Trends of carbon dioxide (CO<sub>2</sub>) emissions from fossil fuels combustion (coal, gas and oil) in the EU member states from 1960 to 2018*. Energy Reports, 2020. **6**: p. 237-242.
3. Mambo, A.D., *ZERO CARBON EMISSION IN UK'S DOMESTIC BUILDINGS*. 2011: VDM Verlag Dr. Müller.
4. Wagiman, K.R., et al., *Lighting system control techniques in commercial buildings: Current trends and future directions*. Journal of Building Engineering, 2020. **31**: p. 101342.
5. Enongene, K.E., et al., *Energy savings and economic benefits of transition towards efficient lighting in residential buildings in Cameroon*. Renewable and Sustainable Energy Reviews, 2017. **78**: p. 731-742.
6. Li, D.H.W. and E.K.W. Tsang, *An analysis of daylighting performance for office buildings in Hong Kong*. Building and Environment, 2008. **43**(9): p. 1446-1458.

7. Begemann, S.H.A., G.J. van den Beld, and A.D. Tenner, *Daylight, artificial light and people in an office environment, overview of visual and biological responses*. International Journal of Industrial Ergonomics, 1997. **20**(3): p. 231-239.
8. Bodart, M. and A. De Herde, *Global energy savings in offices buildings by the use of daylighting*. Energy and Buildings, 2002. **34**(5): p. 421-429.
9. Inchio Lou, Y.Z., *Sludge Bulking Prediction Using Principle Component Regression and Artificial Neural Network*. Mathematical Problems in Engineering, Hindawi Publishing Corporation, India, 2012. **Volume 2012**(Article ID 237693): p. 17.
10. Mohanraj, M., S. Jayaraj, and C. Muraleedharan, *Applications of artificial neural networks for refrigeration, air-conditioning and heat pump systems—A review*. Renewable and Sustainable Energy Reviews, 2012. **16**(2): p. 1340-1358.
11. Cong, T., et al., *Applications of ANNs in flow and heat transfer problems in nuclear engineering: A review work*. Progress in Nuclear Energy, 2013. **62**: p. 54-71.
12. Mellit, A., et al., *Artificial intelligence techniques for sizing photovoltaic systems: A review*. Renewable and Sustainable Energy Reviews, 2009. **13**(2): p. 406-419.
13. Kalogirou, S.A., *Artificial intelligence for the modeling and control of combustion processes: a review*. Progress in Energy and Combustion Science, 2003. **29**(6): p. 515-566.

14. Kalogirou, S.A., *Artificial neural networks in renewable energy systems applications: a review*. Renewable and Sustainable Energy Reviews, 2001. **5**(4): p. 373-401.
15. Hussain, M.A., *Review of the Applications of Neural Networks in Chemical Process Control—Simulation and Online Implementation*. Artificial Intelligence in Engineering, 1999. **13**(1): p. 55-68.
16. Mohanraj, M., S. Jayaraj, and C. Muraleedharan, *Applications of artificial neural networks for thermal analysis of heat exchangers – A review*. International Journal of Thermal Sciences, 2015. **90**: p. 150-172.
17. Zhang, G., B. Eddy Patuwo, and M. Y. Hu, *Forecasting with artificial neural networks:: The state of the art*. International Journal of Forecasting, 1998. **14**(1): p. 35-62.
18. Gardner, M.W. and S.R. Dorling, *Artificial neural networks (the multilayer perceptron)—a review of applications in the atmospheric sciences*. Atmospheric Environment, 1998. **32**(14–15): p. 2627-2636.
19. Chirarattananon, S., P. Chaiwiwatworakul, and S. Pattanasethanon, *Daylight availability and models for global and diffuse horizontal illuminance and irradiance for Bangkok*. Renewable Energy, 2002. **26**(1): p. 69-89.
20. Sayigh, A., *Energy Conservation in Buildings: The Achievement of 50% Energy Saving: An Environmental Challenge?* 2012: Newnes.

21. Alrubaih, M.S., et al., *Research and development on aspects of daylighting fundamentals*. Renewable and Sustainable Energy Reviews, 2013. **21**: p. 494-505.
22. Boyce, P.R., *Review: the impact of light in buildings on human health*. Indoor and Built environment, 2010. **19**(1): p. 8-20.
23. A. Nabil, J.M., *Useful daylight illuminance: A new paradigm for assessing daylight in buildings*. Lighting Research and Technology, 2005. **37**(1): p. 41-57.
24. Hua, Y., A. Oswald, and X. Yang, *Effectiveness of daylighting design and occupant visual satisfaction in a LEED Gold laboratory building*. Building and Environment, 2011. **46**(1): p. 54-64.
25. Veitch, J.A. and R. Gifford, *Assessing beliefs about lighting effects on health, performance, mood, and social behavior*. Environment and Behavior, 1996. **28**(4): p. 446-470.
26. McHugh, J., et al. *Effectiveness of photocontrols with skylighting*. in *IESNA Annual Conference Proceedings*. 2004.
27. Wong, I.L., *A review of daylighting design and implementation in buildings*. Renewable and Sustainable Energy Reviews, 2017. **74**: p. 959-968.
28. Bodart, M., et al., *A guide for building daylight scale models*. Architectural Science Review, 2007. **50**(1): p. 31-36.

29. Littlefair, P., *Daylight prediction in atrium buildings*. Solar Energy, 2002. **73**(2): p. 105-109.
30. Kim, C.-S. and S.-J. Chung, *Daylighting simulation as an architectural design process in museums installed with toplights*. Building and Environment, 2011. **46**(1): p. 210-222.
31. Aghemo, C., A. Pellegrino, and V.R.M. LoVerso, *The approach to daylighting by scale models and sun and sky simulators: A case study for different shading systems*. Building and Environment, 2008. **43**(5): p. 917-927.
32. Li, D.H.W. and J.C. Lam, *Evaluation of lighting performance in office buildings with daylighting controls*. Energy and Buildings, 2001. **33**(8): p. 793-803.
33. Kittler, R., *Daylight prediction and assessment: theory and design practice*. Architectural Science Review, 2007. **50**(2): p. 94-99.
34. Love, J. and M. Navvab, *The vertical-to-horizontal illuminance ratio: a new indicator of daylighting performance*. Journal of the Illuminating Engineering Society, 1994. **23**(2): p. 50-61.
35. Kim, S.-Y. and J.-J. Kim, *The impact of daylight fluctuation on a daylight dimming control system in a small office*. Energy and Buildings, 2007. **39**(8): p. 935-944.
36. Kazanasmaz, T., *Fuzzy logic model to classify effectiveness of daylighting in an office with a movable blind system*. Building and Environment, 2013. **69**: p. 22-34.

37. Su, Y., et al., *Comparative monitoring and data regression of various sized commercial lightpipes*. Energy and Buildings, 2012. **50**: p. 308-314.
38. Swift, P.D. and G.B. Smith, *Cylindrical mirror light pipes*. Solar Energy Materials and Solar Cells, 1995. **36**(2): p. 159-168.
39. Dutton, S. and L. Shao, *Raytracing simulation for predicting light pipe transmittance*. International Journal of Low-Carbon Technologies, 2007. **2**(4): p. 339-358.
40. Kazanasmaz, T., M. Günaydin, and S. Binol, *Artificial neural networks to predict daylight illuminance in office buildings*. Building and Environment, 2009. **44**(8): p. 1751-1757.
41. Jovanović, A., et al., *Importance of building orientation in determining daylighting quality in student dorm rooms: Physical and simulated daylighting parameters' values compared to subjective survey results*. Energy and Buildings, 2014. **77**: p. 158-170.
42. Apian-Bennewitz, P., et al., *Computer-oriented building design: Advances in daylighting and thermal simulation tools*. Renewable Energy, 1998. **14**(1): p. 351-356.
43. Lim, Y.-W., et al., *Building façade design for daylighting quality in typical government office building*. Building and Environment, 2012. **57**: p. 194-204.
44. Krüger, E.L. and A.L. Dorigo, *Daylighting analysis in a public school in Curitiba, Brazil*. Renewable Energy, 2008. **33**(7): p. 1695-1702.

45. Andersen, M., J.M. Gagne, and S. Kleindienst, *Interactive expert support for early stage full-year daylighting design: a user's perspective on Lightsolve*. Automation in Construction, 2013. **35**: p. 338-352.
46. Gagne, J.M.L., M. Andersen, and L.K. Norford, *An interactive expert system for daylighting design exploration*. Building and Environment, 2011. **46**(11): p. 2351-2364.
47. Kota, S., et al., *Building Information Modeling (BIM)-based daylighting simulation and analysis*. Energy and Buildings, 2014. **81**: p. 391-403.
48. Chen, Y., et al., *Experimental and simulation study on the performance of daylighting in an industrial building and its energy saving potential*. Energy and Buildings, 2014. **73**: p. 184-191.
49. Sabry, H., et al., *Balancing the daylighting and energy performance of solar screens in residential desert buildings: Examination of screen axial rotation and opening aspect ratio*. Solar Energy, 2014. **103**: p. 364-377.
50. Tian, C., T. Chen, and T.-m. Chung, *Experimental and simulating examination of computer tools, Radlink and DOE2, for daylighting and energy simulation with venetian blinds*. Applied Energy, 2014. **124**: p. 130-139.
51. Arranz, B., et al., *Evaluation of three solar and daylighting control systems based on Calumen II, Ecotect and radiance simulation programmes to obtain an energy efficient*

- and healthy interior in the experimental building Prototype SD10. Energy and Buildings, 2014. 83: p. 225-236.*
52. Galasiu, A.D. and M.R. Atif, *Applicability of daylighting computer modeling in real case studies: comparison between measured and simulated daylight availability and lighting consumption. Building and Environment, 2002. 37(4): p. 363-377.*
53. Loutzenhiser, P.G., G.M. Maxwell, and H. Manz, *An empirical validation of the daylighting algorithms and associated interactions in building energy simulation programs using various shading devices and windows. Energy, 2007. 32(10): p. 1855-1870.*
54. Acosta, I., J. Navarro, and J.J. Sendra, *Daylighting design with lightscoop skylights: Towards an optimization of shape under overcast sky conditions. Energy and Buildings, 2013. 60: p. 232-238.*
55. Ullah, I. and S. Shin, *Highly concentrated optical fiber-based daylighting systems for multi-floor office buildings. Energy and Buildings, 2014. 72: p. 246-261.*
56. Page, J., et al., *On-site performance of electrochromic glazings coupled to an anidolic daylighting system. Solar Energy, 2007. 81(9): p. 1166-1179.*
57. Esen, H., et al., *Artificial neural network and wavelet neural network approaches for modelling of a solar air heater. Expert Systems with Applications, 2009. 36(8): p. 11240-11248.*

58. Agatonovic-Kustrin, S. and R. Beresford, *Basic concepts of artificial neural network (ANN) modeling and its application in pharmaceutical research*. Journal of Pharmaceutical and Biomedical Analysis, 2000. **22**(5): p. 717-727.
59. Lewis, C.D., *Industrial and business forecasting methods: a practical guide to exponential smoothing and curve fitting*. 1982: Butterworth Scientific.
60. Esen, H., et al., *Artificial neural networks and adaptive neuro-fuzzy assessments for ground-coupled heat pump system*. Energy and Buildings, 2008. **40**(6): p. 1074-1083.
61. Katz, W.T., J.W. Snell, and M.B. Merickel, [29] *Artificial neural networks*, in *Methods in Enzymology*. 1992, Academic Press. p. 610-636.
62. Hosseini, S.A., *Neutron spectrum unfolding using artificial neural network and modified least square method*. Radiation Physics and Chemistry, 2016. **126**: p. 75-84.
63. Mardaljevic, J., *Daylight, indoor illumination and human behavior*. 2012, © Springer Science+ Business Media, LLC.
64. Nick Baker, K.S., *Daylight Design of Buildings*. Earthscan, Oxon, 2013.
65. Halliday, S., *Sustainable construction*. 2008: Routledge.
66. CIBSE, *Lighting Guide 10: Daylighting - a Guide for Designers*. CIBSE, Nov 2014.

67. Reinhart, C.F. and O. Walkenhorst, *Validation of dynamic RADIANCE-based daylight simulations for a test office with external blinds*. Energy and Buildings, 2001. **33**(7): p. p.683-697.
68. Moon, P., Spencer, D., *Illumination for a non-uniform sky*. Illum Eng, 1942. **37**(10): p. 797-826.
69. Li, D.H.W., et al., *A study of the daylighting performance and energy use in heavily obstructed residential buildings via computer simulation techniques*. Energy and Buildings, 2006. **38**(11): p. 1343-1348.
70. Janjai, S. and P. Plaon, *Estimation of sky luminance in the tropics using artificial neural networks: Modeling and performance comparison with the CIE model*. Applied Energy, 2011. **88**(3): p. 840-847.
71. López, G. and C.A. Gueymard, *Clear-sky solar luminous efficacy determination using artificial neural networks*. Solar Energy, 2007. **81**(7): p. 929-939.
72. Tíba, C. and S.S. Leal, *Measuring and modelling illuminance in the semi-arid Northeast of Brazil*. Renewable Energy, 2012. **48**: p. 464-472.
73. Perez, R., R. Seals, and J. Michalsky, *All-weather model for sky luminance distribution—Preliminary configuration and validation*. Solar Energy, 1993. **50**(3): p. 235-245.

74. Pattanasethanon, S., et al., *An accuracy assessment of an empirical sine model, a novel sine model and an artificial neural network model for forecasting illuminance/irradiance on horizontal plane of all sky types at Mahasarakham, Thailand*. *Energy Conversion and Management*, 2008. **49**(8): p. 1999-2005.
75. Sandhyalaxmi G Navada, C.S.A., Savitha G Kini *Prediction of Daylight Availability For Visual Comfort*. *International Journal of Applied Engineering Research* ISSN 0973-4562, 2016. **11**(7): p. 4711-4717.
76. Tarek Hegazy, A.A., *Neural Network Model for Parametric Cost Estimation of Highway Projects*. *Journal of Construction Engineering and Management*, 1998. **124**(3): p. 210-218.
77. Fonseca, R.W.d., E.L. Didoné, and F.O.R. Pereira, *Using artificial neural networks to predict the impact of daylighting on building final electric energy requirements*. *Energy and Buildings*, 2013. **61**: p. 31-38.
78. de Bakker, C., et al., *Occupancy-based lighting control in open-plan office spaces: A state-of-the-art review*. *Building and Environment*, 2017. **112**: p. 308-321.
79. Wong, S.L., K.K.W. Wan, and T.N.T. Lam, *Artificial neural networks for energy analysis of office buildings with daylighting*. *Applied Energy*, 2010. **87**(2): p. 551-557.
80. Dounis, A.I. and C. Caraiscos, *Advanced control systems engineering for energy and comfort management in a building environment—A review*. *Renewable and Sustainable Energy Reviews*, 2009. **13**(6–7): p. 1246-1261.

81. Kim, W., Y. Jeon, and Y. Kim, *Simulation-based optimization of an integrated daylighting and HVAC system using the design of experiments method*. Applied Energy, 2016. **162**: p. 666-674.
82. Li, D.H.W., et al., *An analysis of energy-efficient light fittings and lighting controls*. Applied Energy, 2010. **87**(2): p. 558-567.
83. Lam, M.K.T.W.K.K., *Office Lighting Retrofit Using T5 Fluorescent Lamps and Electronic Ballasts*. HKIE Transactions 2003. **10**(1): p. 55-60.
84. Öztürk, L.D., *Determination of Energy Losses in Lighting in Terms of Good Vision Efficiency*. Architectural Science Review 2008. **51**(1): p. 39-47.
85. Hu, J., E. Shen, and Y. Gu, *Evaluation of Lighting Performance Risk Using Surrogate Model and EnergyPlus*. Procedia Engineering, 2015. **118**: p. 522-529.
86. Hu, J. and S. Olbina, *Illuminance-based slat angle selection model for automated control of split blinds*. Building and Environment, 2011. **46**(3): p. 786-796.
87. Kalogirou, S.A. and M. Bojic, *Artificial neural networks for the prediction of the energy consumption of a passive solar building*. Energy, 2000. **25**(5): p. 479-491.
88. Lam, J.C., *An analysis of residential sector energy use in Hong Kong*. Energy, 1996. **21**(1): p. 1-8.

89. Kumar, R., R.K. Aggarwal, and J.D. Sharma, *Energy analysis of a building using artificial neural network: A review*. Energy and Buildings, 2013. **65**: p. 352-358.
90. Nasr, P., et al., *Influence of cytosolic and mitochondrial Ca<sup>2+</sup>, ATP, mitochondrial membrane potential, and calpain activity on the mechanism of neuron death induced by 3-nitropropionic acid*. Neurochemistry International, 2003. **43**(2): p. 89-99.
91. Yin, C., L. Rosendahl, and Z. Luo, *Methods to improve prediction performance of ANN models*. Simulation Modelling Practice & Theory, 2003. **11**(3-4): p. 211-222.
92. Wijayasekara, D., et al., *Optimal artificial neural network architecture selection for performance prediction of compact heat exchanger with the EBaLM-OTR technique*. Nuclear Engineering & Design, 2011. **241**(7): p. 2549-2557.
93. Liu, H., et al., *An experimental investigation of two Wavelet-MLP hybrid frameworks for wind speed prediction using GA and PSO optimization*. International Journal of Electrical Power & Energy Systems, 2013. **52**(nov.): p. 161-173.
94. May, R.J., H.R. Maier, and G.C. Dandy, *Data splitting for artificial neural networks using SOM-based stratified sampling*. Neural Networks, 2010. **23**(2): p. 283-294.
95. Kubota, N., K. Shimojima, and T. Fukuda, *The role of virus infection in virus-evolutionary genetic algorithm*. 1996.

96. Hou, Z., et al., *Cooling-load prediction by the combination of rough set theory and an artificial neural-network based on data-fusion technique*. *Applied Energy*, 2006. **83**(9): p. 1033-1046.
97. Karatasou, S., M. Santamouris, and V. Geros, *Modeling and predicting building's energy use with artificial neural networks: Methods and results*. *Energy & Buildings*, 2006. **38**(8): p. 949-958.
98. Saxena, N.S.K.K., *Fuzzy Logic Based Students Performance Analysis Model for Educational Institutions*. VIVECHAN International Journal of Research, 2010.
99. Oakley, G., S.B. Riffat, and L. Shao, *Daylight performance of lightpipes*. *Solar Energy*, 2000. **69**(2): p. 89-98.
100. Zastrow, A. and V. Wittwer. *Daylighting with Mirror Light Pipes and with Fluorescent Planar Concentrators. First Results from the Demonstration Project Stuttgart-Hohenheim*. in *30th Annual Technical Symposium*. 1987. International Society for Optics and Photonics.
101. Zhang, Muneer, and Kubie, *A design guide for performance assessment of solar light-pipes*. *Lighting Research & Technology*, 2002.
102. Jenkins, D. and T. Muneer, *Light-pipe prediction methods*. *Applied Energy*, 2004. **79**(1): p. 77-86.

103. Kocifaj, M., et al., *Theoretical solution for light transmission of a bended hollow light guide*. Solar Energy, 2010. **84**(8): p. 1422-1432.
104. Waide, P., S. Tanishima, and I.E. Agency, *Light's Labour's Lost: Policies for Energy-efficient Lighting*. Organization for Economic, 2006.
105. Lin, H., et al., *The energy-saving potential of an office under different pricing mechanisms – Application of an agent-based model*. Applied Energy, 2017. **202**: p. 248-258.
106. Lowry, G., *Energy saving claims for lighting controls in commercial buildings*. Energy and Buildings, 2016. **133**: p. 489-497.
107. Alizadehsalehi, S., A. Hadavi, and J.C. Huang, *From BIM to extended reality in AEC industry*. Automation in Construction, 2020. **116**: p. 103254.
108. Lee, A., et al., *nD modelling - a driver or enabler for construction improvement?* Rics Research Paper, 2005.
109. Wei Yan, M.C., Jeff Haberl, WoonSeong Jeong, Jong Bum Kim, Sandeep Kota, Jose Luis Bermudez Alcocer, Manish Dixit, *Interfacing BIM with building thermal and daylighting modeling*. International Building Performance Simulation Association (IBPSA), Chambery, France, 2013.

110. Nguyen, T.H., T. Shehab, and Z. Gao, *Evaluating Sustainability of Architectural Designs Using Building Information Modeling*. Open Construction & Building Technology Journal, 2010. **4**(1): p. 1-8.
111. Boddy, S., et al., *Computer integrated construction: A review and proposals for future direction*. Advances in Engineering Software, 2007. **38**(10): p. 677-687.
112. Oti, A.H., et al., *Structural sustainability appraisal in BIM*. Automation in Construction, 2016. **69**(SEP.): p. 44-58.
113. Deitel, H.M. and P.J. Deitel. *C# for Programmers (2nd Edition) (Deitel Developer Series)*. 2005.